University of Kentucky

UKnowledge

2023

ROLE OF AUTOPHAGY IN AORTIC ANEURYSMS

Aida Javidan

University of Kentucky, aja252@uky.edu

Digital Object Identifier: https://doi.org/10.13023/etd.2023.032

Right click to open a feedback form in a new tab to let us know how this document benefits you.

STUDENT AGREEMENT:

I represent that my thesis or dissertation and abstract are my original work. Proper attribution has been given to all outside sources. I understand that I am solely responsible for obtaining any needed copyright permissions. I have obtained needed written permission statement(s) from the owner(s) of each third-party copyrighted matter to be included in my work, allowing electronic distribution (if such use is not permitted by the fair use doctrine) which will be submitted to UKnowledge as Additional File.

I hereby grant to The University of Kentucky and its agents the irrevocable, non-exclusive, and royalty-free license to archive and make accessible my work in whole or in part in all forms of media, now or hereafter known. I agree that the document mentioned above may be made available immediately for worldwide access unless an embargo applies.

I retain all other ownership rights to the copyright of my work. I also retain the right to use in future works (such as articles or books) all or part of my work. I understand that I am free to register the copyright to my work.

REVIEW, APPROVAL AND ACCEPTANCE

The document mentioned above has been reviewed and accepted by the student's advisor, on behalf of the advisory committee, and by the Director of Graduate Studies (DGS), on behalf of the program; we verify that this is the final, approved version of the student's thesis including all changes required by the advisory committee. The undersigned agree to abide by the statements above.

<div align="right">

Aida Javidan, Student

Dr. Venkateswaran Subramanian, Major Professor

Dr. Howard Glauert, Director of Graduate Studies

</div>

STUDENT AGREEMENT:

I represent that my thesis or dissertation and abstract are my original work. Proper attribution has been given to all outside sources. I understand that I am solely responsible for obtaining any needed copyright permissions. I have obtained needed written permission statement(s) from the owner(s) of each third-party copyrighted matter to be included in my work, allowing electronic distribution (if such use is not permitted by the fair use doctrine) which will be submitted to UKnowledge as Additional File.

I hereby grant to The University of Kentucky and its agents the irrevocable, non-exclusive, and royalty-free license to archive and make accessible my work in whole or in part in all forms of media, now or hereafter known. I agree that the document mentioned above may be made available immediately for worldwide access unless an embargo applies.

I retain all other ownership rights to the copyright of my work. I also retain the right to use in future works (such as articles or books) all or part of my work. I understand that I am free to register the copyright to my work.

REVIEW, APPROVAL AND ACCEPTANCE

The document mentioned above has been reviewed and accepted by the student's advisor, on behalf of the advisory committee, and by the Director of Graduate Studies (DGS), on behalf of the program; we verify that this is the final, approved version of the student's thesis including all changes required by the advisory committee. The undersigned agree to abide by the statements above.

Aida Javidan, Student

Dr. Venkateswaran Subramanian, Major advisor

Dr. Howard Glauert, Director of Graduate Studies

ROLE OF AUTOPHAGY IN AORTIC ANEURYSMS

_____

DISSERTATION

A dissertation submitted in partial fulfillment of the
requirements for the degree of Doctoral of Philosophy in the
College of Medicine at the University of Kentucky

By

Aida Javidan

Lexington, Kentucky

Director: Dr. Venkateswaran Subramanian, Assistant Professor of Physiology

Lexington, Kentucky

2022

ABSTRACT

Role of Autophagy in Aortic Aneurysms

Abdominal Aortic Aneurysms (AAAs) are permanent dilations of the abdominal aorta with greater than 80% mortality after rupture. Currently, there are no proven non-surgical therapeutics to blunt expansion or rupture, which highlights the need to gain mechanistic insights into AAA formation. AAA formation involves a complex process of destruction of aortic media through activation of matrix metalloproteinases (MMPs), loss of smooth muscle cells, degradation of extracellular matrix proteins like elastin and collagen, and inflammation.

Autophagy is a well-conserved cellular process whereby damaged cytoplasmic organelles and long-lived proteins are degraded. Cellular autophagic activity is usually low under normal conditions but can be markedly dysregulated in pathophysiological conditions. Recent human AAA tissue characterization studies showed an accelerated autophagy process in AAAs. However, the functional association of enhanced autophagy in AAA formation and development is unclear.

In this study, utilizing the well-established AngII-induced AAA mouse model, we identified that, similar to human studies, autophagy proteins like Beclin-1 and LC3-II are increased in the abdominal aorta of the AngII-infused hypercholesterolemic male mice. Then, we utilized both pharmacological and genetic approaches to further elucidate the contribution of autophagy in aortic aneurysms. Administration of 3-methyl adenine (3-MA), an autophagy inhibitor did not influence AngII-induced AAA formation. On the other hand, Celastrol, an autophagy inducer compound

failed to influence autophagy proteins in our AngII-induced AAA mouse model. However, for the first time, we demonstrated that Celastrol supplementation, independent of autophagy activation, promoted AngII-induced AAA formation and ablate sexual dimorphism in male and female mice. Accelerated AngII-induced AAA development by Celastrol supplementation was associated with increased MMP activation and aortic medial destruction.

To further investigate the role of autophagy in aortic aneurysm formation, we generated tamoxifen-inducible smooth muscle cell-specific Beclin-1, a key protein involved in autophagy induction, deficient mice either in normolipidemic or hypercholesterolemic (LDL receptor-deficient) backgrounds. Using this unique mouse model, we demonstrated that, Beclin-1 deficiency in SMCs accelerated ascending and abdominal aortic expansion independent of AngII. Beclin-1 deficiency exacerbated aortic medial elastin fiber destruction, loss of medial SMCs, and collagen deposition in the adventitial layer. In summary, our findings suggested that Beclin-1, an essential autophagic protein, plays a critical role in the maintenance of aortic structural integrity during AAA formation and development.

Aida Javidan

Name of Student

11/29/2022

Date

ROLE OF AUTOPHAGY IN AORTIC ANEURYSMS

By

Aida Javidan

Dr. Venkateswaran Subramanian
_____
Director of Dissertation

Dr. Howard Glauert
_____
Director of Graduate Studies

11/29/2022
_____
Date

In dedication to my mentor, my loving family and friends, and my husband who

had been a constant source of support and encouragement

ACKNOWLEDGMENTS

First and foremost, I'm extremely grateful to my mentor, Dr. Subramanian whose words of encouragement and push for courage taught me to work hard for the things I aspire to achieve. Without his guidance and persistence help, this dissertation would not have been possible. An immense thank you to the current and previous members of the lab team: Weihua Jiang, Lihua Yang, Dr. Michi Okuyama, and Dr. Devi Thiagarajan. Support and help from you all throughout the project were invaluable.

I would like to express gratitude to my advisory committee: Dr. Alan Daugherty, Dr. Ming Gong, Dr. Sidney Whiteheart, and Dr. Qingjun Wang for their insightful comments which were really influential in shaping my experiment and critiquing my results.

Thanks to everyone in Dr. Alan Daugherty's lab for being supportive and available all the time to help me with my projects. I am extremely thankful to Michael Franklin, Deborah Howatt, Jessica Moorleghen, Dr. Hisashi Sawada, and Dr. Hong Lu. Your knowledge, advice, and plentiful experience were great support in my academic research.

My appreciation also goes out to my family and friends for their encouragement and support all through my studies.

From the bottom of my heart, I would like to say a big thank you to my husband, Shayan. Without his tremendous understanding and encouragement in the past few years, it would be impossible for me to complete my study. I am truly thankful for having you in my life.

TABLE OF CONTENTS

LIST OF TABLES

LIST OF FIGURES

CHAPTER 1

Introduction

1.1. Definition to Aortic Aneurysms

Aortic aneurysm is defined as an abnormal and permanent dilation of the aorta. It occurs at any region along the aorta which includes ascending aorta, arch, descending aorta or in abdominal aorta at infrarenal region [1]. The two most common form of aortic aneurysms that are characterized by their different anatomical locations and distinct aetiologias are abdominal aortic aneurysms (AAA) and thoracic aortic aneurysms (TAA).

1.2. Abdominal Aortic Aneurysm

Abdominal Aortic Aneurysm (AAA) which is defined as permanent dilation of abdominal aorta, is one of the most common forms of the aortic aneurysms [2]. AAAs are the cause of more than 175,000 deaths worldwide and the mortality rate associated with aortic rupture is between 60%-80%[3]. AAA is normally happening when the maximal abdominal aortic diameter reaches >50% of the normal diameter and remains asymptomatic until the rupture occurs[3]. Given that, there is not adequate knowledge about underlying mechanisms of AAA development, so far there are no pharmacologic treatments available to prevent AAA expansion and rupture[4]. Currently, open, or endovascular surgical repair of damaged aorta after detection by ultrasound screening is the only available treatment to prevent AAA rupture[5].

1.2.1. Risk Factors

Based on epidemiological screening studies, AAAs are associated with the age, male gender, family history and lifestyle-related risk factors, such as smoking, obesity, hyperlipidemia, and atherosclerosis.[6-8]. The risk of AAA development is known to increase with aging in both genders[9]. The onset of AAA formation significantly increases in men after the age of 60[10]. The prevalence of AAAs is 4–5 times greater in males than females and females seem to be protected from developing AAAs[10, 11]. However, females develop AAAs with higher rate of rupture at smaller size. Family history is also an important risk factor for AAA with about 1–29% prevalence of AAA is among first degree relatives[6]. Familial cases of AAA seem to occur at a younger age and have higher rates of rupture[12]. Smoking is associated with higher rates of aneurysm growth and rupture both in previous and current smokers. Data from the NAAASP screening database published by Ruth A Benson in 2016 revealed a positive smoking history in 90% of patients with diagnosed AAAs[13]. Like other lifestyle risk factors obesity is associated with higher rate of AAAs[14]. Growing evidence showing that high plasma cholesterol concentrations have been associated with an increased risk of AAA development[15]. There are some case-control studies reported that individuals with AAAs have modest elevation of total cholesterol concentrations in fasting lipids compared to normal individuals. However, there are other studies have shown that there is no association between hypercholesterolemia and AAA formation[8, 16].

1.2.2. Pathological events in AAA

The pathologic characteristics of AAA includes an intense inflammatory cell infiltration to the aortic wall, degradation of extracellular matrix proteins like elastin and collagen and depletion of medial smooth muscle cells due to apoptosis and senescence [17], and endothelial dysfunction and death[18].

Pronounced inflammatory infiltration of leukocytes into the aortic wall is one of the primary features in the AAAs. Macrophages are the predominant inflammatory cell types in AAA tissues. Evidence showing that macrophages actively contribute to the AAA developments. MCP-1 receptor, C-C chemokine receptor type 2 (CCR2), that controls the recruitment of monocyte to the site of inflammation and Myeloid differentiation factor 88 (My88), a mediator of signaling cascades that it's stimulation directly promotes leukocyte recruitment to the aortic wall are crucial for macrophage mediated response to inflammation. Deficiency of these two proteins in AngII-induced AAA and calcium-Chloride induced AAA models could attenuate AAA formation[19-22]. Despite the current evidence of the critical role of macrophages in AAA formation, their contribution to the disease needs to be more elucidated.

Infiltration of these inflammatory cells is stimulated by secretion of specific chemokines and cytokines. chemokines like MCP-1 and cytokines such as IL-1β, IL-6, IL-17, IL-23 and TNF-α are upregulated in aneurysmal tissue[23-25]. Among the interleukins, genetic or pharmacological inhibition of IL-1β have been shown to prevent elastase-induced AAA formation[26]. Another cytokine which is elevated

3

in AAAs is transforming growth factor (TGF)-β. Systematic inhibition of this cytokine resulted in AngII-induced AAA augmentation [27, 28]

Elastin and Collagen are the most predominant proteins with extremely long half-lives in extracellular matrix of the aortic wall. They are responsible for compliance and tensile strength of the aortic wall[29]. Degradation of these two proteins in the media layer result in weakening of the aortic wall and dilation of the aortic lumen[30]. A wide variety of proteases like matrix metalloproteinases (MMP), serine proteases and cysteine proteases and are upregulated in AAA developments which lead to the destruction of the extracellular matrix [24, 31, 32]. In response to local inflammatory cytokine production, macrophages, and smooth muscle cells (SMCs) are the two main sources of proteases[33]. The major classes and the most studied proteases are matrix metalloproteinases (MMPs)[34]. Among them MMP-2, MMP-9, and MMP-12 have the highest affinity for elastin as substrate[31, 32, 35]. Elevated concentrations of MMP-9 have been demonstrated in the plasma of individuals afflicted with AAA[31]. Experimental studies demonstrated that deletion of MMP-9 in elastase infused model results in reduction AAA formation whereas lack of MMP-12 in the same model had no impact on the development of the disease[36]. There are no specific pharmacologic inhibitors for MMPs. Doxycycline is one of those nonselective inhibitors that has been used in AAA studies to reduce the MMPs activities [37]. Pre-administration of Doxycycline into AngII-infused hypercholesterolemic mice attenuates the AAA formation[37].

Another hall mark of AAA is smooth muscle cell (SMC) apoptosis and senescence. Vascular SMCs are the predominant cell type in the medial layer of the aortic

wall[38]. SMCs produce elastin, collagen, and other matrix proteins and thereby contribute to the elastic lamellar architecture of the arterial wall [39]. So, decrease in vascular SMC density by apoptosis weakens the aortic wall that leads to aortic wall destruction and aneurysm formation[3, 40]. P53 which is a marker for cell death and its transcriptional target p21, a cyclin-dependent kinase inhibitor, have shown to be upregulated in AAA tissues[39, 41, 42].

On the other hand, SMC senescence which is defined as a cell cycle and growth arrest mechanism in response to the stress conditions, is observed in aneurysmal tissue[42-44]. In vitro studies demonstrated that aneurysm-derived SMC in culture exhibit a limited growth capacity compared to SMC derived from normal aortas[45]. Moreover, vascular SMCs can undergo phenotypic changes in response to vascular injury in both preclinical animal models and human subjects [46]. This phenotype switching is defined as transition from contractile phenotype to a synthetic phenotype[47]. SMC phenotypic switching is characterized by markedly reduced expression of SMC-selective differentiation marker genes like smooth muscle 22alpha (SM22alpha) and alpha smooth muscle actin (αSMA)[3] and increased SMC proliferation, migration with increased MMP-2, MMP-3, and MMP-9 expression [40, 48, 49]. Sustained phenotypic alterations affecting the growth capacity of vascular SMC, possibly reflecting accelerated cellular senescence and an increased susceptibility to apoptosis[47].

Recent evidence suggested that autophagy plays a pivotal role in cardiovascular diseases by regulating SMCs homeostasis [50, 51]. Basal autophagic activity is critical to maintain cell homeostasis and it is considered as a cytoprotective

mechanism to preserve vascular cell functions. Accumulating evidence suggests that autophagy is activated in VSMCs in response to various stimuli including lipids, reactive oxygen species, cytokines, and growth factors and may act as an important mechanism for VSMC survival[52, 53]. But it's functional contribution to AAA development is still unclear.

Reactive Oxygen Species (ROS) play a central role in the development of AAA. Elevated ROS level can affect MMPs activation, pro-inflammatory genes induction and VSMC apoptosis which are the key pathological features of AAA[54, 55]. Different cell types include macrophages, vascular SMC, endothelial cells, and fibroblasts which are contributes to the pathogenesis of AAAs are the main source of ROS[55, 56]. NAPDH oxidative activity and superoxide production have been shown to be elevated in human aneurysmal tissue and inhibition of NAPDH by either pharmacological or genetic methods resulted in attenuation of AAA formation[57].

1.2.3. Mouse models of AAA

The aneurysmal tissue that is normally acquired from the patients during surgical repair to study human AAA, is only a representation of the advanced stages of the disease and provides limited insight into the underlying mechanisms which are involved in the initiation or early stages of disease formation.

To gain mechanistic insight into AAA development, in the last three decades, several experimental mouse models have been generated to study AAAs. These models successfully mimic the cellular and biochemical characteristics of human

AAAs and help us to understand the molecular mechanisms involved in the initiation, progression, and rupture of AAA.

There are multiple methods to induce AAAs in mice including genetic manipulation, oral or sub-cutaneous or intraluminal infusion of different chemical agents. These chemical approaches include the intraluminal infusion of elastase, periaortic incubations of calcium chloride, subcutaneous infusion of AngII, administration of β-aminopropionitrile (BAPN; a lysyl oxidase inhibitor), and subcutaneous implant of Deoxycorticosterone acetate (DOCA) pellet and aldosterone pump in conjunction with high salt water [58-60]. Subcutaneous infusion of AngII by osmotic mini-pumps for a period of 28 days into either LDL receptor-/- or apoE -/- mice leads to AAA formation in the suprarenal region of the aorta [61, 62]. The AngII-induced AAA mouse model mimics most of the characteristics observed in human AAA [63]. The characteristic features of AngII-induced AAA are pronounced leukocyte infiltration of macrophages and immune cells to the aortic wall, early medial disruption, elastin degradation with the presence of matrix metalloproteinases (MMPs)[64, 65], and luminal dilation[66], and subsequent dissection observed by 3 to 10 days after AngII infusion[65, 67]. Like human, male mice are more susceptible than female mice to aneurysm induction by Angiotensin II infusion[11, 68].

The short periaortic incubation of elastase solution in the infrarenal region of the mouse aorta causes extensive elastin destruction and infiltration of leukocytes, predominantly macrophages to the adventitial layer which is followed by immediate dilation of the aorta and an aneurysm formation in 2 to 5 days[69].

7

Application of Calcium chloride ($CaCl_2$) to the adventitia of the infra-renal region is another method for AAA induction[70]. $CaCl_2$led to increases of aortic diameter in the range of 48% to 110% after 2 weeks. Histological analysis of this model demonstrates inflammatory cell infiltration, disruption of the medial layer, and vascular wall thickening.

Administration of β-aminopropionitrile or BAPN (Lysyl oxidase inhibitor) to mice blocks elastin and collagen crosslinking and therefore reduces matrix stability. Adding BAPN into the drinking water in combination with AngII infusion increases the rate of AAA formation and aortic dissection in normolipidemic mice.

DOCA salt mouse model was first developed to study hypertension. But later it was found to be able to induce AAA formation in older mice. Subcutaneous implant of a 50 mg Deoxycorticosterone acetate (DOCA) pellet, a mineralocorticoid agonist, or an osmotic pump containing 200ng/kg/min of aldosterone in conjunction with water containing 0.9% NaCl and 0.2% KCl for 21 days leads to dilation of the aorta in the suprarenal aorta. High salt is very critical in this mouse model and it is required for developing AAs [71] [72, 73]

1.2.4. Current Treatments

Most AAAs are asymptomatic until rupture. Although some of AAAs can be identified during evaluation for abdominal symptoms like pain and tenderness on palpation, most frequently AAAs are detected as an incidental finding during ultrasonography, CT, or magnetic resonance imaging for other purposes.

The current clinical approach to individuals diagnosed with AAAs is to monitor aortic diameter until it reaches sufficient expansion, prompting it to a possibility of rupture and perform the open or endovascular surgical repair[59].

For several decades open surgical repairs were considered standard care for all AAAs. However, trials have identified shortcomings in this form of intervention [74]. There are several risks associated with open surgery. Cardiac complications as the most common morbidity, with an incidence between 2% and 6%, renal failure, and ischemic colitis are the common complications that occur in patients undergoing open surgery.

Endovascular repair (EVAR) is another option of surgical repair that was introduced in early 1990. It includes insertion of an endograft into the lumen that effectively excludes the aneurysm from blood flow, minimizing the risk of rupture. Compared to open surgery, EVAR is a less invasive alternative with a lower postoperative complication [59, 74].

Along with surgical repairs for individuals diagnosed with AAAs, there are some ongoing clinical drug trials to develop medical therapies as an alternative to surgery which is costly and associated with morbidity and mortality. However medical therapy may be helpful only in patients with small-sized aneurysms and not in the individuals who undergo the surgery.

Currently, there are no proven non-surgical therapeutics to blunt AAA progression and rupture which highlights the need to gain mechanistic insights into AAA formation. So, understanding the underlying mechanisms involved in the initiation and progression of AAAs is necessary to develop effective therapies.

1.3. Thoracic Aortic Aneurysm (TAA)

Another form of aortic aneurysm which is less common than AAA is thoracic aortic aneurysm (TAA)[75]. Thoracic aortic aneurysm is considered as a serious medical condition caused by the weakening of the thoracic aortic wall[76]. It may involve one or more aortic segments including aortic root and/or ascending aorta by 60%, aortic arch by 10%, and descending aorta by 40%[77]

The incidence of thoracic aortic aneurysms (TAA) is approximately 9–16 per 100,000 people per year and is associated with significant morbidity and mortality due to the asymptomatic nature of the disease and minimal available therapeutic interventions[78] [76].

Aortic dilation and medial remodeling are two hallmarks of TAA. Like AAA, pathophysiological features of TAA are described as vascular SMC loss, fragmentation of elastin fibers, inflammatory infiltration to the aortic wall, and upregulation of matrix metalloproteinases[5, 79, 80] The underlying molecular mechanism of TAA is not well understood. So therapeutic options are limited to surgical interventions that replace the aneurysmal aorta with an artificial graft either by open surgery or by thoracic endovascular aortic repair (TEVAR). TAAs can be syndromic which happens in less than 30% of cases or sporadic which includes 70% of TAA cases[79]. Growing evidence suggests that mutations in genes encoding the proteins that have a crucial role in controlling the structural and functional properties of the elastin-contractile unit result in syndromic TAAs. Loeys-Dietz syndrome (LDS) is the most recent syndrome discovered in 2005 by Loeys

et al. in LDS, mutations happen in the transforming growth factor receptor 1 and 2 (TGFR1 and TFGR2)[75, 81].

Another syndromic TAA which is the most common genetic syndrome is Marfan syndrome (MFS). It was first described in 1896 and later in 1936 found to be a heritable autosomal-dominant disorder [79]. Marfan syndrome happens in approximately four to six people per every 100,000 and is caused by mutations in one of the genes that encode fibrilin1(FBRN1). Mutation in FBRN1 results in a decrease in the number of elastin fibers, SMC dysfunction, and alteration in TGF-Beta-related signaling pathways which lead to aortic destruction[75, 76].

Sporadic or familial TAAs are more common than syndromic TAA. Sporadic TAA occurs more frequently in men than in females and it is observed more in the younger patient population. Familial TAA and AAA share similarities in risk factors and pathogenesis. Sporadic TAA risk factors include age, sex, hypertension, cigarette smoking, inflammatory diseases, and atherosclerosis [79, 80]. Like AAA, the key features of TAA are SMC depletion, medial elastin degradation with less inflammatory cell infiltration compared to AAA[79].

1.4. An Overview on Autophagy

Autophagy is a complex intracellular process that is essential for cellular homeostasis and stress adaption. This catabolic process is responsible for degrading long-lived or misfolded proteins and damaged organelles to recycle back for biosynthetic processes to maintain cellular homeostasis[82]. There are three types of autophagy include: macroautophagy, herein referred to as

autophagy, microautophagy and chaperone mediated autophagy [83]. Macroautophagy is the most studied autophagic pathway. It is involved in the degradation of whole organelles through an autophagosome in a generalized fashion. On the other hand, microautophagy is referred to an autophagic pathway in that engulfment of cytoplasm directly happens through inward invagination of the lysosomal membrane. Chaperone-mediated autophagy (CMA) is a selective form of autophagy in which, the cytoplasmic proteins translocate across the lysosomal membrane while they are in a complex with chaperone proteins that are recognized by the lysosomal membrane receptor called LAMP.

Autophagy is dynamically regulated. Autophagic activity is usually low under basal conditions, but it can be upregulated in response to several stimuli[83, 84]. The most well-known inducer of cellular autophagy is nutrient starvation [84, 85].Besides starvation, there are other biological stress stimuli including hypoxia, cell injuries, hormonal stimulation, and pharmacological agents that can enhance autophagy activity as well.

1.4.1. The Core Machinery of Autophagy

In general autophagy pathways includes four sequential steps: initiation, elongation, fusion, and degradation[84]. The process of autophagy begins with an expansion of the membrane called the isolation membrane or phagophore. Phagophore then gradually expands and encloses a portion of cytoplasm which result in the formation of a double membrane sequestering vesicle called autophagosome. In mammalian systems, autophagosomes begin to form at multiple sites in the cytoplasm. Although the source of the membrane that makes

12

up the phagophore is highly debated, based on the evidence, it could originate from the cell membrane, golgi complex, endoplasmic reticulum, or mitochondria[82]. Autophagosomes subsequently fuse with lysosomes to form an autolysosome. The fusion process initiates with releasing the enclosed cargo in the autophagosome to the lysosomal lumen. Along with cargo, the inner membrane of doubled membrane autophagosome is degraded by lysosomal enzymes resulting in releasing macromolecules into the cytoplasm for recycling to maintain cellular homeostasis. The autophagy machinery includes a series of autophagy related (ATG) proteins that participate in the induction and progression of the autophagy process[83, 86]. There are two major complexes that are involved in initiation of autophagy process, the PI3K III/Beclin-1 nucleation complex and the ATG1/ULK1. These two complexes facilitate recruitment and regulation of autophagy proteins during phagophore formation. Mammalian target of rapamycin (mTOR) and AMP-activated protein kinase (AMPK) are the most important autophagy regulators. Under nutrient-rich condition, activated mTOR inhibits ATG1/ULK1 from initiation of recruitment of autophagy-essential proteins for phagophore formation. On the other hand, when cellular energy level is low (increased intracellular AMP: ATP ratio), AMPK is activated and phosphorylates ULK1 to activate the autophagy[84]. In the next step of autophagy process, which is called elongation, two ubiquitin-like reactions are involved. First, the ubiquitin-like protein Atg12 is covalently tagged to Atg5. Atg7 an E1 ubiquitin activating enzyme-like protein is required for this reaction. ATG5-ATG12 then conjugated to ATG16 via E2-like ubiquitination enzyme ATG10 to form the ATG5-ATG12-ATG16

complex. Secondly, pro-LC3 is cleaved by ATG4 to form LC3-I. Cytosolic LC3-I is then conjugated to phosphatidylethanolamine (PE-lipid conjugation) by ATG7 to form autophagosome membrane associated LC3-II. Unlike the ATG5-ATG12-ATG16 complex that leaves the autophagosome, LC3-II remains on completed autophagosomes until fusion with the lysosomes. This feature of LC3-II makes it an excellent marker for autophagosome[84]. Fusion to the lysosome is the last step in the autophagy pathway. The completed autophagosome fuses with the lysosome to form an autolysosome. Lysosomal hydrolases can lyse the autophagosome inner membrane and breakdown of the cargo contents[82, 86].

1.4.2. Role of Autophagy in Aortic Aneurysms

Patients with AAA were found to have upregulation of several autophagy-related genes such as LC3, beclin-1, BNIP-1 and VPS-34 in aneurysmal tissue. On the other hand, gene expression profile of peripheral blood in AAA patients showing that ATG5, an autophagy related protein is upregulated compared to the healthy patients [87, 88] . Ramadan et al. extensively reviewed the potential mechanisms by which vascular cells autophagy modulate AAA[89]. In AngII-induced AA model, loss of autophagy in VSMCs through deletion of autophagy protein 5 gene (Atg5) increases the susceptibility of VSMCs to death[90]. Like AAAs, autophagy is also upregulated in cardiac hypertrophy and expression of Atg5, has been shown to be necessary for regression of Angiotensin II- or pressure overload-induced cardiac hypertrophy[91]. Moreover, deficiency in ATG7, which is an essential gene for autophagy, resulted in plaque instability and the risk of plaque rapture in experimental mouse models[92]. Even though autophagy-related genes are

upregulated in AA tissues, it is still unclear whether autophagy acts as a pro-survival or anti-survival mechanism in aortic aneurysm pathogenesis.

CHAPTER 2

Materials and Methods

2.1. Animals

Age-matched (8-12 weeks old) male and female LDL receptor deficient mice (LDLr-/-) (colony bred from original stock from The Jackson Laboratory; stock # 002207; backcrossed to a C57Bl/6N mice; B6NTac; Taconic Biosciences) were used in Celastrol Studies). LDL receptor genotyping was performed as described previously[93]. Mice with inducible deletion of Beclin-1 in SMCs were produced by breeding male mice hemizygous for Acta2-CreERT2 (Cre+) to female Beclin-1 floxed mice (obtained from Dr. Edmund B Rucker 3rd) in an LDLR -/- background. At 8 weeks of age, male Beclin-1 x Acta2-CreERT2 (Cre+) and non-Cre littermates (Cre-) mice were injected with tamoxifen (75 mg/kg, i.p.) for 5 consecutive days.

2.2. Angiotensin II infusion

All mice were anesthetized with isoflurane at a concentration of 2% in oxygen for subcutaneous osmotic mini-pump implantation. Mice were infused with either saline or AngII (0.5 or 1.0 µg/kg/min, Bachem, Torrance, CA) for 7 days, 14 days, and 28 days by Alzet osmotic minipumps (Model 2004 for males and 1004 for females, Durect Corporation, Cupertino, CA) as described previously.[93]

2.3. Celastrol Diet

Mice were fed a saturated fat-enriched diet (21%wt/wt milk fat; TD.170793, Envigo, Madison, WI) supplemented with or without Celastrol (10mg/kg/day, BOC Science, NY) for five weeks. Celastrol was added to the high fat diet in the ratio of 80 ppm and the dose was calculated based on the average diet consumption per day.

2.4. Blood pressure Measurements

 Systolic blood pressure (SBP) was measured on conscious mice by using a computerized tail-cuff blood pressure system (Kent Scientific Corp, Torrington, CT). Mice were placed on the warming platform. Twenty cycles of blood pressure were measured for each mouse. SBP was measured on 3 consecutive days prior to pump implantation and in the final week of AngII infusion. Measurements <50 mmHg and >220 mmHg were excluded.

2.5. 3-Methyladenine (3-MA) administration

Autophagy inhibitor, 3-MA (M9281; Sigma-Aldrich) dissolved in PBS. Mice were orally gavaged with 3-MA at the dose of 30 mg/kg/day) using a 22-gauge gavage needle in a fluid volume of 100 µl once daily for 35 days.

2.6. Total Cholesterol Measurement

Blood was collected by cardiac puncture in tubes containing EDTA (0.2 mol/L), centrifuged at 2,000 rpm for 20 min (4ºC) and plasma was stored at -80°C. Total plasma cholesterol concentrations were measured using enzymatic assay kit (Pointe Scientific Kit) according to the manufacturer's instruction.

2.7. Quantification of AAAs by ultrasound and ex-vivo measurements

Internal suprarenal lumen diameter was measured on days 0, 14, 28 in Saline or AngII infused mice by using a high frequency ultrasound imaging system (Vevo 2100, Visual Sonics, Toronto, Canada) using a MS550 MicroScanTM transducer. Mice were anesthetized and restrained in a supine position to acquire ultrasonic images. Short axis scans of abdominal aortas were performed from the left renal arterial branch level to the suprarenal region. For measuring external aortic width, dissected aorta stored in 10% formalin for 48 hours. Once fixed, aortas were put in saline buffer for a few hours before the cleaning procedure. Formalin fixed aorta were cleaned and pinned on black wax. Images were taken using a Nikon dissecting microscope. Mice with a 50% increase in abdominal aortic lumen compared to baseline were considered with an AAA. Image analysis to measure maximal aortic width was performed by using Nikon elements. AAA incidence was defined as a 50% increase of abdominal aortic width after 28 days of AngII infusion including mice that died of aortic rupture during the study.

2.8. Quantification of TAA (In Situ measurement)

For TAA measurement, formalin fixed ascending aortic images were captured using Nikon Imaging system. Using the polyline tool available in the Nikon Imaging software, a line created in the middle of the aorta that extends from where the aorta is attached to the heart to the 1 mm below the left subclavian artery. Then, by using parallel line tool, a line was created 0.5 mm from the innominate artery extending into the ascending aorta. Using the simple line tool six lines were created perpendicular to the middle line that extend from one edge to other edge of the

aorta to measure the aortic width at the ascending, arch and descending thoracic aorta.

2.9. Enface Measurements

At the study endpoint, formalin-fixed aorta were cleaned and cut into thoracic part including ascending and arch area and abdominal part. Thoracic part was cut open from the outer curvature through the innominate artery then the left common carotid artery, and then to the left subclavian artery. The aorta was pinned on black wax and the pictures of en face aortas were taken with Nikon camera. Measurements included ascending and arch region to 3 mm above the celiac artery. Atherosclerosis was quantified on aortic arches as lesion area, and percent lesion area on the intimal surface by *en face* analysis as described previously. [94] Lesion areas were measured using Image-Pro Plus software (MediaCybernetics, Bethesda, MD) by direct visualization of lesions under a dissecting microscope.

2.10. Immunohistochemistry and histology

For immunohistochemistry and histology studies, the suprarenal aorta was fixed first by keeping sample in 70% alcohol and then in 5% formaldehyde for 24 hours, followed by paraffin embedding. The embedded tissue cut in series (10 slides and 2 sections on each slide per mice) with the thickness of 5 µm. Samples were deparaffinized by heating at 60°C for 10 min, this was followed by a series of incubation of hydration: Xylene for 10 min, Xylene 1:1 with 100% ethanol for 6 min, 100% ethanol for 5 min, 95% ethanol for 3 min, 70% ethanol 3 min, 50% ethanol

19

for 3 min, 25% ethanol for 1 min and water for 1 min. For immunohistochemistry purposes, after deparaffinization, antigen retrieval was performed on samples.

For Verhoeff's elastin staining, the samples stained with Verhoeff's iron hematoxylin (5% hematoxylin in absolute alcohol, 10% Ferric chloride, Verhoeff's iodine) for 20 min. It was followed by 3 times of rinsing with water and differentiation in 2% ferric chloride for 1 to 3 min. Next, samples were rinsed in water for 3 times and dehydrated in 95% ethanol and 100% ethanol for 30 sec and mounted.

For Picro Sirius Red staining (ScyTek PSR kit), deparaffinized sections were hydrated in distilled water and immersed in Picro Sirius Red solution and stained for 60 min at room temperature. Then, sections were rinsed quickly in 2 changes of acetic acid solution. It was followed by dehydration in 2 changes of absolute alcohol. Slides were mounted using resinous mounting medium.

For α-SMC staining, sections were deparaffinized, rehydrated, and treated with antigen unmasking solution for 20 min in 95-100°C to reveal the antigen. Sections were incubated with 0.5% Triton X-100 for 10 min in 40°C. It was followed by incubation with Redusol and hydrogen peroxide for 2 min and washing with automation buffer between each step. After blocking endogenous background with Avidin/Biotin blocking kit (Vector/Laboratories) and non-specific binding (normal goat serum, Vectastain ABC Kit), slides were incubated with the α-SMC primary antibodies (Abcam, catalog No: ab5694) for 30 min at 40°C. Slides were then incubated with biotinylated secondary antibody for another 30 min at 40°C. This incubation was followed by signaling detection VECTASTAIN Elite ABC system

(Vector Laboratories) for 10 mi. Then, samples counterstained with hematoxylin for 10 seconds and mounted with glycine.

2.11. Quantification of elastin fragmentation

Fragmentation is defined as the presence of free ends for elastin layers in aortic media layer. Verhoeff's elastin-stained aortic section images were taken using 20 and 40X Nikon objective lens. Each group includes three mice and for each mouse, 2-3 slides with 2 sections per slide were measured for elastin breaks.

2.12. Quantification of α-SMCs positive Area

Pictures were taken using Axioscan 7 using 10X objective lens. By using NIS elements Analysis software, region of interest (ROI) was defined in each section. The threshold was defined in one section and used as a reference for the rest of the samples. To quantify the α-SMCs positive area, the proportion of binary area (μm^2) to ROI area (μm^2) was calculated. Each group includes three mice and for each mouse, 2-3 slides with 2 sections per slide were measured for elastin breaks.

2.13. Gel zymography

Male and female mice (n=3-5 mice/group) were infused with saline or AngII (500 and 1000 ng/kg/day) for 14 days. Aortic protein (10 µg) was extracted from abdominal aorta and resolved by using SDS-PAGE (7.5%) in the presence of gelatin (20 mg/mL) to detect matrix metalloproteinase (MMP) activity. Gels were washed with 2.5% Triton X-100 (1 hr) followed by distilled water (30 min) and incubated overnight (37°C) in Tris buffer containing 5 mM calcium chloride. Gels were stained with Brilliant Blue for 30 min and destained using destain solution

21

(1X). Gel images were captured by using Chemi.Doc Imager (Comerssie Blue Gel Mode); the unstained regions represented areas of matrix metalloproteinases (MMPs) activity.

2.14. Western blotting

Protein was extracted from frozen aortic samples in RIPA buffer (Sigma) containing a protease inhibitor cocktail (Roche) and quantified with the BCA Protein Assay Reagent (Thermo Scientific). Twenty micrograms of protein were loaded in SDS-polyacrylamide gel and then transferred to nitrocellulose membranes and probed with primary antibodies for ATG7 (abcam, ab207612), Beclin-1(abcam, ab207612), LC3B (MBL, PM036), and β-actin (Sigma-Aldrich, A5441). Following incubation with the appropriate horseradish peroxidase-linked secondary antibodies (Vector Laboratories, Newark, CA), signals were visualized with an enhanced chemiluminescence detection system. The chemiluminescent signal was acquired using a charge-coupled device camera (VersaDoc, Bio-Rad Laboratories, Hercules, CA) and quantified by Image Lab software (Bio-Rad Laboratories).

2.15. Statistics

Data are represented as mean ± SEM. Statistical analyses were performed using SigmaPlot 14.5 (Systat Software Inc). Data were tested for normality and equal variance using the Shapiro-Wilk and Brown-Forsythe test. For two-group comparisons, un-paired Student's t test was performed for normally distributed and equally variant values, while Mann-Whitney Rank Sum test was performed for

variables not passing normality or equal variance test. Two-way repeated ANOVA or two-way ANOVA with Holm-Sidak *post hoc* analyses were performed for multiple-group and multiple-manipulation analysis. The incidence of aneurysm formation and mortality due to rupture was analyzed by using Fisher's exact tests. Repeated measurement data were analyzed with SAS fitting a linear mixed model expressing the temporal trend in systolic blood pressure as a quadratic polynomial in time for each treatment. Values of $P<0.05$ were considered statistically significant.

2.16. Study approval

All study procedures were approved by the University of Kentucky Institutional Animal Care and Use Committee (Protocols 2011-0907 and 2020-3634). This study followed the recommendations of The Guide for the Care and Use of Laboratory Animals (National Institutes of Health).

CHAPTER 3

Results

3.1. Autophagy related proteins increased in AngII-infused aorta

Initially in 2009, Giusti *et al.,* provided a gene expression profile of peripheral blood in AAA patients showing that ATG5, an autophagy related protein is upregulated compared to the healthy patients[88]. Later in 2012, Zheng *et al.,* demonstrated that expression of autophagy-related genes such as Beclin1, Atg4b, VPS34, and protein levels of LC3I/II are upregulated in human aneurysmal tissues[87]. Experimental studies have shown that angiotensin-II (AngII), a primary mediator of adverse vascular remodeling and AAA stimulates autophagic response in cultured aortic SMCs and cardiac tissues[91, 95-98]. Based on the above evidence suggesting an associative link between autophagy and AAAs, we were interested to see whether autophagy markers were influenced in our experimental mouse model of AngII-induced AAA. To address this question, male LDLr$^{-/-}$ mice (8 weeks old) were fed a saturated fat-enriched diet. After 1 week of diet feeding, mice were infused with either saline or high dose of AngII (1.0 µg/kg/min) by osmotic minipumps for 7 days. Western blot analyses of aortic tissue demonstrated a strong increase in autophagy proteins, Beclin-1 **(Figure 1A, B)** and LC3B-II **(Figure 1C, D)** in AngII-infused aorta. Similar to published literature [87, 88], my data data suggested an associative link between autophagy and AngII-induced AAAs. However, it is still unclear whether upregulation of autophagy has a causative role (beneficial or detrimental) in AngII-induced AAA. Therefore, for the next step, we utilized pharmacological approaches to either inhibit or over activate

the autophagy to investigate how autophagy dysregulation could influence AngII-induced AAA formation.
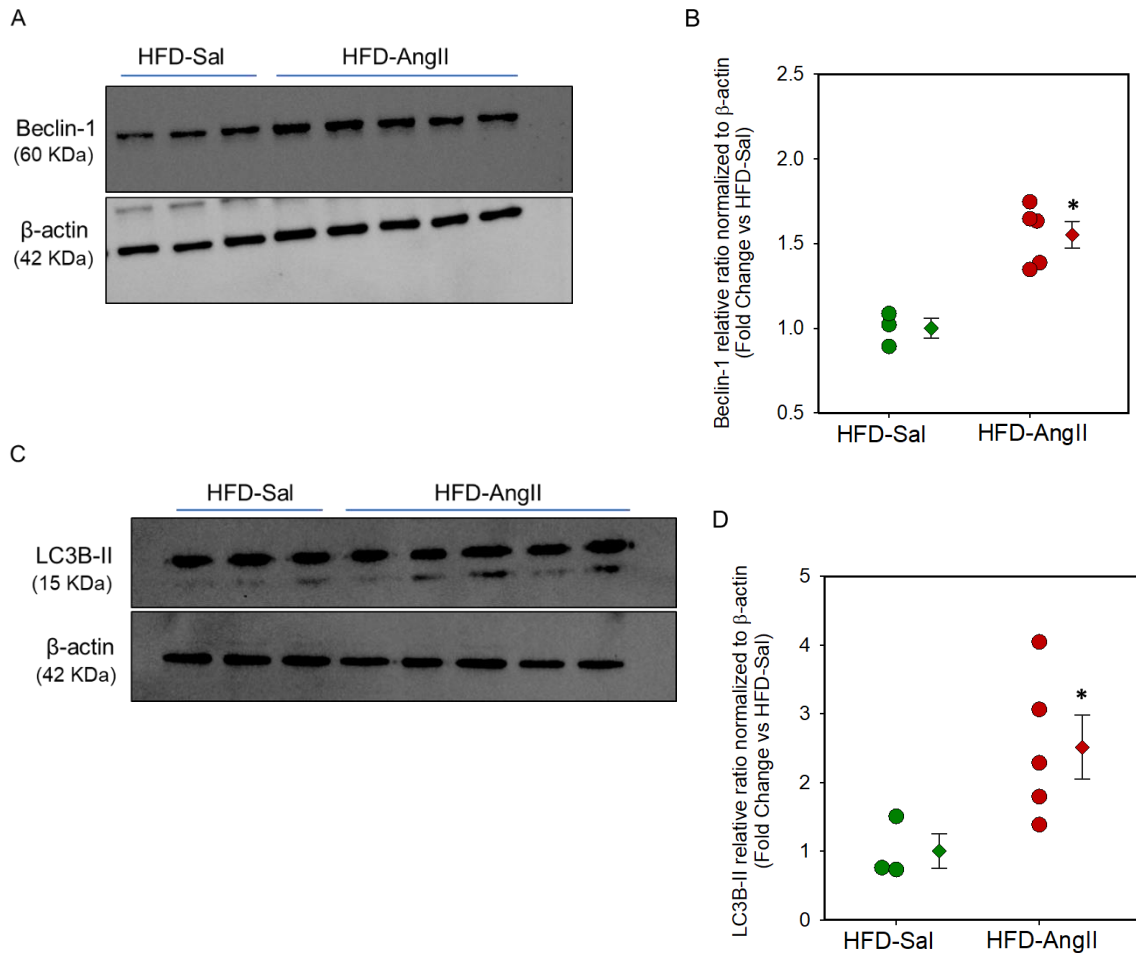
Figure 1. Increased expression of autophagy markers in AngII-infused aorta.

After one week of either Saline or AngII infusion (1.0 μg/kg/min) into male LDLr $^{-/-}$ mice, aortic tissue lysates were collected and western blot analysis was performed. **(A, B)** Protein expression of Beclin-1 in aortic tissue. **(C, D)** Protein expression of LC3B-II in aortic tissue. Circles represent each induvial mouse. Means of each group are represented by triangles and error bars are SEM. Statistical analysis was performed using Two-tailed Student's t-test. * denotes P<0.05.

3.2. Pharmacological loss of function approach: 3-MA administration into AngII-induced AAA mouse model

3-Methyladenine (3-MA), a group of phosphoinositide 3-kinase (PI3K) inhibitors is a widely used inhibitor of autophagy[99, 100]. 3-MA has been proposed to suppress autophagy by inhibiting the class III phosphoinositide 3-kinase (PI3K) to block the production of phosphatidylinositol 3-phosphate (PI3P), which is essential for the initiation of autophagy[99, 101]. In this study we used the 3-MA as inhibitor of autophagy to investigate the potential role of autophagy in AngII-induced AAA formation. High fat diet fed male LDLr$^{-/-}$ mice (10 weeks old) were given either vehicle (water) of 3-MA (30 mg/kg/day), by gavage, starting 1 week prior to AngII infusion. After one week of 3-MA administration, mice were subcutaneously infused with high dose of AngII (1.0 µg/kg/min) by osmotic mini-pump implantation for 28 days. 3-MA administration had no effect on body weight and AngII-induced blood pressure compared to vehicle group **(Table I)**. To track the aneurysm formation, 3-MA and vehicle groups were subjected to ultrasound imaging in vivo at week 0, week 2 and week 4. Although Ultrasonic measurements showed a significant increase in luminal diameter at week 4 in both groups compared to their baseline, the luminal dilation was not different between the groups at week 4 **(Figure 2.1A, B)**. Consistent with ultrasound data, external aortic width measurements did not show any significant differences in AAA formation **(Figure 2.2A, B)** and incidence **(Figure 2.3)** between the groups**.** As a conclusion, administration of 3-MA, under the conditions used, had no influence on AngII-induced AAA development in mice.

27

Table I. Effects of 3-MA administration in male LDL receptor -/- mice infused with AngII

Groups	Vehicle	3-MA
Infusion	AngII (1.0 µg/kg/min)	AngII (1.0 µg/kg/min)
N	10	9
Body Weight (g)	24.3 ± 0.5	24.3 ± 0.3
Systolic BP Pre-Infusion (mmHg)	151 ± 4	154 ± 2*
Systolic BP Post-Infusion (mmHg)	181 ± 4	172 ± 4*

Table I. Values are represented as means ± SEMs. Body weights were determined at termination. Systolic blood pressure was measured prior to (week 0) and during AngII infusion (week 4). Student's t=test was performed to analyze body weight at week 4Two-way repeated measures ANOVA was used to analyze systolic blood pressures. (P=0.69) * Denotes *P*<0.05 systolic BP post-infusion *vs.* pre-infusion, by two-way repeated measures ANOVA.
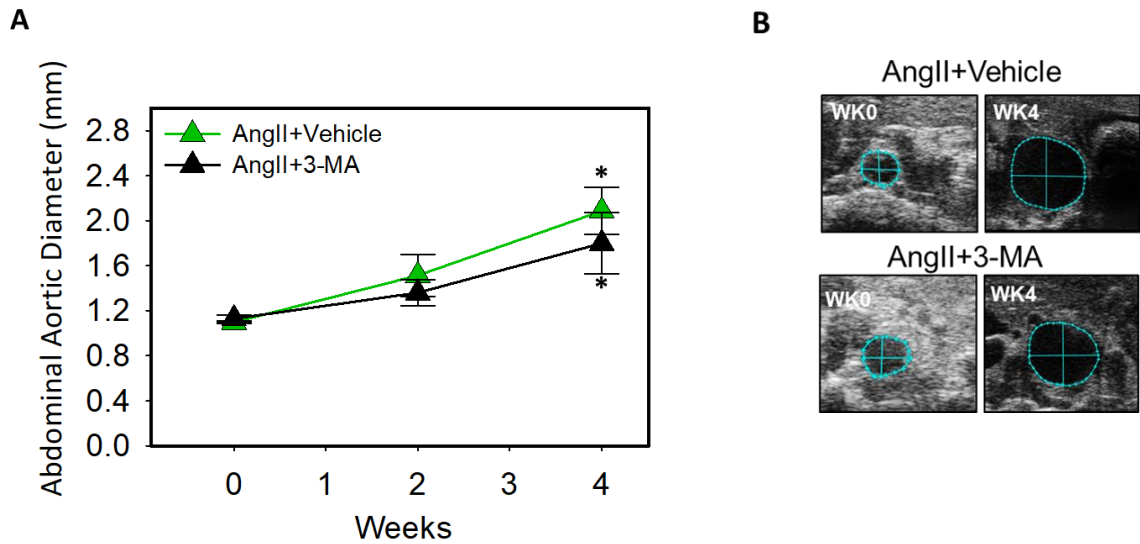
Figure 2.1. 3-MA administration had no effect on abdominal aortic luminal diameter in AngII-infused hypercholesterolemic male mice. (A) The maximal luminal diameter of suprarenal aorta at three different time points during 28 days of AngII infusion (1.0 µg/kg/min) +/- 3-MA. **(B)** Representative ultrasound images of the abdominal aorta. Means of each group are represented by triangles and error bars are SEM Statistical analysis was performed using Two-tailed Student's t-test. * denotes $P<0.001$ when comparing week4 *vs.* week0.
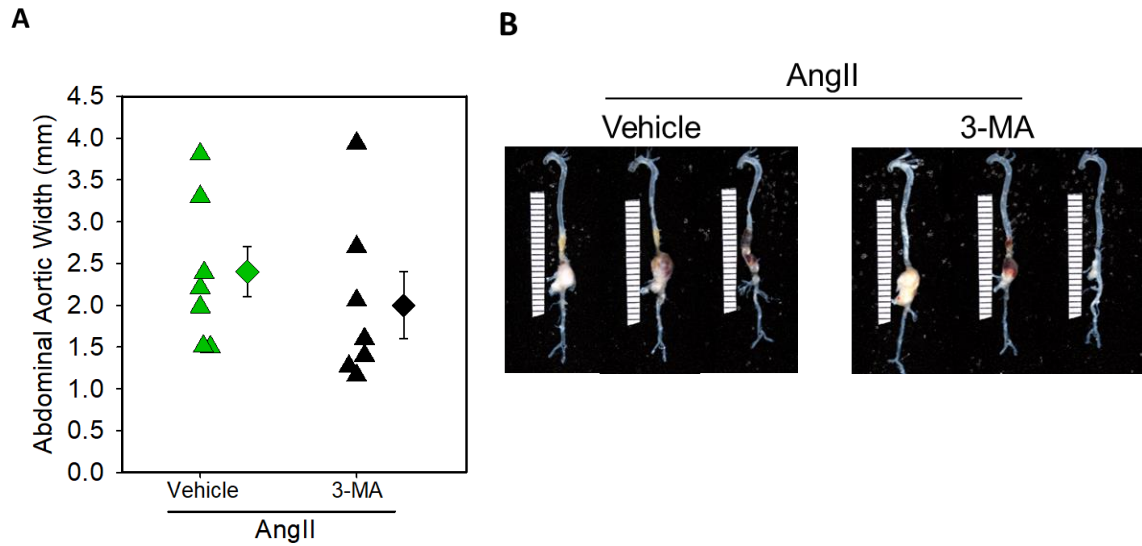
Figure 2.2. 3-MA administration did not affect AngII-induced AAA formation.

(A) Measurements of maximal external width of abdominal aortas after 28 days of AngII infusion (1.0 µg/kg/min) +/- 3-MA administration. **(B)** Representative images of the aortas. Triangles represent individual mice, diamonds represent means and error bars are SEM. Statistical analyses were performed using Two-tailed Student's t-test (P=0.383)
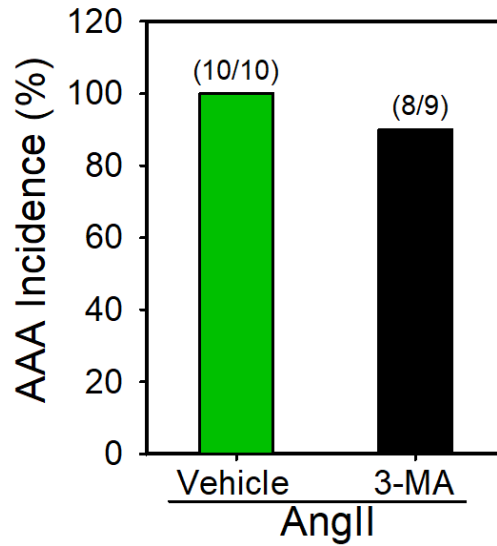
Figure 2.3. 3-MA administration had no effect on AngII-induced AAA incidence. The incidence of AAA (>50% increase in aortic width and ruptured aorta) in AngII-infused mice with or without 3-MA administration. Statistical analyses were performed by Fisher's Exact test.

3.3. Pharmacological gain of function approach: Effect of Celastrol, an autophagy inducer, on AngII-induced AAA formation in hypercholesterolemic male mice

Along with performing an inhibition strategy to reduce autophagic activity in mice, we used another pharmacological approach to induce autophagy to investigate the effect of autophagy activation on AngII-induced AAA development.

Celastrol is a pentacyclic triterpene from the root extracts of Thunder God Vine (*Tripterygium wilfordii*) [102] [103]. Recently, emerging reports suggest the involvement of Celastrol in restoring autophagy level by upregulating of autophagy related proteins like LC3B and Beclin1[104, 105]. Here, we utilized Celastrol as an autophagy inducer to examine whether upregulation of autophagy influence AngII-induced AAA in mice.

To evaluate the effect of Celastrol supplementation on AngII-induced AAA formation in hypercholesterolemic mice, we initiated a pilot study utilizing male LDLR$^{-/-}$ mice (8 weeks old; n=12 per group). In this study, mice were fed a saturated fat-enriched diet supplemented with or without Celastrol (10 mg/kg/day) for five weeks. After one week of the diet, mice were infused with a high dose of AngII (1.0 µg/kg/min) for 28 days via osmotic mini-pump and sacrificed at day 28 for AAA assessments.

3.4. Celastrol supplementation affected body weight and AngII-induced blood pressure in male LDLR$^{-/-}$ mice

Celastrol supplementation significantly decreased high fat diet-induced body weight gain and AngII-induced blood pressure compared to control group **(Table II)**. However, Celastrol supplementation had no effect on total plasma cholesterol concentrations **(Table II).**

3.5. Celastrol supplementation accelerated aortic luminal dilation in high dose of AngII-induced AAA formation

After two weeks of AngII infusion, ultrasonography measurements showed an acceleration in AAA formation in Celastrol supplemented group **(Figure 3.1A, B)**. Despite the significant difference (P<0.05) between the two groups in week 2, intraluminal measurement by sonography **(Figure 3.1A, B)** and maximal aortic width measurements in week 4 **(Figure 3.2A, B)** did not show any significant difference between the control and Celastrol groups. AAA incidence rate was similar in both groups **(Figure 3.3)**. Additionally, Celastrol supplementation modestly increased AngII-induced ascending aortic expansion **(Figure 3.4A, B)**, but had no effect on atherosclerotic lesion areas in aortic arches **(Figure 3.4C)**.

Table II. Effects of Celastrol on male LDLR$^{-/-}$ mice infused with high dose AngII

Groups	HFD	Celastrol
Infusion	AngII (1.0 µg/kg/min)	AngII (1.0 µg /kg/min)
N	12	12
Body Weight (g)	25.1 ± 0.7	18.1 ± 0.6*
Plasma Cholesterol (mg/dL)	951.5 ± 32.2	961 ± 56.5
Systolic BP Pre-Infusion (mmHg)	138 ± 4	133 ± 4
Systolic BP Post-Infusion (mmHg)	188 ± 5^	169 ± 8^#

Table II. Values are represented as means ± SEMs. Body weights and plasma cholesterol concentrations were determined at termination. Systolic blood pressure was measured prior to (week 0) and during AngII infusion (week 4). Two-way repeated measures ANOVA was used to analyze systolic blood pressures. *Denotes P<0.05 Celastrol vs HFD by Student's t=test. ^ Denotes *P*<0.05 systolic BP post-infusion *vs.* pre-infusion, by two-way repeated measures ANOVA. # Denotes *P*<0.05 Celastrol *vs.* HFD by two-way repeated measures ANOVA with Bonferroni t-test *post hoc* analysis.
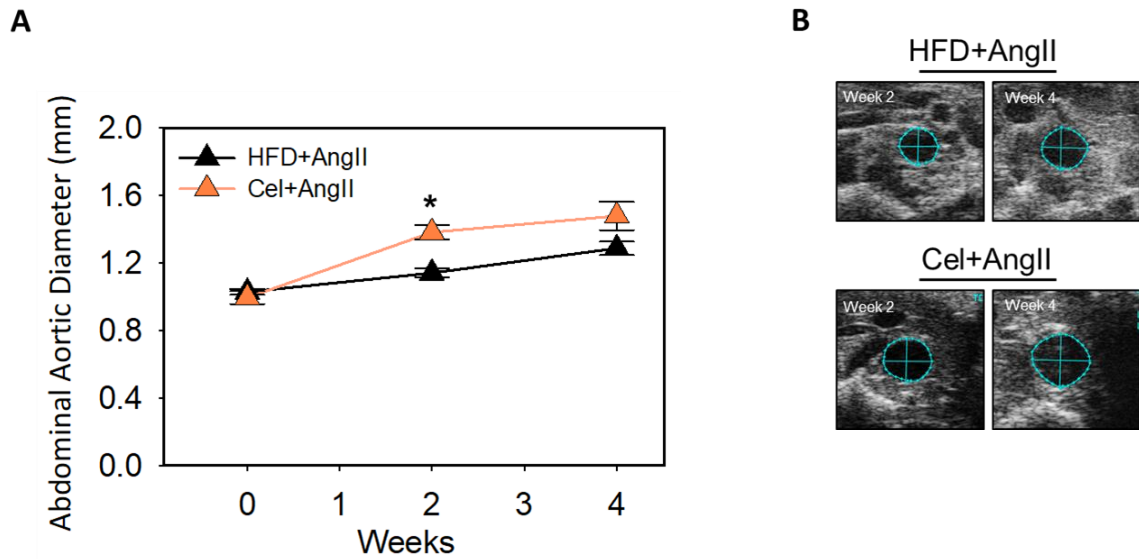
Figure 3.1. Celastrol supplementation accelerated high-dose, AngII-induced luminal dilation. (A) Ultrasonic measurements of abdominal aortic diameters at three different time points during 28 days of **high dose** of AngII infusion (1.0 µg/kg/min) +/- Celastrol supplementation into male LDLR$^{-/-}$ mice. **(B)** Representative ultrasound images of the abdominal aorta week 2 compared to week 4. Means of each group are represented by triangles and error bars are SEM. Statistical analysis was performed using Two-tailed Student's t-test. * denotes P<0.05 when comparing HFD+AngII *vs.* Celastrol+AngII at week 2.

A

B
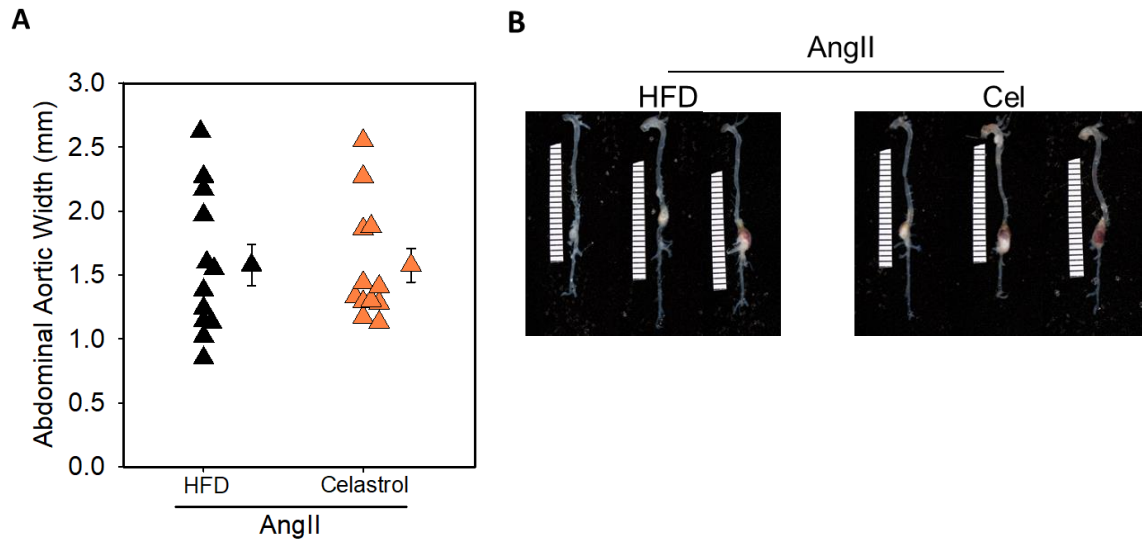
Figure 3.2. Celastrol supplementation did not exacerbate final high-dose of AngII-induced AAA formation. (A) Measurements of maximal external width of abdominal aortas after 28 days of high dose of AngII infusion. **(B)** Representative images of the abdominal aorta. Triangles represent individual mice and diamonds, and error bars are means and SEM respectively Statistical analyses were performed using Two-tailed Student's t-test (P=0.840).
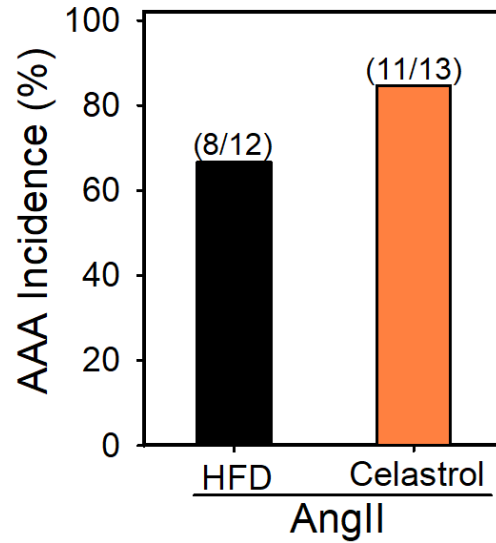
Figure 3.3. Celastrol supplementation did not affect AAA incidence in high-dose of AngII-infused mice. The incidence of AAA (>50% increase in aortic width and ruptured aorta) in AngII-infused mice -/+ Celastrol supplementation. Statistical analyses were performed by Fisher's Exact test.
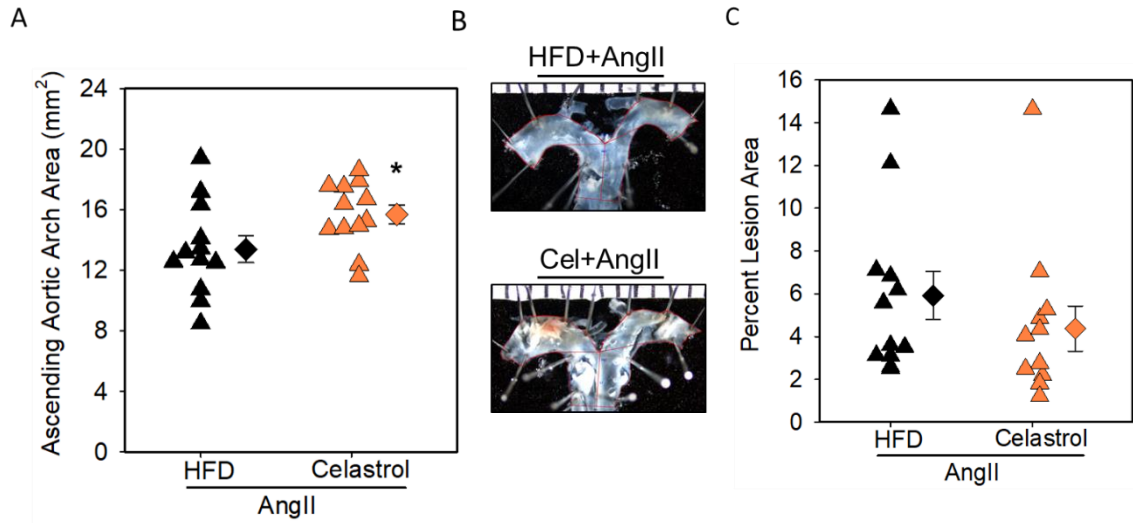
Figure 3.4. Celastrol supplementation slightly increased ascending arch area but had no effect on atherosclerosis in mice infused with a high dose of AngII. (A) Ascending aortic arch area measurement. **(B)** Representative images of Ascending aortic arch. **(C)** Percent lesion areas in aortic arches were measured by an en face technique. Triangles represent individual mice. Diamonds and error bars represent mean ± SEM.* denotes $P < 0.05$ by a two-tailed Student's t-test.

3.6. Celastrol supplementation significantly increased low-dose of AngII-induced AAA formation in male mice

Based on the observed Celastrol supplementation accelerated high-dose, AngII-induced aortic dilation at early times points (week 2). Given that AngII promotes AAA severity and incidence in a dose dependent manner [61, 98, 106], we next tested the effects of Celastrol supplementation with low dose of AngII (0.5 µg/kg/min) to examine if there is any effect of Celastrol supplementation on the acceleration of low dose AngII-induced AAA formation in hypercholesterolemic mice. Male LDLR$^{-/-}$ mice (8-10 weeks old; n=5-13 per group) were fed a saturated fat-enriched diet supplemented with or without Celastrol (10 mg/kg/day) for five weeks. After one week of the diet, mice were infused with either saline or a low dose of AngII (0.5 µg/kg/min) using osmotic mini-pumps for 28 days. Celastrol supplementation significantly decreased high fat diet-induced body weight gain in both saline and AngII-infused groups of mice but had no effect on total plasma cholesterol concentrations and AngII-induced blood pressure **(Table III)**. Dietary supplementation of Celastrol significantly promoted low dose of AngII-induced abdominal aortic luminal dilation **(Figure 4.1A, B)** and external aortic width **(Figure 4.2A, B)** in male mice as measured by ultrasonography and *ex vivo* measurement, with 90% AAA incidence (10/11) compared to 36% (4/11) in the control group **(Figure 4.3)**. In addition, Celastrol supplementation significantly increased AngII-induced ascending aortic expansion **(Figure 4.4A, B)** but had no effect on atherosclerotic lesion areas in aortic arches **(Figure 4.5).**

Table III. Effects of Celastrol in male LDL receptor -/- mice infused with saline or low dose of AngII

Groups	HFD		Celastrol	
Infusion	Saline	AngII (0.5 µg/kg/min)	Saline	AngII (0.5 µg/kg/min)
N	5	10	5	11
Body Weight (g)	30.8 ± 1.4	29.6 ± 0.8	20.1 ± 1.2*	20.8 ± 0.4*
Plasma Cholesterol (mg/dL)	1192 ± 81	1208 ± 98	1351 ± 89	1437 ± 48
Systolic BP Pre-Infusion (mmHg)	136 ± 4	146 ± 3	145 ± 4	150 ± 3
Systolic BP Post-Infusion (mmHg)	154 ± 7	182 ± 6#	138 ± 4	181 ± 4#

Table III. Values are represented as means ± SEMs. Body weights and plasma cholesterol concentrations were determined at termination. Systolic blood pressure was measured prior to (week 0) and during AngII infusion (week 4). * Denotes $P<0.05$ celastrol vs HFD by two-way ANOVA. # Denotes $P<0.05$ systolic BP post-infusion vs pre-infusion, by two-way repeated measures ANOVA.
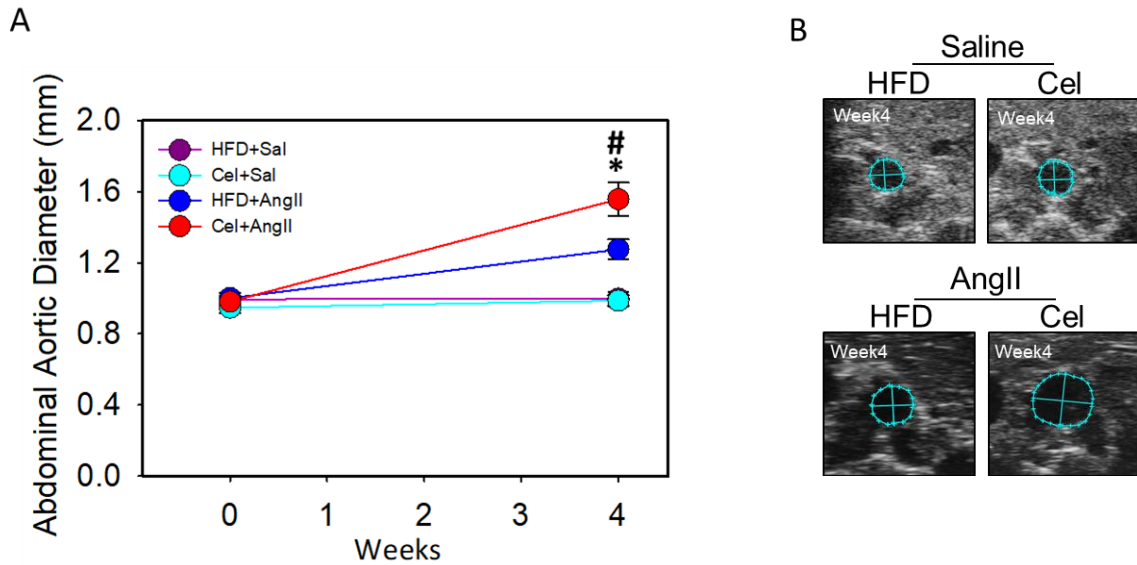
Figure 4.1. Dietary supplementation of celastrol significantly promoted low dose of AngII-induced abdominal aortic luminal dilation. (A) Ultrasonic measurements of abdominal aortic diameters at week 0 and week 4 after 28 days of either saline or **low dose** of AngII (0.5 μg/kg/min) infusion -/+ Celastrol supplementation. **(B)** Representative ultrasound images of the abdominal aorta at week 4. Statistical analyses were performed using Two Way RM ANOVA. * denotes $P<0.05$ when comparing HFD+AngII vs Cel+AngII at week 4. # denotes $P<0.05$ when comparing Week 4 vs week 0 for Cel+AngII.
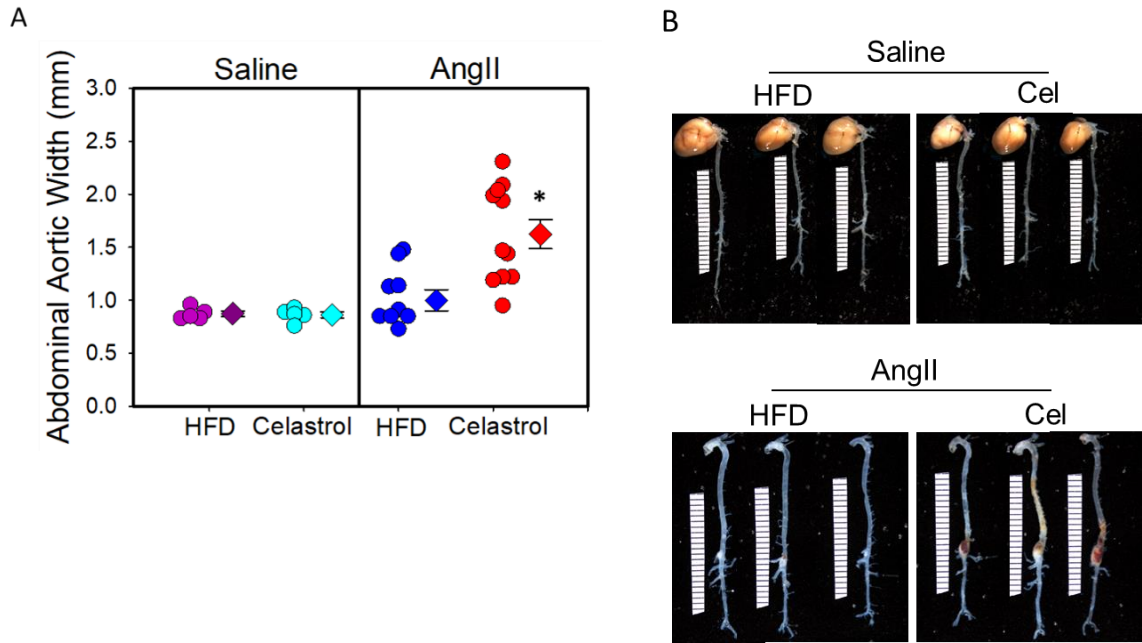
Figure 4.2. Celastrol supplementation profoundly increased low dose of AngII-induced AAA formation in male mice. (A) Measurements of maximal external width of abdominal aortas in saline and lose dose of AngII (0.5 µg/kg/min) infused mice -/+ Celastrol supplementation at week 4. **(B)** Representative images of the abdominal aorta. Circles represent individual mice and diamonds represent means. Statistical analyses were performed using Two Way ANOVA. * denotes P<0.05 when comparing HFD+AngII vs Cel+AngII at week 4.
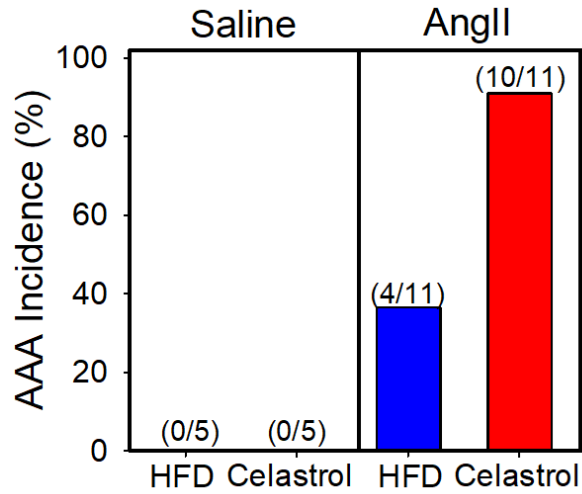
Figure 4.3. Celastrol supplementation increased AAA incidence in male mice. The incidence of AAA in saline and AngII-infused mice -/+ Celastrol supplementation. Statistical analyses were performed by Fisher Exact test.
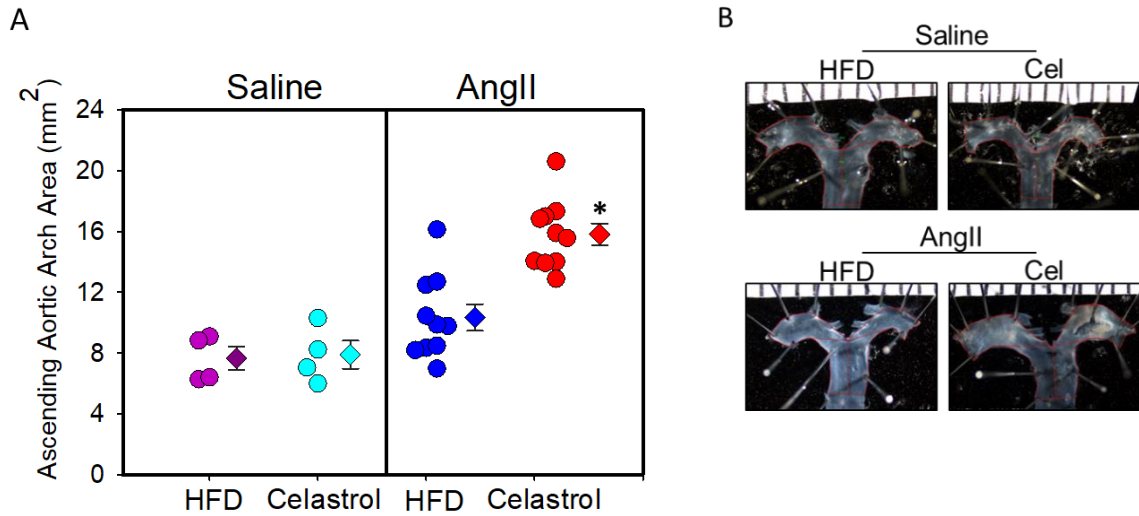
Figure 4.4. Celastrol supplementation significantly increased the low dose of AngII-induced ascending aortic expansion. (A) Ascending aortic arch area measurement. **(B)** Representative images of Ascending aortic arch. Circles represent individual mice. Diamonds and error bars represent mean ± SEM. * denotes $P < 0.05$ by Two Way ANOVA.
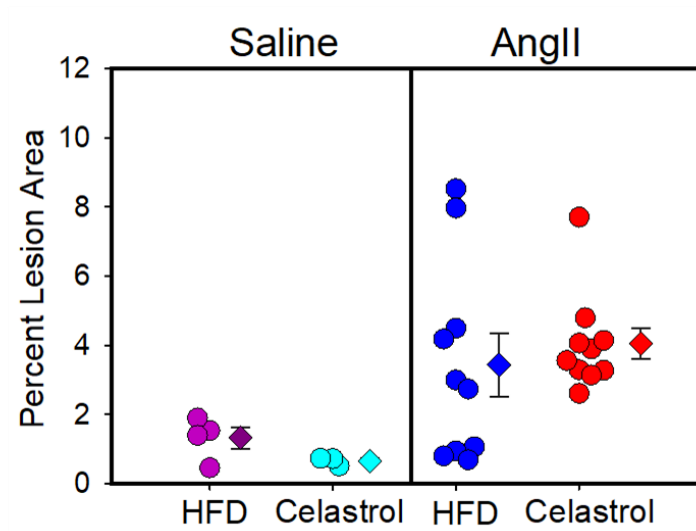
Figure 4.5. Celastrol supplementation had no effect on atherosclerosis in male hypercholesterolemic mice. Percent lesion areas in aortic arches were measured by an *en face* technique. Circles represent individual mice. Diamonds and error bars represent mean ± SEM. Statistical analyses were performed using Two Way ANOVA (P=0.51).

3.7. Celastrol Supplementation Increased AngII-induced AAA in Female Mice

Based on the results obtained from male studies, we next tested whether Celastrol supplementation would influence AAA formation in female LDLR$^{-/-}$ mice. Since female mice are highly resistant to AngII-induced AAA formation, in this study, female LDLR$^{-/-}$ mice were infused with either saline or high dose of AngII (1.0 μg/kg/day) for 4 weeks and fed HFD with or without Celastrol for 5 weeks starting one week before AngII infusion. As with males, Celastrol supplementation significantly decreased high fat diet-induced body weight gain in both saline and AngII-infused groups of mice but had no effect on total plasma cholesterol concentrations and AngII-induced blood pressure (Table IV). Interestingly, Celastrol supplementation in females resulted in a significant increase in AngII-induced abdominal aortic luminal dilation **(Figure 5.1A, B)** and external aortic width **(Figure 5.2A, B)** as measured by ultrasonography and ex vivo measurement with 80% incidence (11/14) compared to 6% (1/15) in the control group **(Figure 5.3)**. In addition, Celastrol supplementation modestly, but significantly increased AngII-induced ascending aortic expansion (**Figure 5.4A, B**) but had no effect on atherosclerotic lesion areas in aortic arches (**Figure 5.5**).

Table IV. Effects of Celastrol in female LDLR$^{-/-}$ mice infused with saline or high dose of AngII

Groups	HFD		Celastrol	
Infusion	Saline	AngII (1.0 µg/kg/min)	Saline	AngII (1.0 µg/kg/min)
N	5	10	5	11
Body Weight (g)	21.9 ± 0.6	22.8 ± 0.5	16.6 ± 0.9*	16.7 ± 0.3*
Plasma Cholesterol (mg/dL)	982 ± 87	1079 ± 86	1032 ± 87	1147 ± 54
Systolic BP Pre-Infusion (mmHg)	150 ± 4	139 ± 3	147 ± 3	149 ± 3
Systolic BP Post-Infusion (mmHg)	169 ± 5#	166 ± 5#	133 ± 3	176 ± 4#

Table IV. Values are represented as means ± SEMs. Body weights and plasma cholesterol concentrations were determined at termination. Systolic blood pressure was measured prior to (week 0) and during AngII infusion (week 4). * Denotes $P<0.05$ Celastrol vs HFD by two-way ANOVA. # Denotes $P<0.05$ systolic BP post-infusion vs pre-infusion, by two-way repeated measures ANOVA.
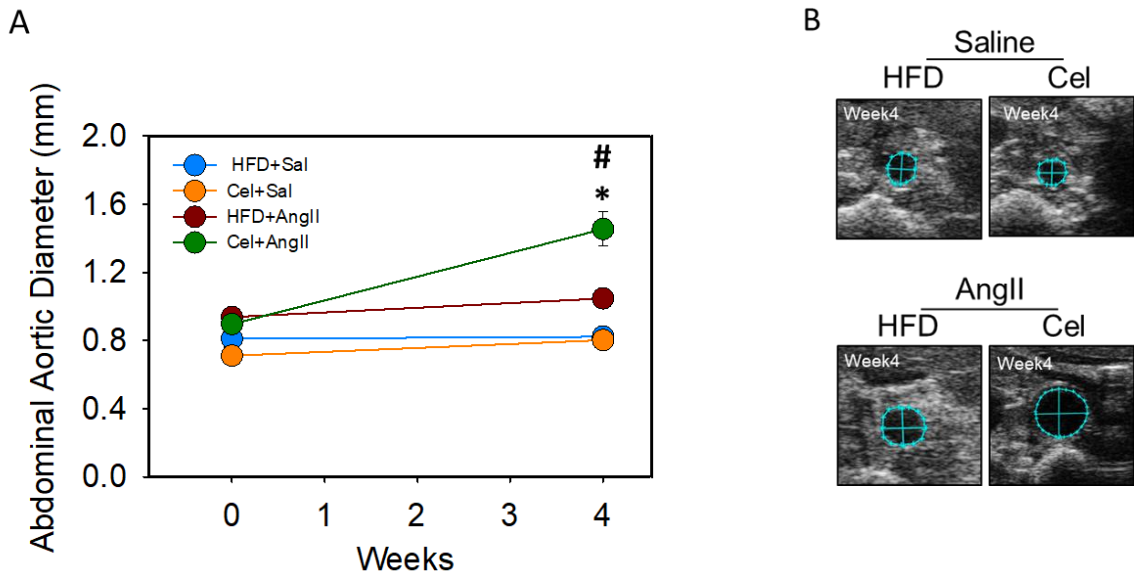
Figure 5.1. Celastrol supplementation in female mice resulted in a significant increase in AngII-induced abdominal aortic luminal dilation. (A) Ultrasonic measurements of abdominal aortic diameters at week 0 and week 4 during 28 days of either saline or AngII (1.0 µg/kg/min) infusion +/- Celastrol supplementation. **(B)** Representative ultrasound images of the abdominal aorta. Circles represent individual mice and diamonds and error bars represent means and SEM. Statistical analyses were performed using Two Way RM ANOVA. * denotes $P<0.05$ when comparing HFD+AngII vs Cel+AngII at week 4. # denotes $P<0.05$ when comparing Week 4 *vs.* week 0 for Cel+AngII.
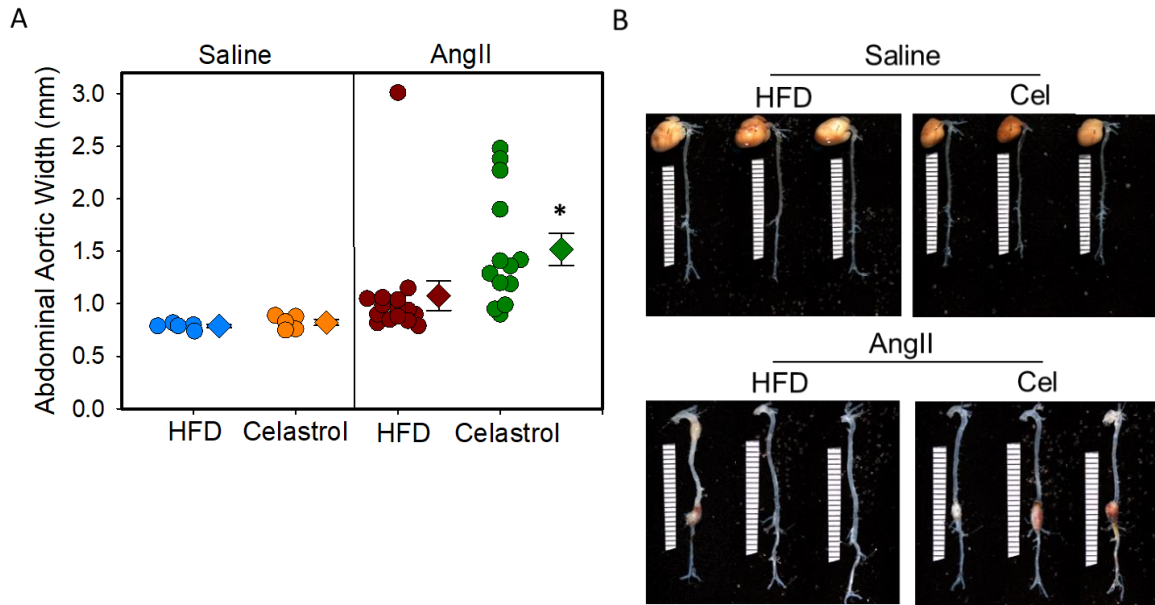
Figure 5.2. Celastrol supplementation significantly promoted AngII-induced AAA development in female mice. (A) Measurements of maximal aortic width of abdominal part in saline and AngII (1.0 µg/kg/min) infused mice -/+ Celastrol supplementation at week 4. **(B)** Representative images of the abdominal aorta. Circles represent individual mice and diamonds represent means. Statistical analyses were performed using Two Way ANOVA. * denotes *P*<0.05 when comparing HFD+AngII *vs.* Cel+AngII at week 4.
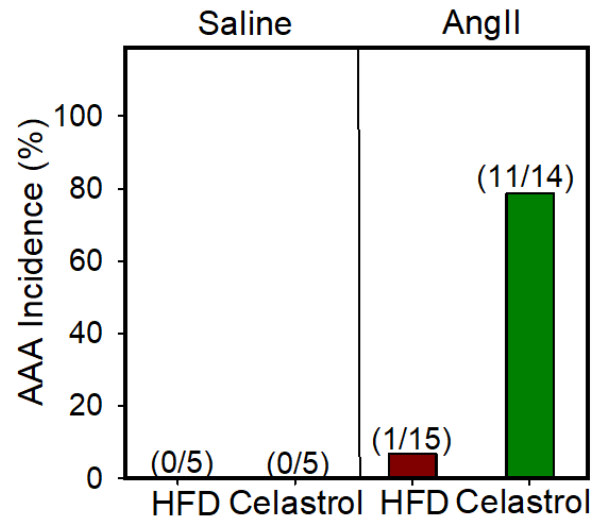
Figure 5.3. Celastrol supplementation significantly increased AAA incidence in female mice. The incidence of AAA in saline and **high dose** of AngII-infused mice -/+ Celastrol supplementation. Statistical analyses were performed by Fisher Exact test.
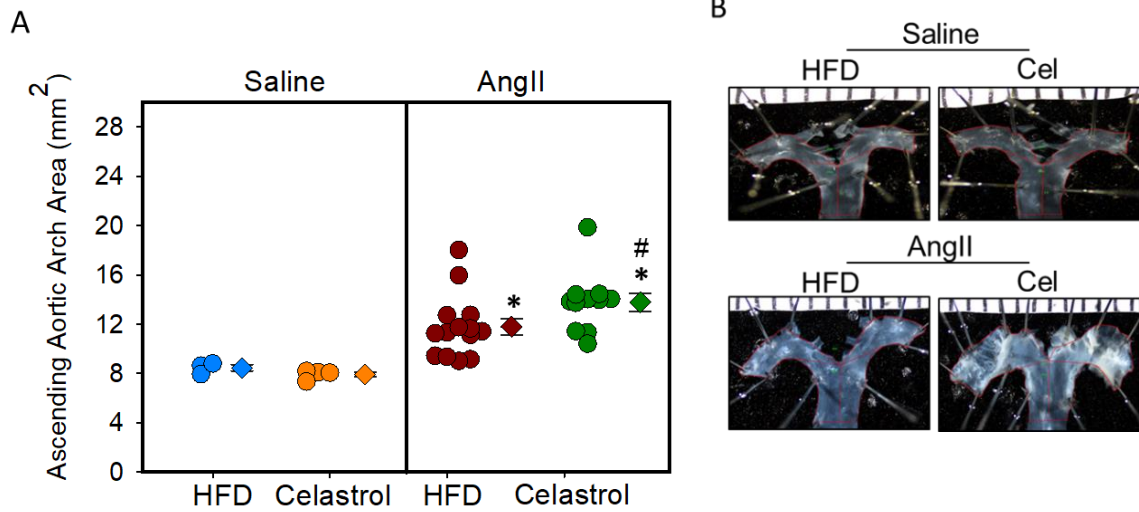
Figure 5.4. Celastrol supplementation significantly increased AngII-induced ascending aortic expansion in female mice. (A) Ascending aortic arch area measurement. **(B)** Representative images of Ascending aortic arch. Circles represent individual mice. Diamonds and error bars represent mean ± SEM. * denotes P<0.05 when comparing week 4 *vs.* week 0. # denotes P<0.05 when comparing Cel+AngII vs HFD+AngII at week 4. Statistical analyses were performed by Two Way ANOVA.
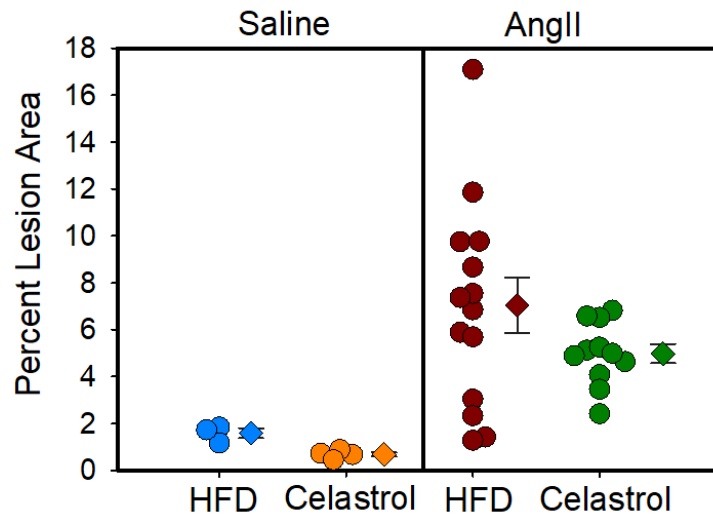
Figure 5.5. Celastrol supplementation had no effect on atherosclerosis in female hypercholesterolemic mice. Percent lesion areas in aortic arches were measured by an en face technique. Circles represent individual mice. Diamonds and error bars represent mean ± SEM. Statistical analyses were performed using Two-Way ANOVA.

3.8. Celastrol supplementation increased abdominal aortic medial elastin break and MMP9 activity in both male and female mice infused with AngII

Histological characterization of abdominal aortic sections obtained from male and female mice showed aortic wall disruption in AngII-infused aortas that received Celastrol supplementation. Verhoef's elastin staining and α-smooth muscle cell actin immunohistochemical staining revealed that Celastrol supplementation significantly promoted AngII-induced medial elastin breakage, and a significantly reduced medial α-smooth muscle cell actin-positive area in both male **(Figure 6.1A, B and 6.2A, B)** and female (**Figure 6.3A, B and 6.4A, B**) mice. Additionally, Picrosirius Red staining analyses revealed that Celastrol supplementation exhibited pronounced collagen deposition thickening in the adventitia of both male and female mice (**Figure 6.5**). In addition, in-gel gelatin zymographic analyses of abdominal aortic lysates revealed that Celastrol supplementation significantly increased AngII-induced matrix metalloproteinases (MMP) -9, not -2 activities in both male **(Figure 6.6A, B)** and female **(Figure 6.7A, B)** mice, compared to AngII and Saline controls.
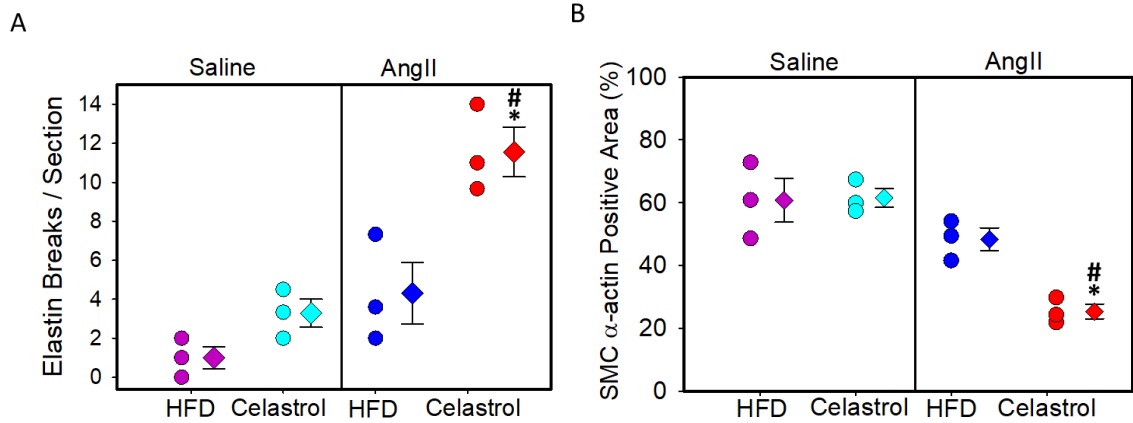
Figure 6.1 Aortic wall disruption in AngII-infused aortas of male mice that received Celastrol supplementation. (A) Quantification of elastin fragmentation with Verhoeff elastin stain and **(B)** Quantification of immunohistochemical staining for α-smooth muscle actin positive area in abdominal aorta after 28 days of saline or AngII (0.5 µg/kg/min) -/+ Celastrol supplementation in male mice (N=3) mice/group. Circles represent individual mice. Diamonds and error bars represent mean ± SEM. Statistical analyses were performed using Two Way ANOVA. * denotes $P<0.05$ when comparing HFD+AngII vs Cel+AngII at week 4. # denotes $P<0.05$ when comparing Week 4 *vs.* week 0 in Cel+AngII.
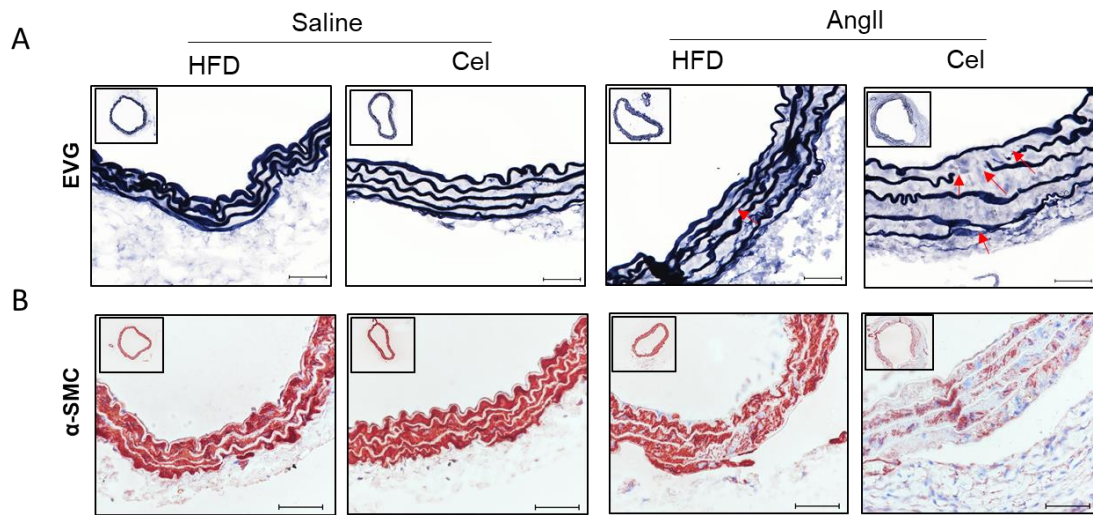
Figure 6.2 Representative images of (A) Verhoeff's elastin staining and **(B)** α-smooth muscle actin staining in abdominal aortic sections from male mice after 28 days of saline or AngII (0.5 µg/kg/min) infusion -/+ Celastrol supplementation.
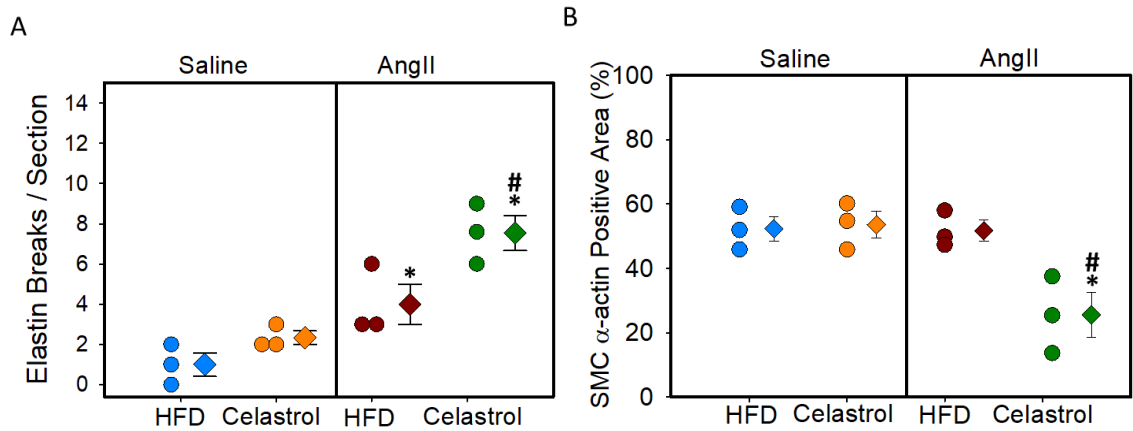
Figure 6.3 Aortic wall disruption in AngII-infused aortas of female mice that received Celastrol supplementation. (A) Quantification of elastin fragmentation with Verhoeff elastin stain and **(B)** Quantification of α-smooth muscle actin positive area in abdominal aorta after 28 days of saline or AngII (1.0 µg/kg/min) -/+ Celastrol supplementation in female mice (N=3 mice/group). Circles represent individual mice. Diamonds and error bars represent mean ± SEM. Statistical analyses were performed using Two Way ANOVA. * denotes $P<0.05$ when comparing week 4 *vs.* week0. # denotes $P<0.05$ when comparing Cel+AngII *vs.* HFD+AngII at week 4.
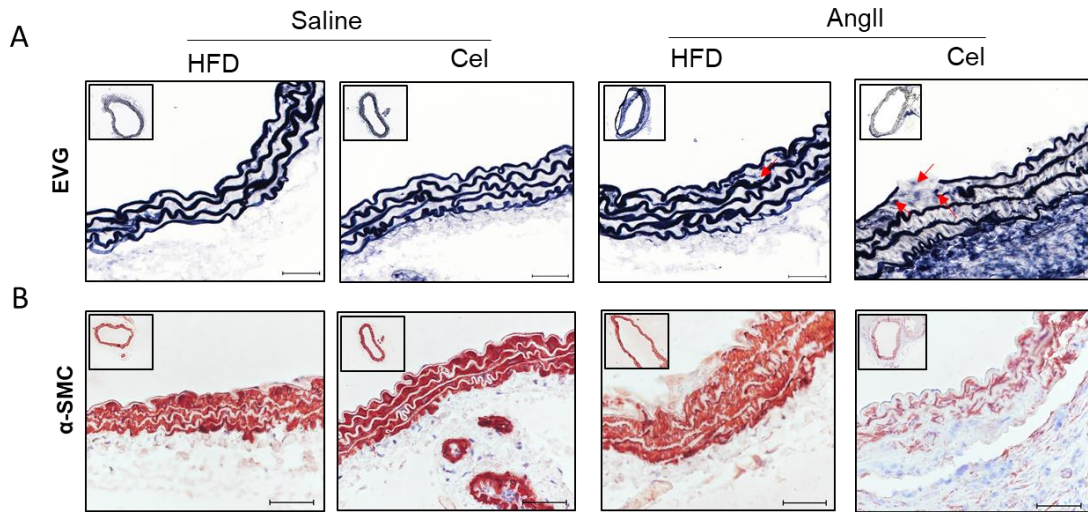
Figure 6.4 Representative images of (A) Verhoeff's elastin staining and **(B)** α-smooth muscle actin staining in abdominal aortic sections from female mice after 28 days of saline or AngII infusion (1.0 μg/kg/min) -/+ Celastrol supplementation.
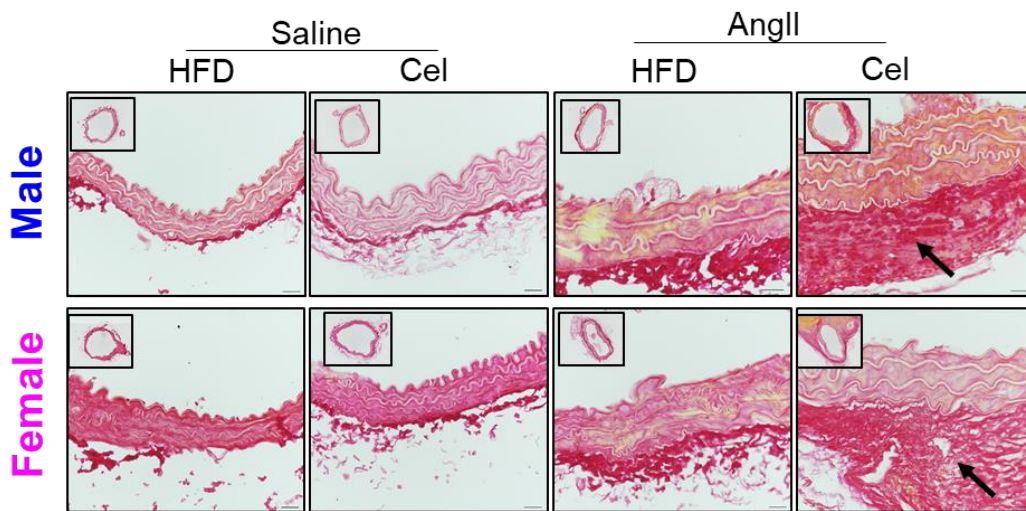
Figure 6.5 Representative images of Picrosirius red-stained suprarenal aortic sections showing collagen deposition (arrows) in adventitia with Celastrol supplementation in AngII-infused male and female mice.
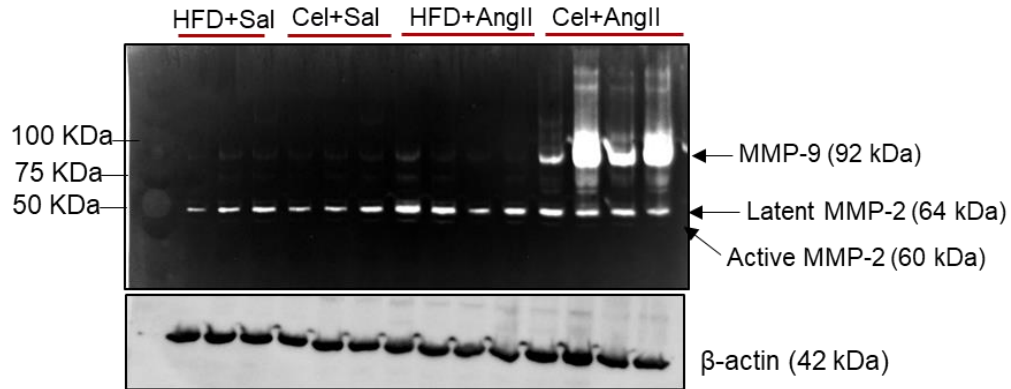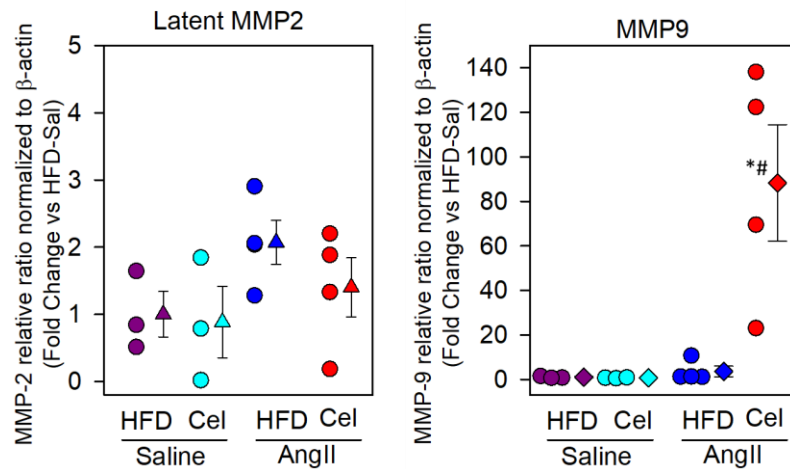
Figure 6.6 Aortic expression of MMP-9 and MMP2 after 2 weeks of AngII infusion in the aorta of male mice. (A) Gelatin zymography of protein extracts from mouse abdominal aortas infused with saline or AngII (0.5 µg/kg/min) +/- Celastrol supplementation. **(B)** Gelatinase activity quantification by Image Lab Software. Circles represent individual mice. Diamonds and error bars represent mean ± SEM. Statistical analyses were performed using Two Way ANOVA. * denotes $P<0.05$ when comparing saline vs AngII. # denotes $P<0.05$ when comparing Celastrol vs HFD.
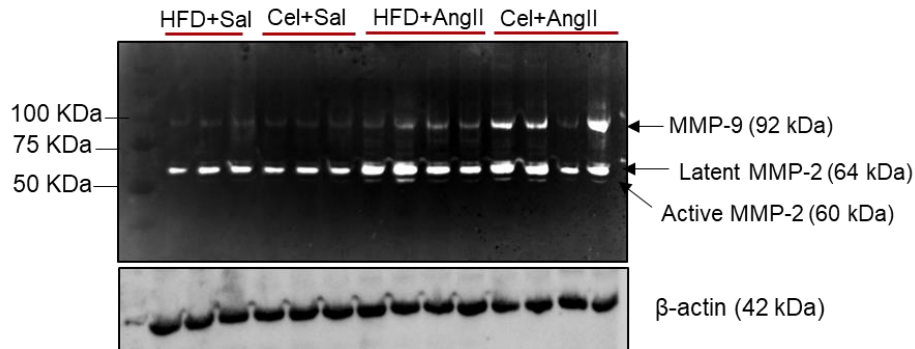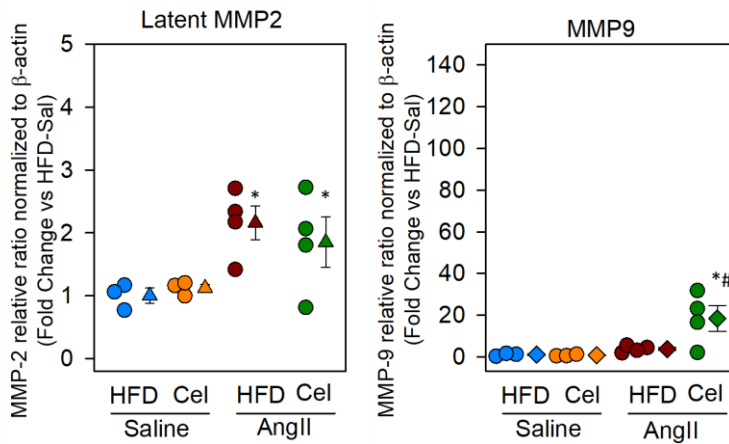
Figure 6.7 Aortic expression of MMP-9 and MMP2 after 2 weeks of AngII infusion in the aorta of female mice. (A) Gelatin zymography of protein extracts from mouse abdominal aortas (1.0 μg/kg/min) +/- Celastrol supplementation. **(B)** Gelatinase activity quantification by image Lab Software. Circles represent individual mice. Diamonds and error bars represent mean ± SEM. Statistical analyses were performed using Two Way ANOVA. * denotes *P*<0.05 when comparing saline vs AngII. # denotes *P*<0.05 when comparing Celastrol vs HFD.

3.9. Celastrol supplementation had no impact on autophagy activation in AngII-infused LDLR $^{-/-}$ mice

Since Celastrol supplementation caused profound increased in AngII-induced AAA development and incidence in both male and female mice, we were interested to see whether Celastrol influenced autophagy proteins in mediating AngII-induced AAAs. To address this question, male LDLR-/- mice (8 weeks old) were fed a fat-enriched diet +/- Celastrol. After 1 week of diet feeding, mice were infused with either saline or AngII (0.5 µg/kg/min) by osmotic minipumps for 2 weeks. Western blot analysis using aortic tissue lysate obtained after 2 weeks of AngII infusion revealed that Celastrol supplementation had no effect on autophagy proteins in the aorta. Although Beclin-1 and ATG7, an E1-like activating enzyme, which play a critical role in autophagy process, slightly increased by AngII infusion but there was no difference between these two autophagy related proteins after celastrol supplementation **(Figure 7A-D)**. These data suggested that Celastrol supplementation accelerated AngII-induced AAA formation without influencing autophagy pathway proteins in the aorta.
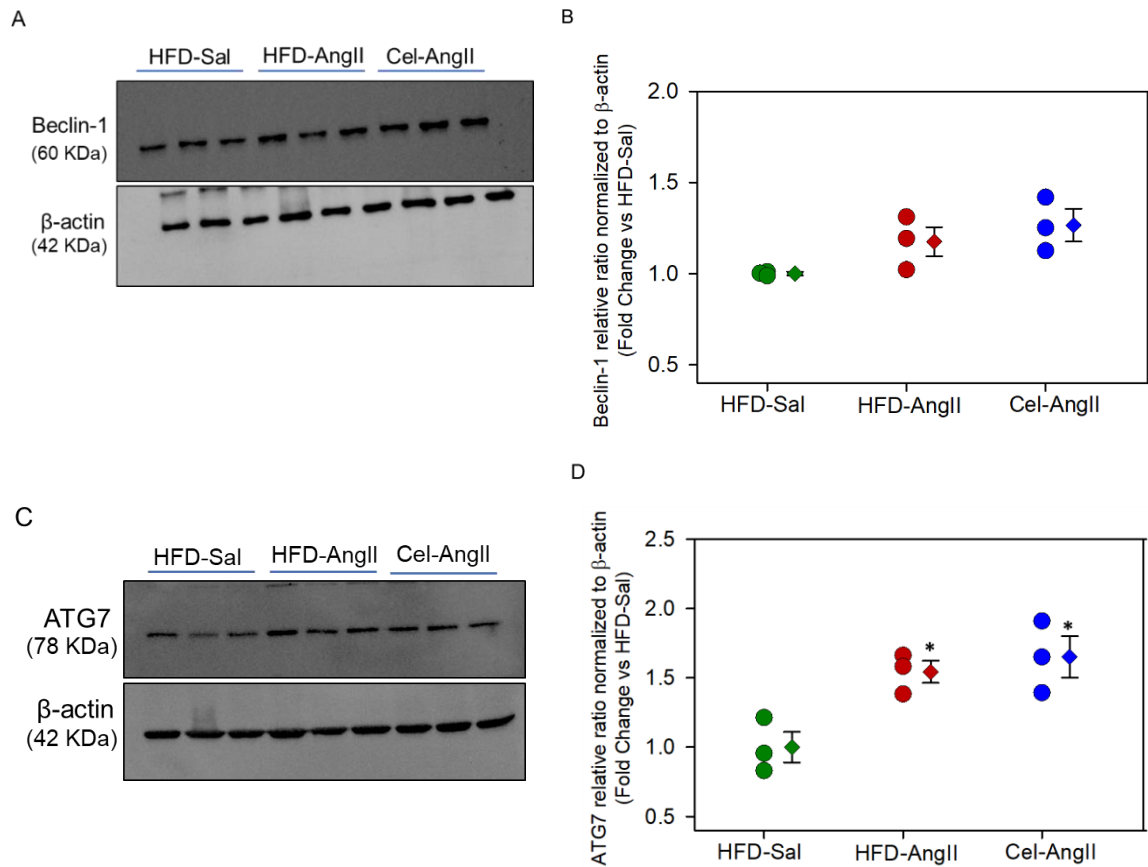
Figure 7. Celastrol supplementation did not increase autophagy related proteins. After two weeks of either Saline or AngII infusion (0.5 µg/kg/min) into male LDLr $^{-/-}$ mice, aortic tissue lysates were collected and western blot analysis was performed **(A, B)** Protein expression of Beclin-1 in aortic tissue. **(C, D)** Protein expression of Atg7 in aortic tissue. Circles represent each individual mouse. Means of each group are represented by triangles and error bars are SEM. Statistical analysis was performed using one-way ANOVA. * Denotes *P*<0.05 when comparing AngII groups to the control.

3.10. Generation of SMC-Beclin-1 knockout mice

Based on the outcome of the above 2 different studies using 3-MA and Celastrol, currently, it is not clear that if autophagy plays a critical role in the development of AngII-induced ascending and abdominal aortic aneurysms. To understand the functional contribution of autophagy in AA development, next we utilized a genetic mouse model approach.

Recent clinical studies highlighted that Beclin-1, a gene indispensable for autophagy process and function, is highly upregulated in human AAA tissues[87]. Similar to human data, our findings demonstrated that AngII infusion increased Beclin-1 protein expression in abdominal aorta **(Figure 1A&B, Figure 7A&B).** To examine the functional role of autophagy, we generated a transgenic mouse in which the autophagy protein Beclin-1 was deleted in SMCs. The rational for exclusively focusing on SMCs is based on the fact that SMCs are the predominant cell type in the aortic medial layer and have a pivotal role in maintaining aortic structural and integrity [39].In addition, SMC-rich aortic medial stability is highly disrupted in AAs[46].

Since Beclin-1 deficiency in mice are embryonically lethal [107], to achieve SMC-specific Beclin-1 deficiency in mice, our overall strategy was to develop age-, strain- and sex- matched mice that are homozygous for Beclin-1 floxed (f/f) alleles and express tamoxifen-inducible Cre recombinase driven by the SMC-specific Acta2 promoter (SMA- ERT2) [108]. Beclin-1 floxed mice were obtained from Dr. Rucker at the University of Kentucky,[109] and the SMA-ERT2 Cre mice were obtained from Dr. Chambon, IGBMC via Dr. Dichek, University of Washington

[110]. To develop SMC-specific Beclin-1 deficient mice in a LDLR$^{-/-}$ background, female LDLR$^{-/-}$ Beclin-1 homozygous f/f mice were bred to male LDLR$^{-/-}$ Beclin-1$^{f/f}$ mice that are hemizygous (+/0) for the ERT2-SMA promoter driving Cre expression. Breeding strategies have ensured strain equivalency between Beclin-1$^{f/f}$ mice that are either WT (Cre$^{0/0}$) or in combination with hemizygous ERT2-SMA Cre (Cre$^{+/0}$) **(Figure 8.1)**. To induce Cre recombinase activity, tamoxifen (75 mg/kg body weight) was administered intraperitoneally for 5 days [111]. After 2 weeks, Western blot analyses showed depletion of Beclin-1 protein in the aortic media but not in adventitia from Cre$^{+/0}$ mice compared to Cre$^{0/0}$ littermates **(Figure 8.2A, B)**. Using the well-established Angiotensin II (AngII) infusion model of AAs[98], we examined the role of SMC-Beclin-1 during the development of AAs in hypercholesterolemic mice.
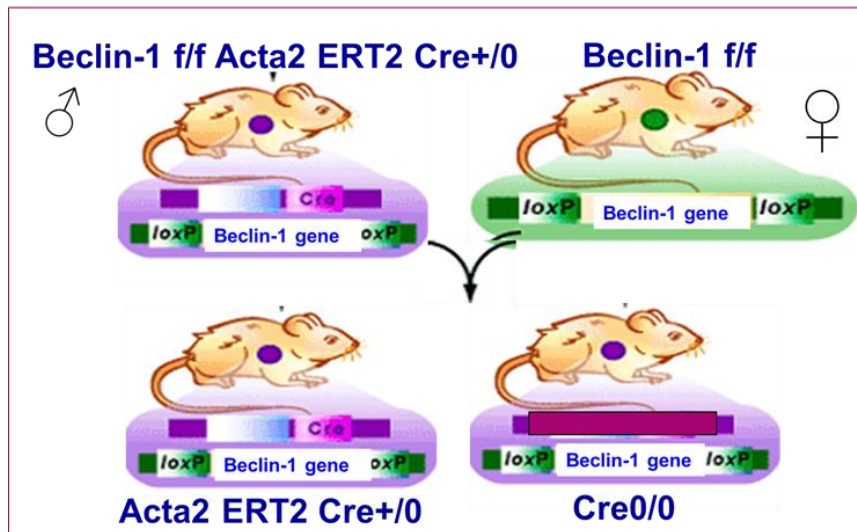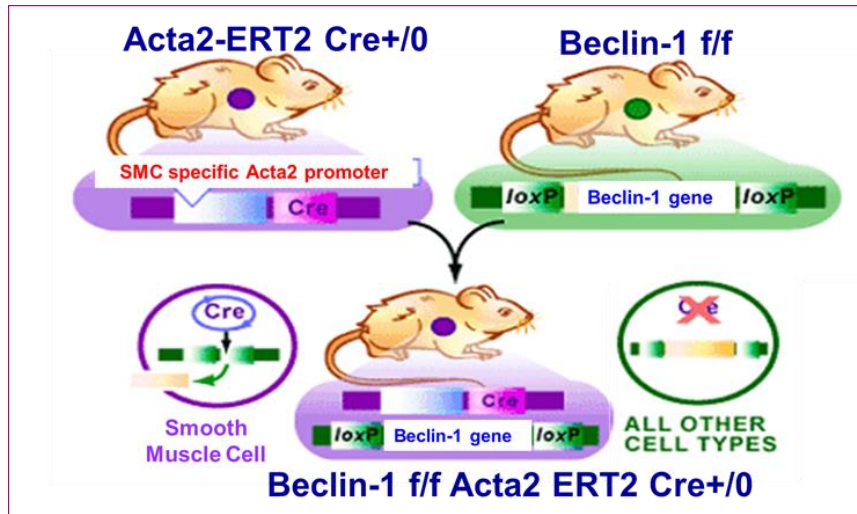
Figure 8.1 Breeding scheme for the generation of Beclin-1[f/f] Acta2 ERT2Cre[+/0] x LDLR^{-/-} mice.
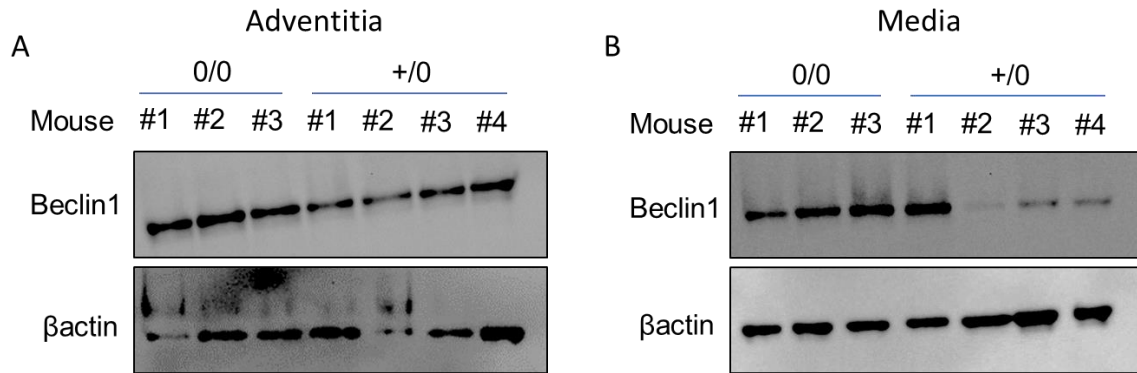
Figure 8.2 Western blot analyses showed a reduction of Beclin-1 protein in SMC-rich aortic medial tissue of Acta2 ERT2 Cre$^{+/0}$ mice. Beclin-1 protein level in aortic **(A)** Adventitia and **(B)** Media from SMC-*Beclin1$^{-/-}$* mice and SMC-*Beclin1$^{+/-}$* littermates 2 weeks after Tamoxifen injection.

3.11. SMC-Beclin-1 deficiency accelerates abdominal aortic aneurysms in low dose AngII-infused mice

To study the role of Beclin-1 in SMCs, 6-8 weeks old male LDLR$^{-/-}$ Beclin-1 floxed mice that are either SMA- ERT2 Cre$^{+/0}$ or Cre$^{0/0}$ (N=6-15 per group) were injected with tamoxifen for 5 days. After 2 weeks, mice were fed a high-fat diet for 5 weeks. After 1 week of diet feeding, mice were infused subcutaneously with either saline or a low dose of AngII (0.5 μg/kg/min) by osmotic mini-pumps for 4 weeks. Body weight analyses showed beclin-1 deletion significantly slowed down the weight gain in hypercholesterolemic mice fed a high-fat diet compared to their wild type control **(Table V)**. In addition, total cholesterol measurements revealed significant reduction in plasma cholesterol of SMC-Beclin-1 deficient mice compared to their wild type controls in dependent of AngII infusion **(Table V)**.

Interestingly, SMC-Beclin-1 deficiency significantly promoted the expansion of aorta starting from the ascending aorta to the lower part of the abdominal aorta up to the renal branch, just above the infrarenal aorta in both saline and AngII-infused mice compared to the littermate controls **(Figure 8.4B).**

Ultrasound and *ex vivo* aortic width measurement of abdominal aortas revealed that SMC-Beclin-1 deficiency (Cre$^{+/0}$) caused a significant increase in abdominal aortic luminal dilation **(Figure 8.3A&B)** and external aortic width **(Figure 8.4A&B).** in both saline and AngII-infused groups compared to the littermate controls (Cre0/0). Among the saline infused groups, SMC-Beclin-1 deficiency (Cre$^{+/0}$) showed a significant increase of 66% (4/6) AAA incidence compared to Cre$^{0/0}$-Saline controls (0/6) **(Figure 8.5).** Low dose of AngII (0.5 μg/kg/min) -infusion

showed a modest but not significant increase in abdominal aortic width and AAA incidence (6%; 1/15) in $Cre^{0/0}$ mice compared to saline controls **(Figure 8.5)**. However, in SMC-Beclin-1 deficient mice ($Cre^{+/0}$), low dose of AngII infusion showed an incidence of 93% (14/15) compared to 6% (1/15) incidence in AngII-infused littermate controls ($Cre^{0/0}$). Furthermore, among the SMC-Beclin-1 deficient ($Cre^{+/0}$) saline and AngII infused groups of mice, there is no significant difference in abdominal aortic expansion and AAA incidence **(Figure 8.5)**.

Table V. Effect of SMC-Beclin-1 deletion on body weight and plasma cholesterol in hypercholesterolemic male mice infused with either saline or AngII

Groups	Cre0/0		Cre+/0	
Infusion	**Saline**	**AngII(0.5 µg/kg/min)**	**Saline**	**AngII (0.5 µg /kg/min)**
N	7	14	6	13
Baseline Body Weight	26.4 ± 0.9	26.4 ± 0.5	24.5 ± 0.7	26.2 ± 0.5
End Point Body Weight (g)	34.2 ± 0.9#	32.0 ± 1#	28.2 ± 0.7*#	27.1 ± 0.3*
Plasma Cholesterol (mg/dL)	1540 ± 132.5	1383 ± 86.8	985 ± 102.5*	754.7± 61.1*

Table V. Values are represented as means ± SEMs. Body weights were determined at baseline and termination. Plasma cholesterol concentrations were determined at termination. * Denotes $P<0.05$ Cre+/0 vs Cre0/0 at week 4 and # Denotes $P<0.05$ Week 4 *vs.* Week0 by Two-Way RM ANOVA.
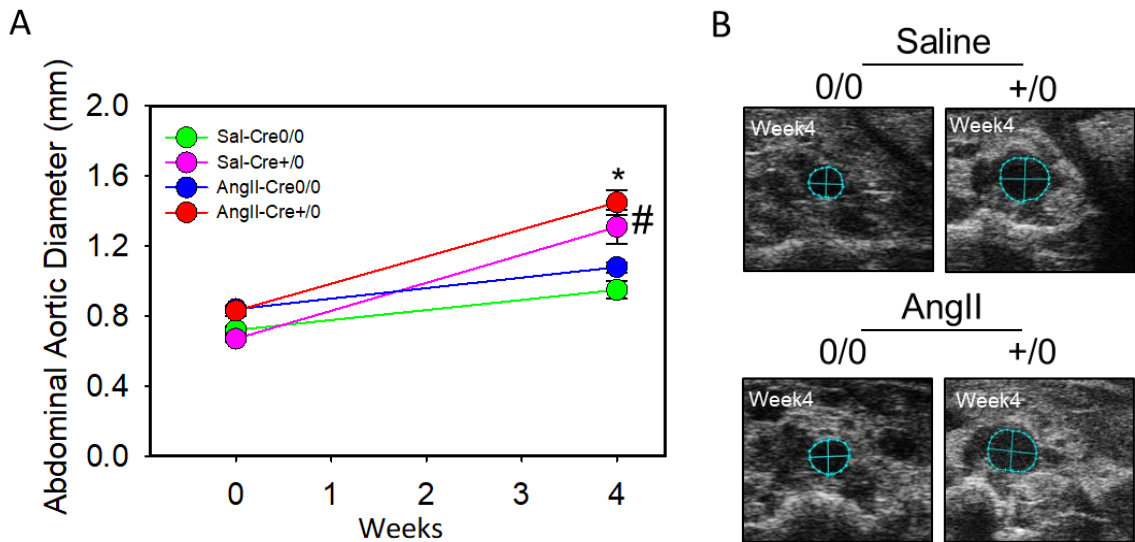
Figure 8.3 SMC-Beclin-1 deficiency increased aortic luminal diameter in male hypercholesterolemic mice. (A) Ultrasonic measurements of abdominal aortic luminal diameter of Beclin-1 Acta2 ERT2 $Cre^{0/0}$ (n=7-15) and $Cre^{+/0}$ (n=6-15) mice fed with high-fat diet and infused with either saline or AngII (0.5 µg/kg/min) measured at week 0 and week 4. **(B)** Representative ultrasound images of the abdominal aorta after 28 days of AngII infusion. Circles represent means of each group and error bars are SEM. Statistical analyses were performed using Two Way RM ANOVA. * Denotes $P < 0.001$ when comparing AngII-Cre $^{+/0}$ mice to AngII-Cre0/0; # denotes $P < 0.001$ when comparing Sal-$Cre^{+/0}$ to Cre $^{0/0}$ in either saline or AngII-infused mice.
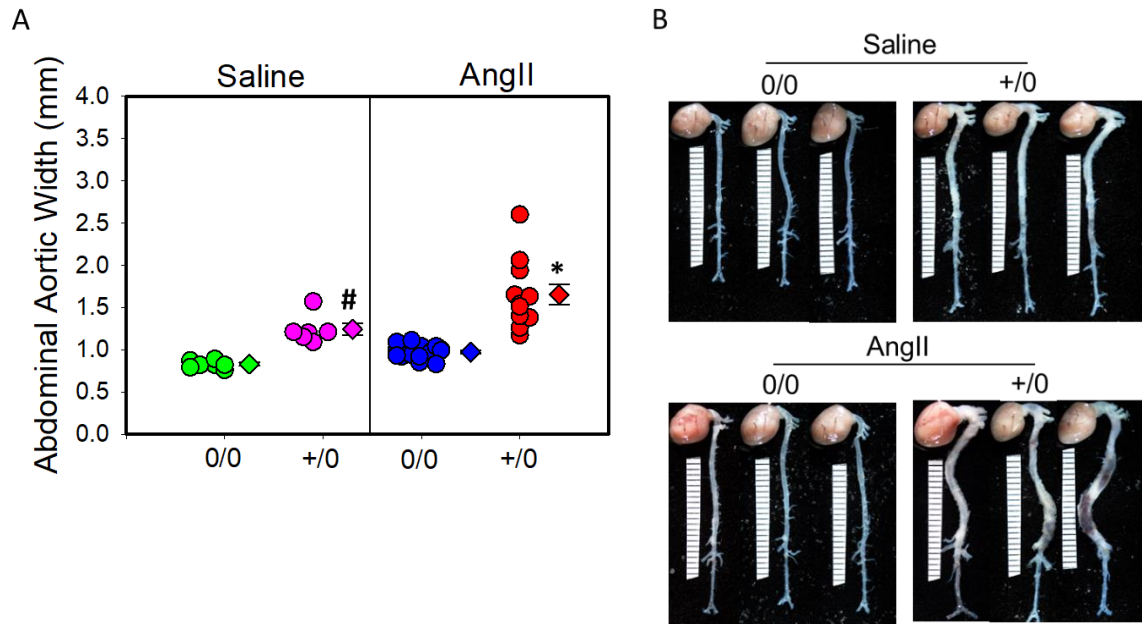
Figure 8.4 Beclin-1 deficiency in SMCs increased abdominal aortic width in both Saline and AngII-infused aortas. (A) *Ex-vivo* abdominal diameters of Beclin-1 Acta2 ERT2 Cre$^{0/0}$ (n=5-10) and Cre $^{+/0}$ (n=4-11) mice fed with high-fat diet and infused with either saline or AngII. Circles represent individual mice in each group. Means of each group are represented by diamonds and error bars are SEM. **(B)** Aortic pictographs nearest the mean. Means of each group are represented by diamonds and error bars are SEM. * denotes $P < 0.05$ when when comparing AngII-Cre $^{+/0}$ mice to AngII-Cre$^{0/0}$; # denotes $P < 0.05$ when comparing Sal-Cre+/0 to Cre $^{0/0}$ in either saline or AngII-infused mice.
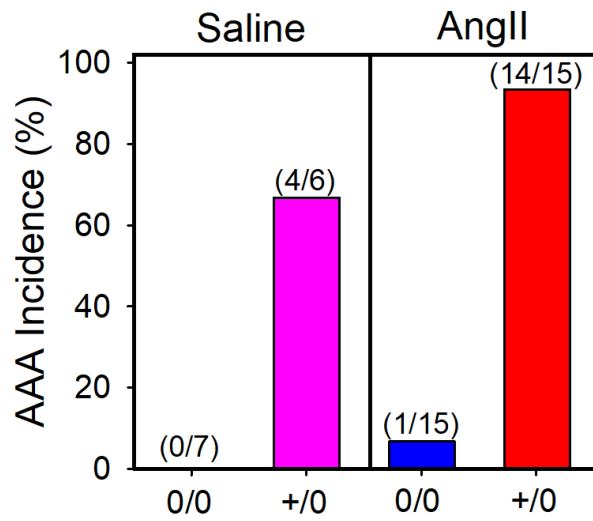
Figure 8.5 Beclin-1 deficiency profoundly increased AAA incidence independent of AngII infusion in hypercholesterolemic male mice. The incidence of AAA in Beclin-1 Acta2 ERT2 Cre[0/0] and Cre [+/0] (n=4-11) mice fed with high-fat diet and infused with either saline or AngII measured at week 4. Statistical analyses were performed by Fisher Exact test.

3.12. Beclin-1 deficiency in SMCs increased AngII-induced thoracic aortic expansion

In addition to the crucial role of SMC-Beclin-1 in AAA formation, analysis of in situ measurement of thoracic aorta revealed that inducible depletion of Beclin-1 in SMCs profoundly increased aortic expansion in the regions of ascending aorta **(Figure 8.6A)**, arch **(Figure 8.6B)**, and descending **(Figure 8.6C)** thoracic aorta in both saline and AngII-infused male LDLR$^{-/-}$ mice compared to the littermate controls. Similar to AAA, the effect of Beclin-1 deficiency was independent of AngII infusion, as Beclin-1 deficiency in SMCs significantly increased the aortic expansion in saline control groups as equivalent to AngI-infused groups. **(Figure 8.7).**
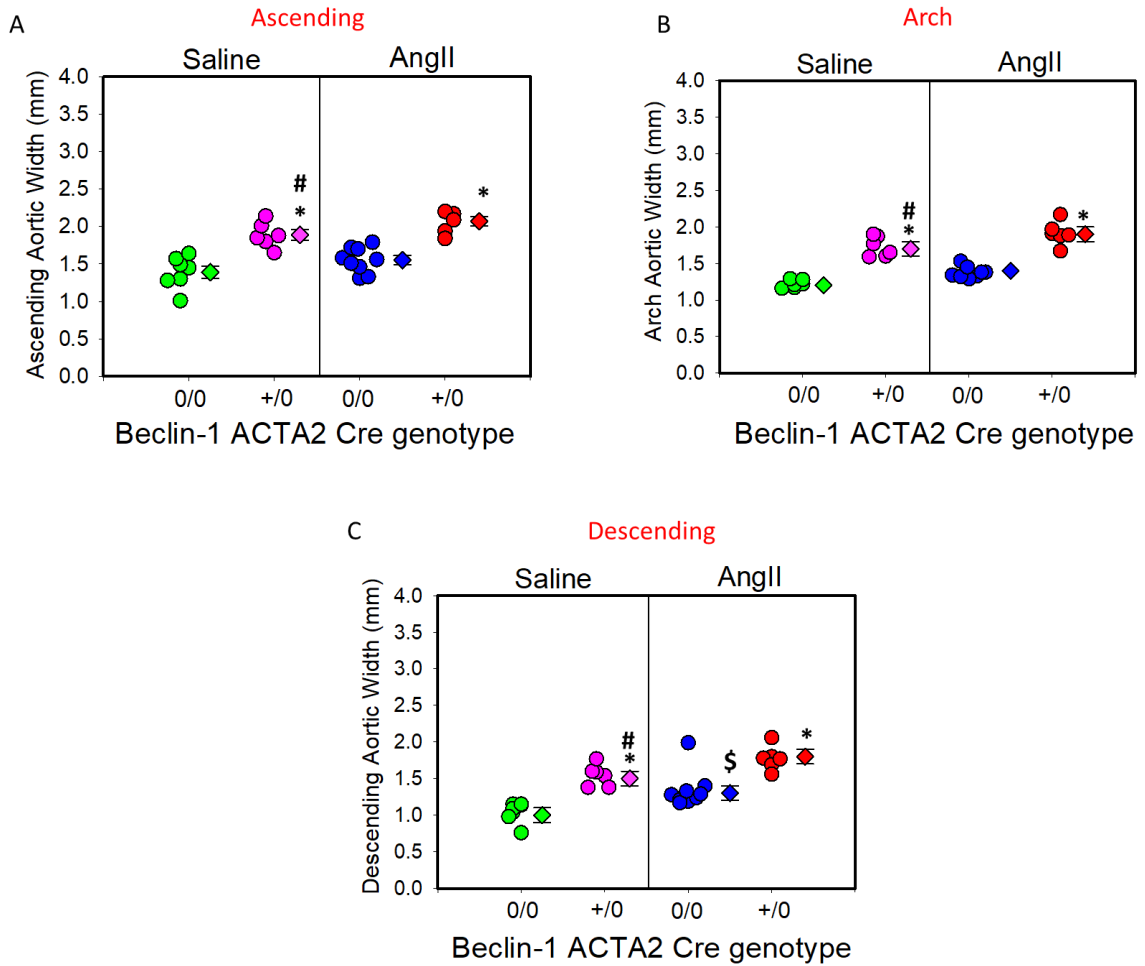
Figure 8.6 Beclin-1 deficiency accelerated thoracic aortic expansion in hypercholesterolemic male mice. *In situ* measurement of **(A)** ascending aortic width**, (B)** arch aortic width and **(C)** descending aortic width in Beclin-1 Acta2 ERT2 Cre$^{0/0}$ and Cre $^{+/0}$ mice fed with high fat diet and infused with either saline or AngII at week 4. Circles represent individual mice in each group. Means of each group are represented by diamonds and error bars are SEM. * denotes *P* < 0.05 when comparing SMC-Beclin1 Cre $^{+/0}$ mice to their WT controls. # denotes *P* < 0.05 when comparing Cre $^{+/0}$ *vs.* Cre 0/0 in either saline or AngII-infused mice. $ denotes *P* < 0.05 when comparing saline vs AngII in wild type mice.
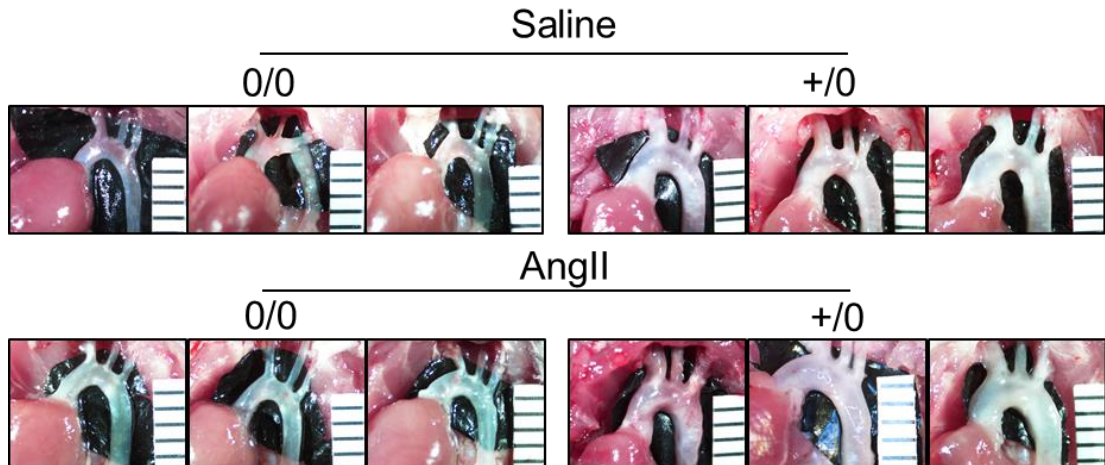
Figure 8.7 Representative images of thoracic aorta from SMC-Beclin1 Cre +/0 and Cre$^{0/0}$ infused with either saline or AngII

3.13. Beclin-1 deficiency markedly diminished population of medial SMCs and disrupted aortic wall integrity

To further characterize SMC-Beclin-1 deficient phenotype during AngII-induced AA formation, the abdominal and ascending segments of the aorta were dissected, processed and subsequently sectioned to perform analysis for medial elastin break, alpha-SMC positive area and collagen deposition. As determined by Verhoef's staining, deletion of Beclin1 in SMCs profoundly increased aortic medial thickening and medial elastin breaks in both abdominal and ascending aortic sections. In addition, SMC-Beclin-1 deficiency further accelerated AngII-induced aortic medial thickening and elastin breaks in both abdominal **(Figure 8.8A, 8.9A)** and ascending aortic **(Figure 8.8B, 8.9B)** sections, Immunohistochemical staining for SMC α-actin positive area revealed severe depletion of SMC α-actin markers in aortic medial layer both in abdominal **(Figure 8.10A, 8.11A)** and ascending **(Figure 8.10B, 8.11B)** segment in Beclin-1 deficient mice that was independent of the effect of AngII infusion. Moreover, Picro Sirius Red staining showed a strong adventitial collagen deposition and thickenings in Beclin-1 deficient mice compare to their WT littermates infused with either saline or AngII **(Figure 8.12).**
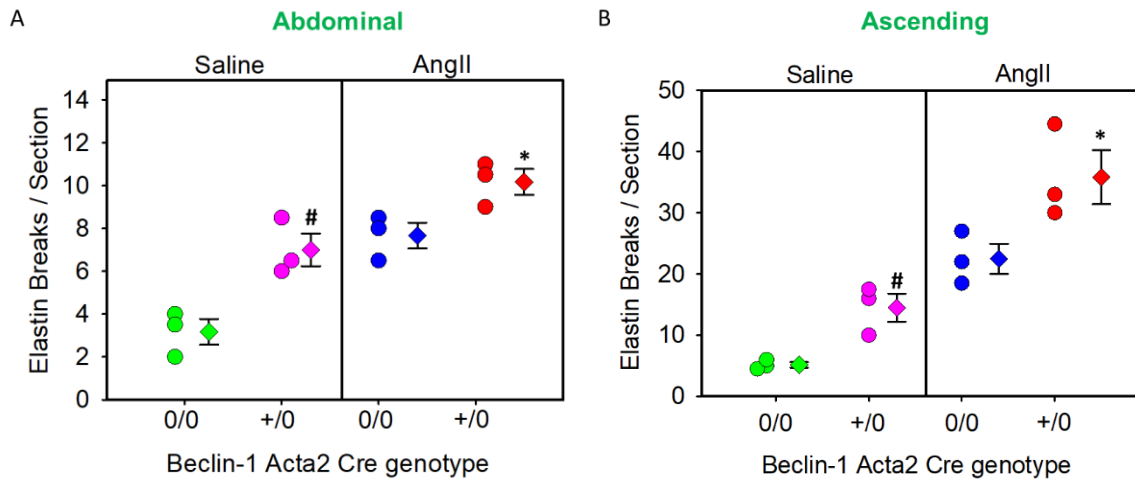
Figure 8.8 Beclin-1 deficiency significantly increased elastin breaks abdominal and ascending aorta. Quantification of elastin fragmentation with Verhoeff elastin stain in **(A)** Abdominal aortic segment and **(B)** Ascending aortic segment in Cre[+/0] male mice and their WT littermates infused with saline or AngII (0.5 µg/kg/min) for 28 days. Circles represent each individual mouse. Diamonds and error bars represent mean ± SEM. Statistical analyses were performed using Two Way ANOVA. * Denotes $P<0.05$ when comparing Cre+/0 to Cre0/0 infused with AngII and # denotes $P<0.05$ when comparing Cre+/0 to Cre0/0 infused with saline.
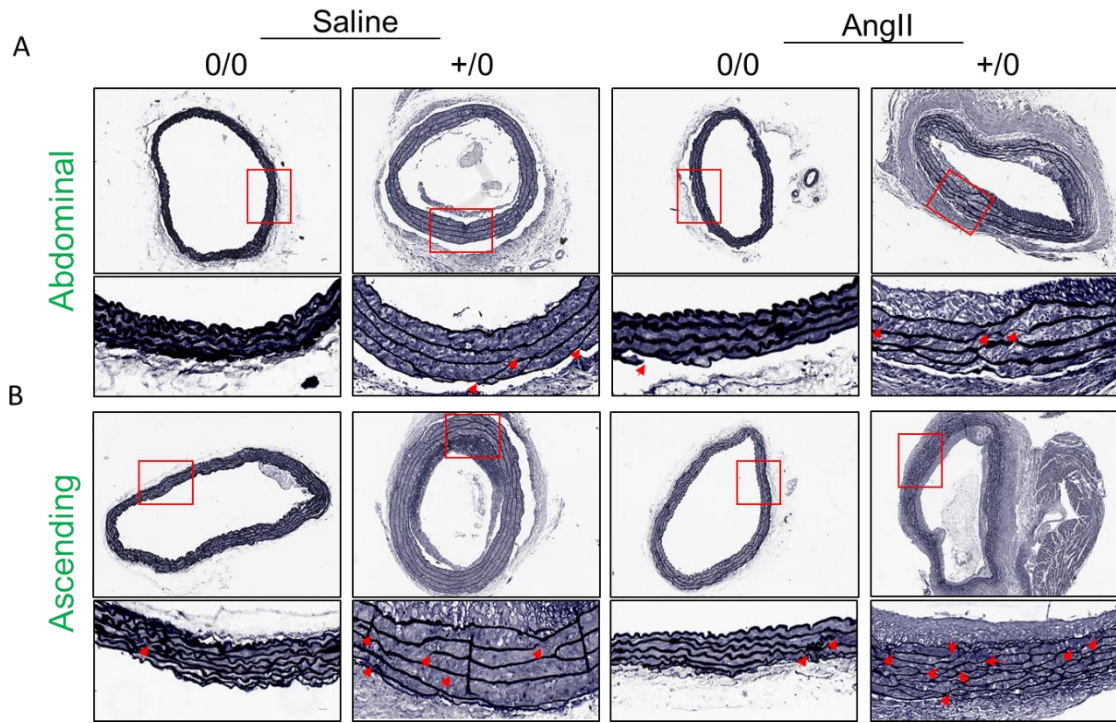
Figure 8.9 Representative images of Verhoeff's elastin staining on **(A)** Abdominal aortic sections and **(B)** Ascending Aortic Sections form SMC-Beclin1 WT and KO mice infused with either saline or AngII for 28 days.
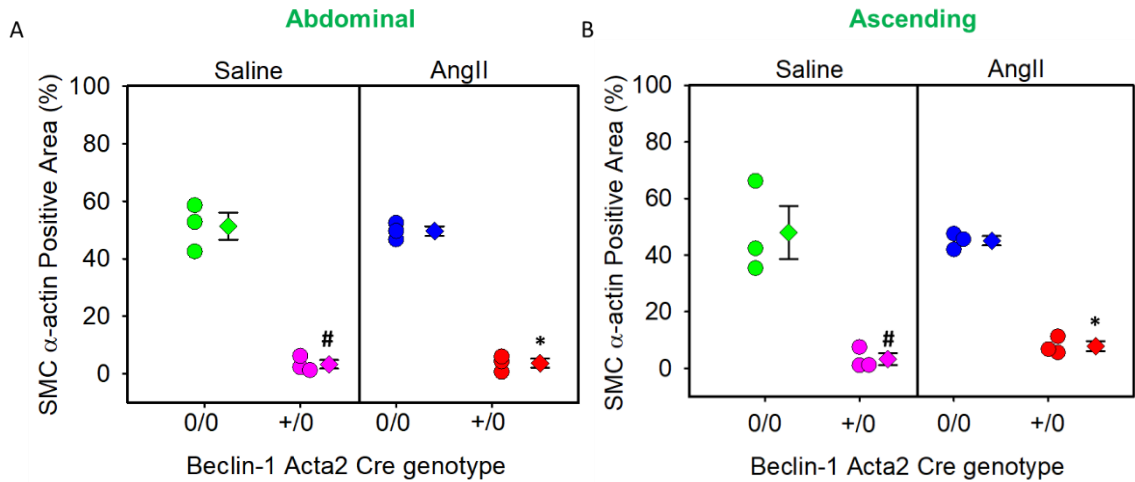
Figure 8.10 Beclin-1 deficiency significantly decreased SMC α-actin positive area in both abdominal and ascending aorta. Quantification of immunohistochemical staining for SMC α-actin in **(A)** Abdominal aortic segment and **(B)** Ascending aortic segment in Cre[+/0] male mice and their WT littermates infused with saline or AngII (0.5 µg/kg/min) for 28 days. Circles represent each individual mouse. Diamonds and error bars represent mean ± SEM. Statistical analyses were performed using Two Way ANOVA. * Denotes $P<0.001$ when comparing Cre[+/0] to Cre[0/0] infused with AngII and # denotes $P<0.01$ when comparing comparing Cre+/0 to Cre[0/0] infused with saline.
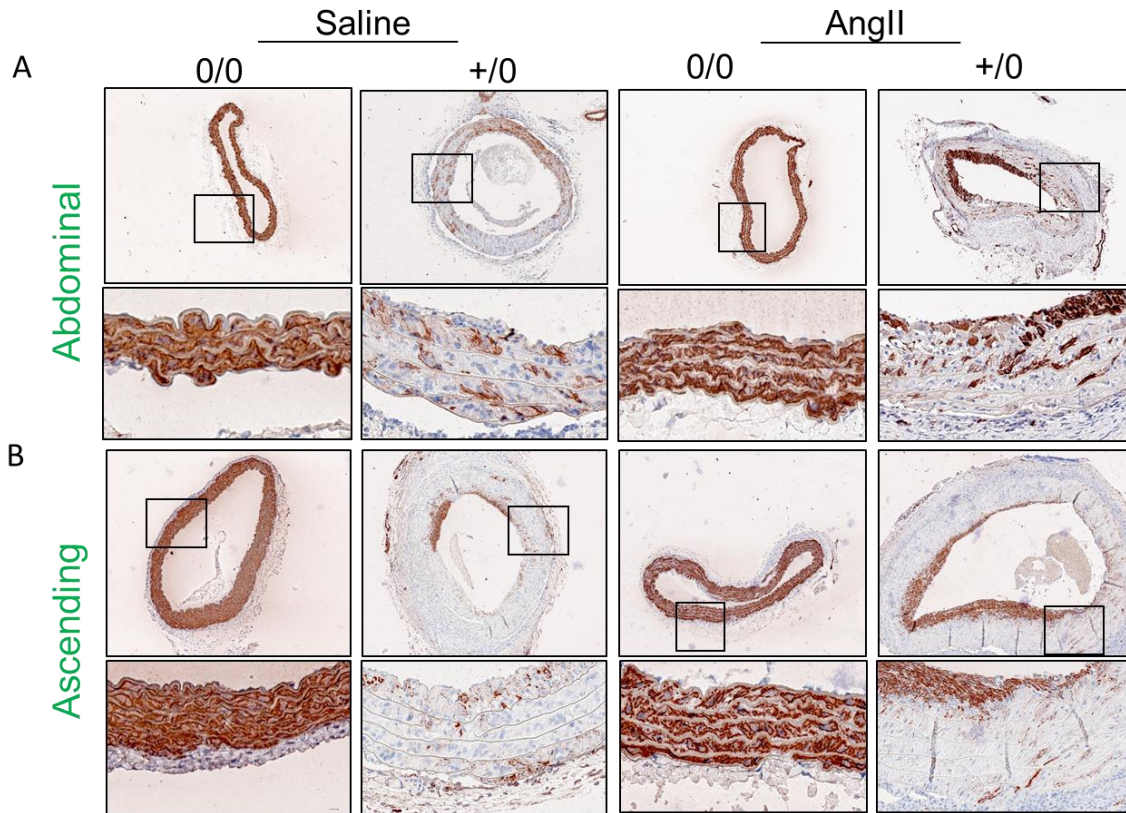
Figure 8.11 Representative images of SMC α-actin positive area on **(A)** Abdominal aortic sections and **(B)** Ascending Aortic Sections form SMC-Beclin1 WT and KO mice infused with either saline or AngII for 28 days.
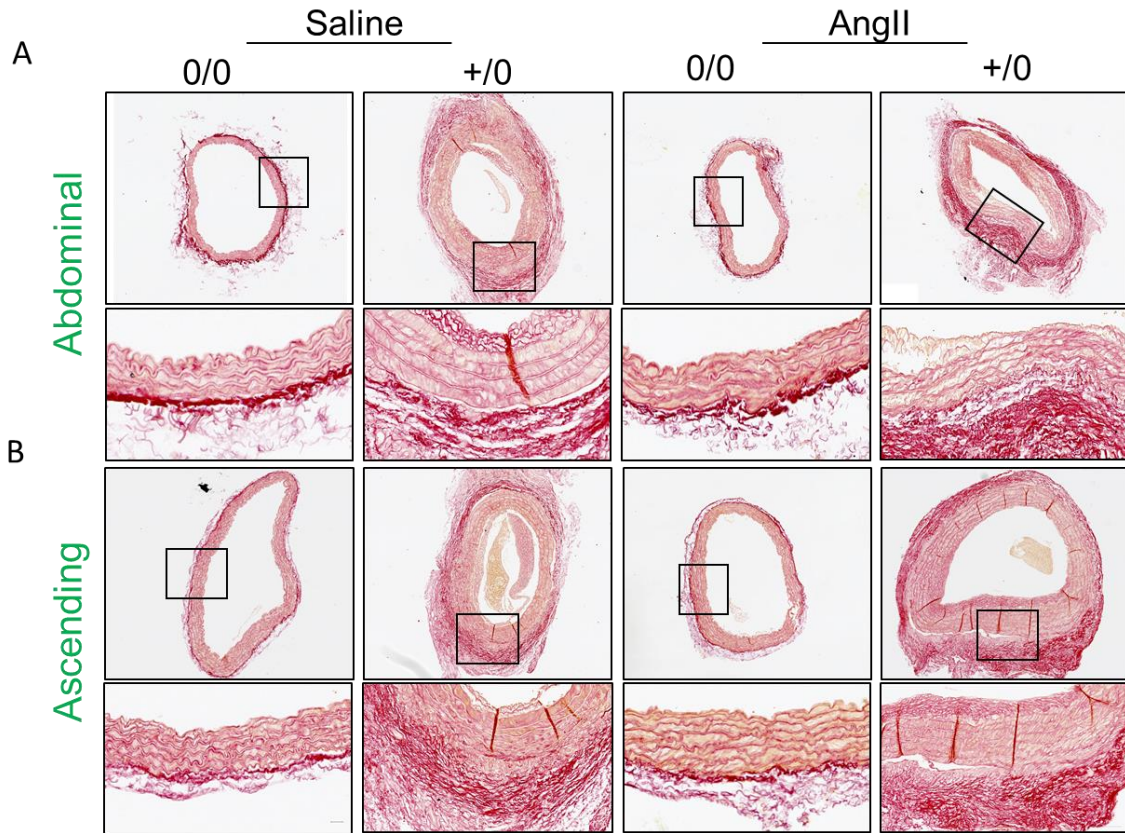
Figure 8.12 Representative images of PSR-staining for Collagen content on **(A)** Abdominal aortic sections and **(B)** Ascending Aortic Sections form SMC-Beclin1 WT and KO mice infused with either saline or AngII for 28 days.

3.14. High dose of AngII had no further effect on SMC- Beclin-1 deficiency accelerated aortic expansion in LDLR$^{-/-}$ mice

Based on the observed increased expansion of aorta starting from the ascending aorta to the lower part of the abdominal aorta with SMC-Beclin-1 deficiency in LDLr$^{-/-}$ mice, we were interested to examine whether increasing the dose of AngII had any localized effect on AAA formation instead of whole aortic expansion.

To address this question, we performed a pilot study utilizing male SMC-Beclin-1 Cre$^{+/0}$ (n=6) and Cre$^{0/0}$ (n=7) mice in LDLr$^{-/-}$ background. Mice were fed a high-fat diet for 5 weeks. After 1 week of diet feeding, they were infused subcutaneously with high dose of AngII (1.0 µg/kg/min) by osmotic mini-pumps for 4 weeks. After 4 weeks of the high dose of AngII infusion, ultrasonography **(Figure 9.1A&B)** and ex-vivo measurements **(figure 9.2A&B)** showed significant aortic luminal dilation and expansion in the Cre0/0 littermate control as expected with the high dose of AngII in hypercholesterolemic mice.   However, in SMC-Beclin-1 deficient mice (Cre$^{+/0}$), the absence of Beclin-1 promoted aortic expansion in all regions including ascending and abdominal aortas. The high dose of AngII did not cause any specific localized AAA expansion in the SMC-Beclin-1 deficient mice compared to the littermate controls. SMC-Beclin-1 deficiency had no influence on high dose AngII-induced AAA incidence **(Figure 9.3).** Furthermore, SMC-Beclin-1 deficiency had no effect on high dose AngII-induced thoracic aortic expansion in LDLr$^{-/-}$ mice **(Figure 9.4A, B&C and Figure 9.5)**
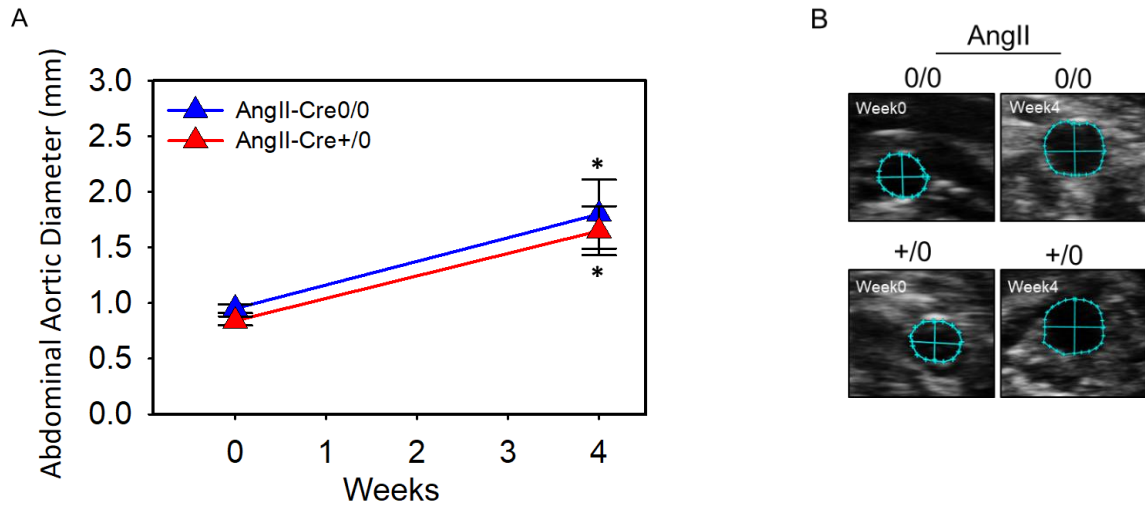
Figure 9.1 High dose of AngII had no effect on SMC- Beclin-1 deficiency accelerated aortic luminal dilation in LDLr$^{-/-}$ mice. (A) Ultrasonic measurements of abdominal aortic diameters at week 0 and week 4 after 28 days of AngII infusion (1.0 µg/kg/min) into Beclin-1 Cre$^{0/0}$ and Cre$^{+/0}$ male LDLr$^{-/-}$ mice. **(B)** Representative ultrasound images of the abdominal aorta week 0 compared to week 4. Statistical analysis was performed using Two-tailed Student's t-test. Means of each group are represented by triangles and error bars are SEM. * denotes $P<0.05$ when comparing Week 4 *vs.* week0 in both groups.
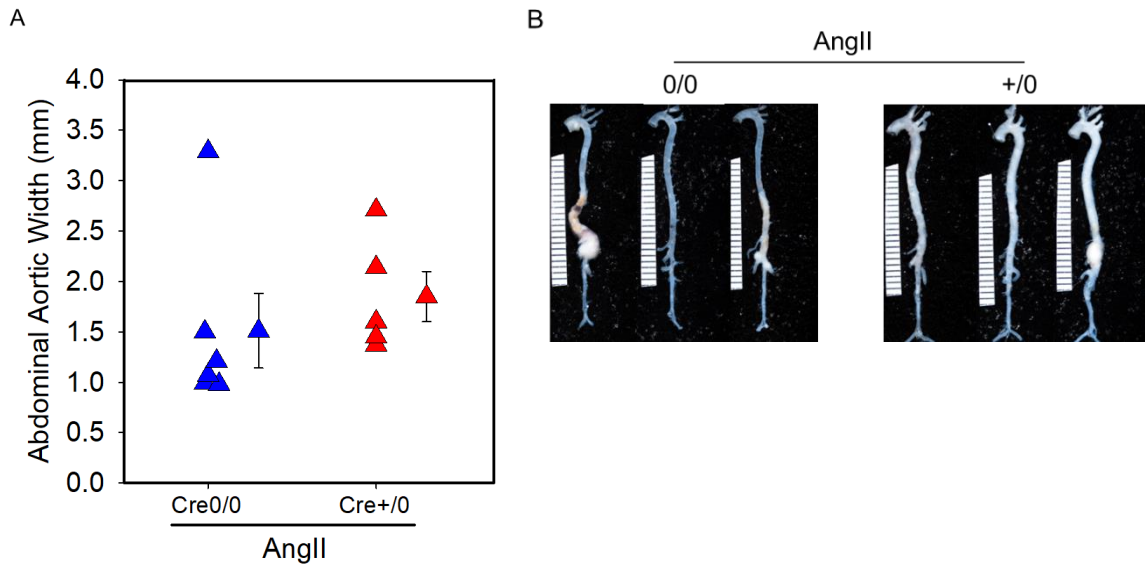
Figure 9.2. High doses of AngII had no effect on SMC- Beclin-1 deficiency accelerated aortic expansion in LDLr$^{-/-}$ mice. (A) Measurements of maximal external width of abdominal aortas after 28 days of AngII infusion. **(B)** Representative images of the abdominal aorta. Statistical analyses were performed using Two-tailed Student's t-test (P=0.177). Triangles represent individual mice and diamonds, and error bars are means and SEM respectively.
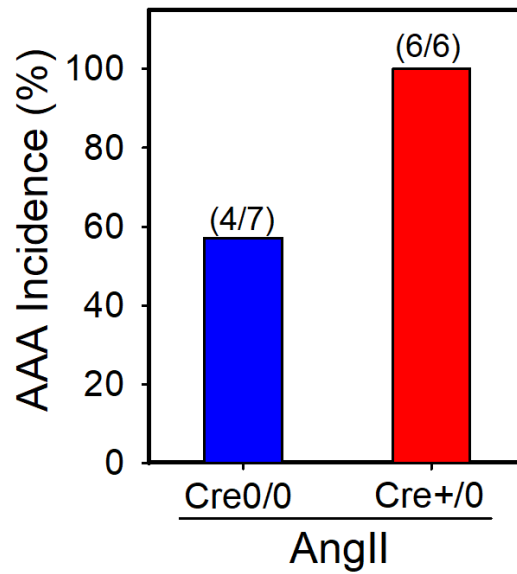
Figure 9.3. Beclin-1 deficiency did not affect AAA incidence in high-dose of AngII-infused mice. The incidence of AAA (>50% increase in aortic width and ruptured aorta) in AngII-infused Beclin-1 $Cre^{0/0}$ and $Cre^{+/0}$ mice. Statistical analyses were performed by Fisher's Exact test (not significant).
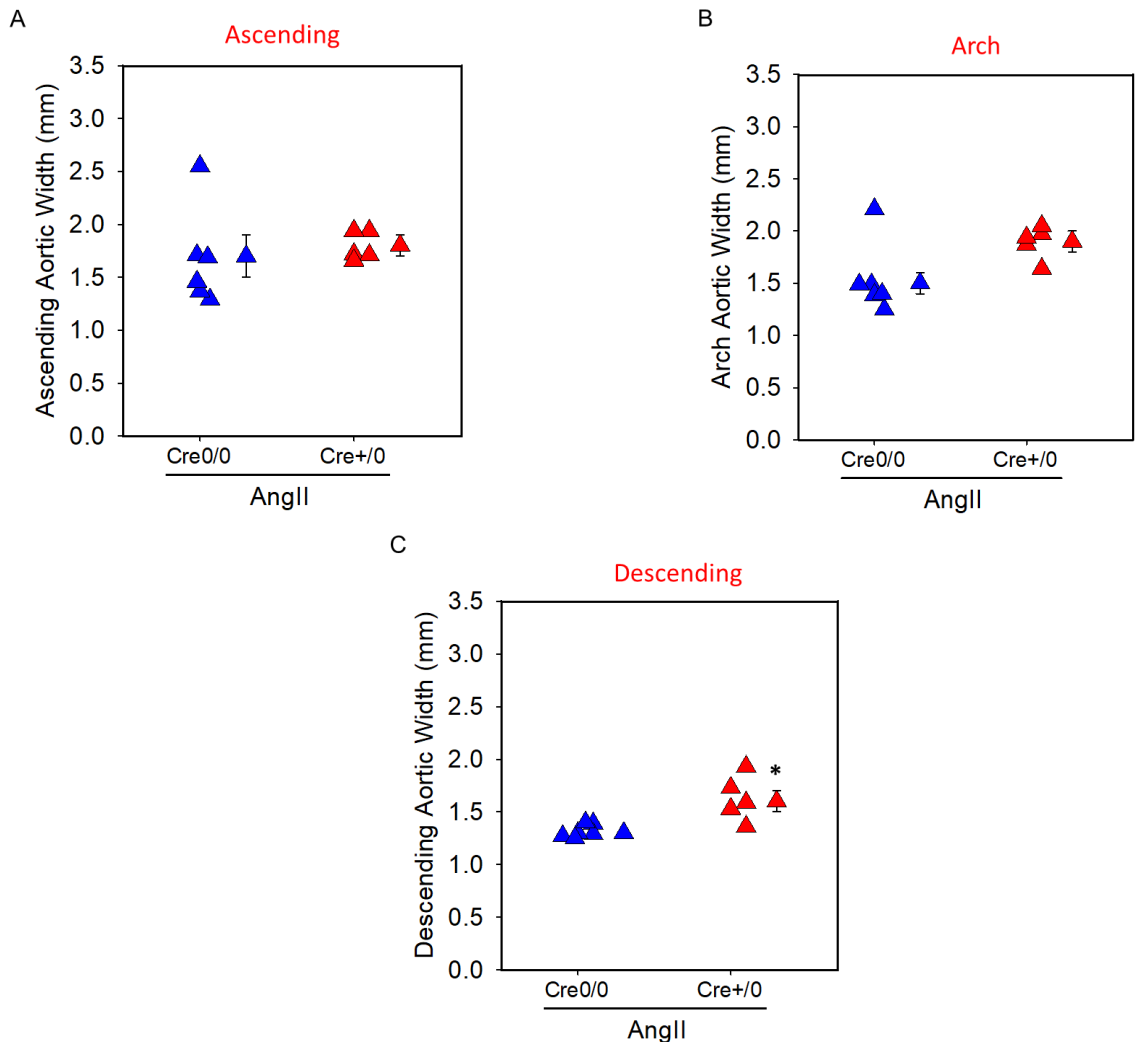
Figure 9.4 Beclin-1 deficiency had no impact on High dose AngII- induced thoracic aortic expansion. *In situ* measurement of **(A)** ascending aortic width, **(B)** arch aortic width and **(C)** descending aortic width in Beclin-1 Acta2 ERT2 Cre[0/0] (n=7) and Cre [+/0] (n=6) mice fed with high fat diet and infused with AngII (1.0 µg/kg/min) at week 4. Circles represent individual mice in each group. Means of each group are represented by diamonds and error bars are SEM. Statistical analyses were performed by Student t-test. * Denotes *P*<0.05
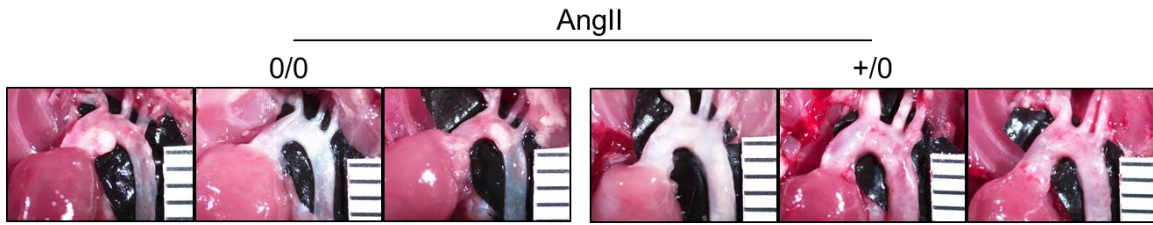
Figure 9.5 Representative images of thoracic aorta from SMC-Beclin1 Cre [+/0] and Cre[0/0] hypercholesterolemic male mice infused with either saline or AngII.

3.15. Beclin1 deficiency in SMCs had no impact on the AAA formation but significantly increased the thoracic aortic expansion in normolipidemic mice

Based on the strong findings on aortic expansion in SMC-Beclin-1 deficiency in hypercholesterolemic LDLr$^{-/-}$ mice, as a next step, we want to understand whether hypercholesterolemia play any critical role in the development of aortic pathology in SMC-Beclin-1 deficient mice. Published literatures demonstrated that high dose of AngII (1.0 µg/kg/min) infusion into normolipidemic mice also resulted in AAA formation but in a less extent compared to the hyperlipidemic mice showing that hyperlipidemia could be a driving force in acceleration of AAA development in mice [67] However, high dose of AngII (1.0 µg/kg/min)-induced ascending aortic aneurysms are shown to be independent of hypercholesterolemia in [112]**.**

To address the role of hypercholesterolemia in SMC-Beclin-1 deficiency induced aortic pathology, we generated SMC-Beclin-1 deficient (Cre+/0) mice and littermate controls (Cre$^{0/0}$) in a normolipidemic B6 background and fed with normal chow diet. After 2 weeks of tamoxifen injection for 5 days, SMC-Beclin-1 Cre0/0 and Cre+/0 mice were infused with either saline or AngII (1.0 µg/kg/min) (n=7 per genotype and infusion). SMC-Beclin-1 deficiency in normolipidemic mice had no impact on end point body weight **(Table VI)** and AAA **(Figure 10.1A&B).** but resulted in significant expansion of the thoracic aorta **(Figure 10.2A-C & Figure 10.3)** in both saline and AngII-infused groups as similar to the hypercholesterolemic mice study **(Figure 8.6A-C).**

AngII infusion had no additional effect on SMC-Beclin-1 deficiency accelerated aortic expansion observed in saline infused mice. In addition, SMC-Beclin-1 deficiency in normolipidemic mice had no effect on AngII-induced AAA expansion. This data clearly suggests that the effect of SMC-Beclin-1 deficiency on aortic expansion in mice is independent of hypercholesterolemia.

Table VI. Effect of SMC-Beclin-1 deletion on body weight and plasma cholesterol in normolipidemic male mice infused with either saline or AngII

Groups	Cre0/0		Cre+/0	
Infusion	Saline	AngII (1000ng/kg/min)	Saline	AngII (1.0 µg/kg/min)
N	7	7	7	6
Baseline Body Weight	27.4 ± 1.2	30.2 ± 0.8	28.5 ± 1.4	30.2± 0.5
End Point Body Weight (g)	30.4 ± 1.3	29.1 ± 0.7	29.7 ± 1.2	26.8 ± 0.3*

Table VI. Values are represented as means ± SEMs. Body weights were determined at baseline and termination. * Denotes *P*<0.05 Week 4 vs Week0 by Two-Way RM ANOVA.
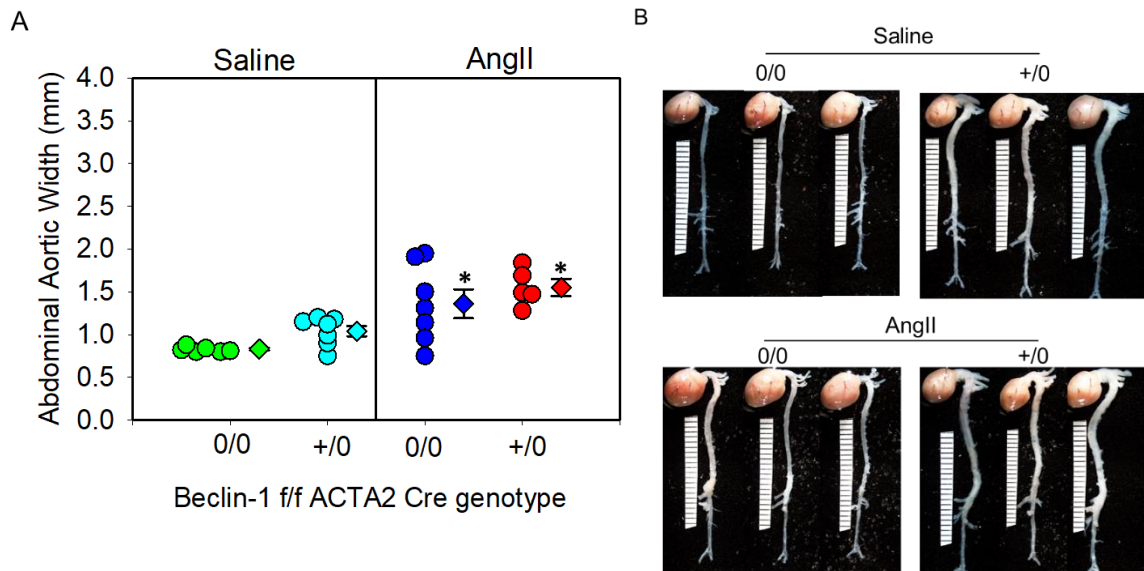
Figure 10.1 Beclin-1 deficiency in SMCs had no impact on AngII-induced abdominal aortic width in normolipidemic mice. (A) *Ex-vivo* abdominal diameters of Beclin-1 Acta2 ERT2 Cre[0/0] (n=7) and Cre [+/0] (n=7) mice fed with chow diet and infused with either saline or AngII (1.0 µg/kg/min). **(B)** Aortic pictographs nearest the mean. Circles represent individual mice in each group. Means of each group are represented by diamonds and error bars are SEM. * denotes $P < 0.05$ when comparing AngII infused mice to saline groups. Statistical analyses were performed by Two-way ANOVA.
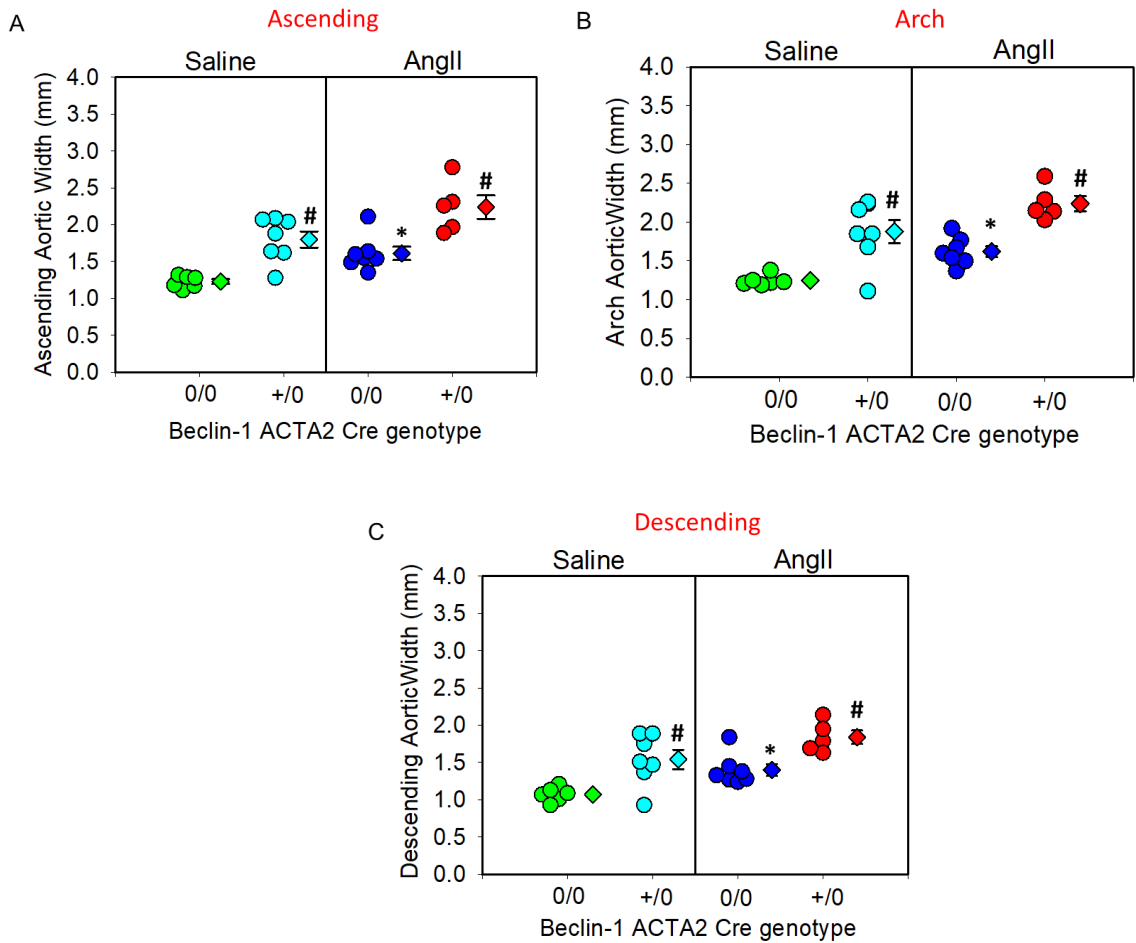
Figure 10.2 Beclin-1 deficiency accelerated ascending aortic expansion in normolipidemic male mice. (A) *In situ* ascending aortic width measurement of Beclin-1 Acta2 ERT2 Cre[0/0] and Cre +/0 mice fed with chow diet and infused with either saline or AngII at week 4. **(B)** Representative images of ascending aorta. Circles represent individual mice in each group. Means of each group are represented by diamonds and error bars are SEM. * denotes $P < 0.05$ when comparing AngII vs saline groups. # denotes $P < 0.001$ when comparing Cre [+/0] *vs.* Cre 0/0 in either saline or AngII-infused mice.

Saline

0/0   +/0

AngII

0/0   +/0
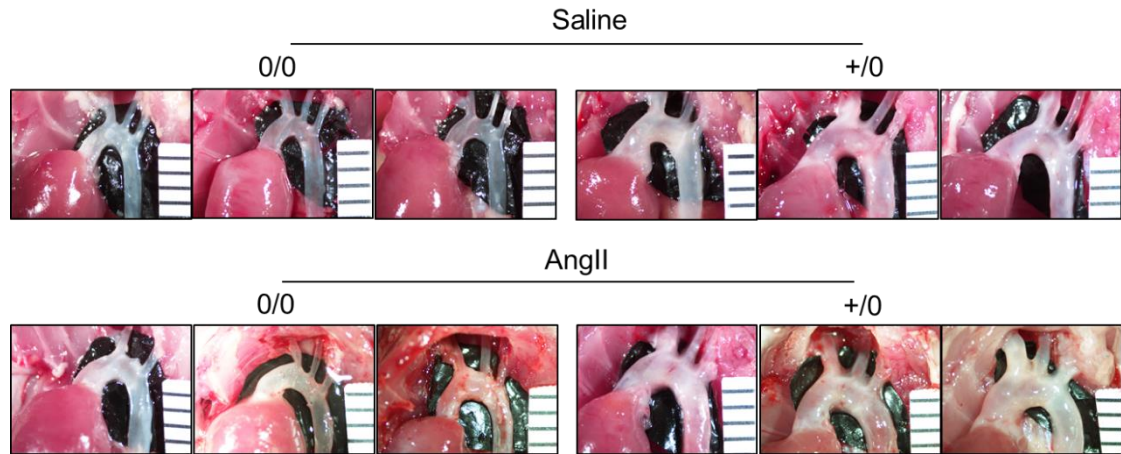
Figure 10.3 Representative images of thoracic aorta from SMC-Beclin1 Cre $^{+/0}$ and Cre$^{0/0}$ normolipidemic male mice infused with either saline or AngII.

CHAPTER 4

Discussion and Future Direction

By utilizing the highly reproducible AngII-induced AAA mouse model in hypercholesterolemic LDLr-/- mice, I demonstrated that autophagy proteins are increased in AngII-infused abdominal aortas. Using 3-methyaladenine, a common autophagic inhibitor, we did not demonstrate any effect of autophagy inhibition on AngII-induced AAA formation. Furthermore, using Celastrol, an autophagy inducer, we demonstrated that Celastrol supplementation accelerated AngII-induced AAA formation in male mice. Surprisingly, Celastrol supplementation also abolished sexual dimorphic effect of AAAs, and promoted AngII-induced AAAs in female mice as similar to male mice. Interestingly, Celastrol supplementation accelerated AngII-induced AAAs is strongly associated with the activation of matrix metalloproteinase (MMP) -9 but had no effect on autophagy proteins. Using a novel SMC-specific autophagy protein, Beclin-1, inducible deficient mice, we examined the contribution of autophagy to AngII-induced AAAs and identified that inducible depletion of Beclin-1 strongly promoted the development of aortic aneurysms in mice which supports a critical role for SMC-derived autophagy proteins in maintaining aortic structural integrity during AAA development.

AngII infusion into male hypercholesterolemic mice markedly increased key proteins involved in autophagic process including Beclin-1, a marker for required for initiation of autophagy and autophagosome formation and LC3B-II, an autophagosome marker associated with autophagic vacuoles throughut the autophagy process[82, 84, 85] **,** in the abdominal aorta which is in correlation with

94

published reports of increased autophagy protein in human AAAs[87, 88]. A published study using cultured rat aortic SMCs incubated with AngII suggests a possible contribution of RhoA -Rho kinase dependent mechanism in increasing AngII-induced autophagy proteins[97]. However, the mechanism underlying the accelerated autophagy proteins in human AAAs or in AngII-infused mice aortas are yet to be defined.

In our study, 3-MA, a PI3 kinase inhibitor widely used as an autophagy inhibitor, at the dose of 30mg/kg/day had no effect on AngII-induced AAAs in hypercholesterolemic mice. The 3-MA was administered daily via oral gavage. Previous studies demonstrated that 3-MA administration via intraperitoneal injection at the dose of 30 mg/kg/day significantly suppressed AngII-induced hypertension in normolipidemic mice[113].The observed no effect on AngII-induced AAA with 3-MA administration in our present study could be due to insufficient dosage of 3-MA by oral gavage or it is because of the fact that 3-MA is not a specific inhibitor and could affect class I PI3K which has opposite effect to class III PI3K to induce the autophagy. Otherwise, it may suggest that 3-MA mediated autophagy inhibition had no effect on AngII-induced AAA in hypercholesterolemic mice. Further dose dependent studies are needed to understand the effect of pharmacological inhibition of autophagy on AAAs in mice.

Celastrol supplementation significantly increased AngII-induced AAA formation in male hypercholesterolemic mice. Celastrol a pentacyclic triterpene was shown to accelerate autophagy in both cultured cells and mice under various disease

conditons[104, 105]. In addition to its effect on autophagy, Celastrol also shown to suppress obesity and inflammation[114]. An important point to note that Celastrol supplementation accelerated AAA formation only with low dose of AngII (0.5 µg /kg/min for 28 days), not with the high dose of AngII (1.0 µg/kg/min). AngII is well known to induce AAA formation in hypercholesterolemic mice in a dose dependent manner. With the dose of 1.0 µg/kg/min, AngII causes an AAA incidence of about 80% whereas it shows 30-40% AAA incidence with the dose of 0.5 µg/kg/min, in male hypercholesterolemic mice[67, 80]. Therefore, to study an accelerated effect on AngII-induced AAA formation with any gene deficiency or pharmacological drugs, the dose of 0.5 µg/kg/min is optimal to arrive any statistical difference. The observed acceleration on AngII-induced AAA with Celastrol supplementation is not anticipated. Based on the observed early acceleration in aortic luminal dilation in Celastrol supplementation group of mice with high dose of AngII (1.0 µg/kg/min), we reduced the dose of AngII to 0.5 µg/kg/min for the subsequent study, which showed a significant increase in AAA compared to the control group. Like humans, AAA formation in mice is 4-5 times greater in males than females. By infusion of a high dose of AngII into female mice, only 20-30% of female mice get aneurysms [68, 115]. Based on this evidence, we were interested in how Celastrol supplementation affects AAA formation in female mice. Our data indicated that Celastrol supplementation combined with AngII infusion resulted in propounding increase in internal luminal dilation and AAA formation in female mice as comparable to male mice. Celastrol supplementation dramatically ablated the sexual dimorphism of AAA in mice.

Furthermore, Western blot analyses using aortic tissue from Celastrol supplemented AngII-infused mice clearly demonstrated that Celastrol had no effect on aortic autophagy proteins in our model. Consistent with the published literatures [116, 117], in our study, Celastrol supplementation significantly suppressed Western diet-induced body weight gain. The decreased body weight gain observed with Celastrol supplementation could be due to its effect on demonstrated leptin sensitization [116]. However, we did not observe any difference in diet consumption. The Celastrol is shown to mediate its anti-obesity effect through interleukin-1 receptor (IL1R) as IL1R mice are totally resistant to Celastrol mediated anti-obesity effect [116]. In addition, diet-mediated calorie reduction in mice is shown to reduce AngII-induced AAA formation in ApoE-/- mice[118]. However, interestingly, in our study, irrespective of body weight loss, Celastrol supplementation significantly increased AngII-induced AAA formation in both male and female LDLr$^{-/-}$ mice without influencing aortic autophagy proteins.

One of the hallmarks of aortic aneurysm is elastin degradation which leads to aortic dilation and rupture[5, 24]. Therefore, we investigated whether Celastrol supplementation could exacerbate the AngII-induced elastin breaks in male and female mice. Verhoeff's Van Gieson (EVG) elastin staining revealed significant elastin degradation in the aortic wall. Additionally, Celastrol reduced medial SMC positive area and increased adventitial thickness and adventitial collagen deposition in these mice. Since Verhoef's staining revealed a dramatic increase in elastin breaks by Celastrol supplementation, we studied the effect of Celastrol on matrix metalloprotease (MMP) activity in abdominal aortic tissues obtained from

male and female mice 2 weeks after AngII infusion. MMPs like MMP2 and MMP9 play a crucial role in AAA formation by degradation of elastin fibers in the aortic media layer [119]. Although MMP2 and MMP9 activities increased with AngII infusion compared to saline groups, only MMP9 were significantly upregulated by Celastrol supplementation in both male and female mice. The Celastrol supplementation mediated increase in AngII-induced aortic MMP9 activity may partially explain the mechanism through which Celastrol promotes AngII-induced elastin break and aortic dilation in both male and female mice. However, in the literature, several studies in different disease conditions such as intrahepatic cholestatic of pregnancy [120], or breast cancer [121, 122], Celastrol is shown to suppress MMP-2 and -9 activities which is in contrary with our current observation in AngII-induced AAA model. Further studies are warranted to understand mechanisms by which Celastrol promotes AngII-induced MMP activation and AAA.

Based on the outcomes of our pharmacological (3-MA and Celastrol) approach studies, we were not able to conclude the role of autophagy in AngII-induced AAAs. To further understand if there is any potential role or contribution of autophagy in AngII-induced AAAs, we utilized the genetic mouse model of autophagy. Based on our preliminary findings that Beclin-1 is highly increased in AngII-infused aortas, we generated a transgenic mouse with SMC-specific deficiency of Beclin-1. The rationale for generating Beclin-1 deficient mice in SMCs was based on the fact that Beclin-1 plays a critical role in the induction of autophagy process[107, 109]. Furthermore, SMCs are an integral part of the thick aortic medial layer which helps to maintain the structural integrity [38, 40]. As a

key component of autophagy process, Beclin-1 deficiency results in embryonic lethality in mice[107]. By utilizing Beclin-1 floxed mice and tamoxifen-inducible SMC-Acta2 Cre recombinase mice, we generated the tamoxifen-inducible SMC-Specific Beclin-1 deficient mice.

SMC-specific inducible depletion of Beclin-1 in hypercholesterolemic significantly increased Aortic dilation in both saline and AngII-infused mice. Our data clearly demonstrates that depletion of Beclin-1 mediated autophagy in SMCs is sufficient to accelerate aortic dilation/expansion irrespective of AngII infusion, which strongly indicates that SMC-derived autophagy play a critical role in aneurysm formation. Very interestingly, in SMC-specific Beclin-1 deficient mice, the aortic dilation originates from the ascending aorta to the diaphragm of the abdominal aorta. Earlier studies using SMC-ATG7 mice, Azza Ramadan *et al.,* reported that SMC-ATG7 deficiency results in increase AAA incidence accompanied by higher mortality rate in AngII-infused mice due to cardiac failure[38]. In addition, using SMC-ATG5 deficient mice, showed deletion of ATG5 in VSMCs is also related to higher rate of aortic dissection in normolipidemic mice[90]. However, in our present study, the observed phenotype of aortic dilation starting from ascending aorta to the suprarenal abdominal aorta with SMC-Beclin-1 deficiency is highly unique and suggests that Beclin-1-mediated autophagy play a unique and critical role in the regulation of aortic aneurysmal development. Furthermore, the observed reduction in body weight and plasma cholesterol in SMC-Beclin-1 deficient mice under high fat diet conditions could be due to defect in dietary fat absorption. In support, SMCs present in the gastro-intestinal tract are shown to play an important

role in gastrointestinal motility[123]. However, further studies are warranted to understand the underlying mechanisms in observed reduced body weight and plasma cholesterol concentrations in SMC-Beclin-1 deficient mice under high fat diet.

Histological characterization of aortic sections from ascending and abdominal aorta revealed that SMC-Beclin-1 deficiency resulted in a significant aortic medial expansion, elastin layer breaks, loss of α-SMC actin positive area in the aortic media and thickened adventitia with accumulated Picrosirius positive collagen proteins. By utilizing SMC-Beclin-1 deficient mice in normolipidemic background, we observed a similar phenotype of aortic dilation, medial expansion, and elastin layer breaks without any change in body weight, which highlights that effect of SMC-Beclin-1 deficiency on aortic pathology is independent of hypercholesterolemia. However, currently, it is not clear if the increased medial thickening is due to medial hyperplasia or hypertrophy. AngII infusion is shown to promote ascending aortic medial hyperplasia and aortic medial hypertrophy in mice [124, 125]**.** In addition, autophagy is shown to promote AngII-induced SMC hypertrophy [126]. Interestingly, in our study, irrespective of AngII infusion, inducible depletion of Beclin-1 in SMCs in matured mice resulted in significant medial thickening in both ascending and abdominal aortas. In summary, our findings strongly suggest that Beclin-1 in vascular SMCs plays a critical role in suppressing aortic aneurysmal development in mice.

Our future studies will focus to understand the mechanism of aortic expansion in SMC-Beclin-1 deficient mice by addressing:

(i)   The potential role of Beclin-1-mediated autophagy on SMC hyperplasia and hypertrophy.

(ii)   The effect of SMC-Beclin-1 deficiency on ECM proteins – elastin and collagen distribution and stability.

(iii)   The effect of SMC-Beclin-1 deficiency on SMC phenotype switch during aortic aneurysmal development.

(iv)   The effect of SMC-Beclin-1 deficiency on sexual dimorphism on aortic aneurysmal development.

(v)   The effect of SMC-Beclin-1 deficiency on hypercholesterolemia and atherosclerosis in mice.

References

1. Kuivaniemi, H., et al., Understanding the pathogenesis of abdominal aortic aneurysms. Expert Rev Cardiovasc Ther, 2015. 13(9): p. 975-87.
2. Anagnostakos, J. and B.K. Lal, Abdominal aortic aneurysms. Prog Cardiovasc Dis, 2021. 65: p. 34-43.
3. Zhong, L., et al., SM22alpha (Smooth Muscle 22alpha) Prevents Aortic Aneurysm Formation by Inhibiting Smooth Muscle Cell Phenotypic Switching Through Suppressing Reactive Oxygen Species/NF-kappaB (Nuclear Factor-kappaB). Arterioscler Thromb Vasc Biol, 2019. 39(1): p. e10-e25.
4. Golledge, J., et al., Abdominal aortic aneurysm: pathogenesis and implications for management. Arterioscler Thromb Vasc Biol, 2006. 26(12): p. 2605-13.
5. Davis, F.M., D.L. Rateri, and A. Daugherty, Abdominal aortic aneurysm: novel mechanisms and therapies. Curr Opin Cardiol, 2015. 30(6): p. 566-73.
6. Altobelli, E., et al., Risk Factors for Abdominal Aortic Aneurysm in Population-Based Studies: A Systematic Review and Meta-Analysis. Int J Environ Res Public Health, 2018. 15(12).
7. Cornuz, J., et al., Risk factors for asymptomatic abdominal aortic aneurysm: Systematic review and meta-analysis of population-based screening studies. European Journal of Public Health, 2004. 14(4): p. 343-349.
8. Derubertis, B.G., et al., Abdominal aortic aneurysm in women: prevalence, risk factors, and implications for screening. (0741-5214 (Print)).
9. Singh, K., et al., Prevalence of and risk factors for abdominal aortic aneurysms in a population-based study : The Tromsø Study. (0002-9262 (Print)).
10. Lo, R.C. and M.L. Schermerhorn, Abdominal aortic aneurysms in women. J Vasc Surg, 2016. 63(3): p. 839-44.
11. Hannawa, K.K., G.R. Eliason Jl Fau - Upchurch, Jr., and G.R. Upchurch, Jr., Gender differences in abdominal aortic aneurysms. (1708-5381 (Print)).
12. Kapila, V., et al., Screening for abdominal aortic aneurysms in Canada: 2020 review and position statement of the Canadian Society for Vascular Surgery. Canadian Journal of Surgery, 2021. 64(5): p. E461.
13. Benson, R.A., et al., Screening results from a large United Kingdom abdominal aortic aneurysm screening center in the context of optimizing United Kingdom National Abdominal Aortic Aneurysm Screening Programme protocols. (1097-6809 (Electronic)).
14. Stackelberg, O., et al., Alcohol Consumption, Specific Alcoholic Beverages, and Abdominal Aortic Aneurysm. Circulation, 2014. 130(8): p. 646-652.
15. Golledge, J., et al., Association between serum lipoproteins and abdominal aortic aneurysm. (1879-1913 (Electronic)).
16. Törnwall, M.E., et al., Life-Style Factors and Risk for Abdominal Aortic Aneurysm in a Cohort of Finnish Male Smokers. Epidemiology, 2001. 12(1).

17.   Daugherty, A. and L.A. Cassis, Mechanisms of abdominal aortic aneurysm formation. Current Atherosclerosis Reports, 2002. 4(3): p. 222-227.

18.   Siasos, G., et al., The Role of Endothelial Dysfunction in Aortic Aneurysms. (1873-4286 (Electronic)).

19.   Daugherty, A., et al., Angiotensin II infusion promotes ascending aortic aneurysms: attenuation by CCR2 deficiency in apoE-/- mice. Clin Sci (Lond), 2010. 118(11): p. 681-9.

20.   Ishibashi, M., et al., Bone marrow-derived monocyte chemoattractant protein-1 receptor CCR2 is critical in angiotensin II-induced acceleration of atherosclerosis and aneurysm formation in hypercholesterolemic mice. Arterioscler Thromb Vasc Biol, 2004. 24(11): p. e174-8.

21.   MacTaggart, J.N., et al., Deletion of CCR2 but not CCR5 or CXCR3 inhibits aortic aneurysm formation. Surgery, 2007. 142(2): p. 284-8.

22.   Owens, A.P., 3rd, et al., MyD88 deficiency attenuates angiotensin II-induced abdominal aortic aneurysm formation independent of signaling through Toll-like receptors 2 and 4. Arterioscler Thromb Vasc Biol, 2011. 31(12): p. 2813-9.

23.   Daha, M.R., et al., Interleukin-1[beta] and tumor necrosis factor-[alpha] release in normal and diseased human infrarenal aortas. Journal of Vascular Surgery, 1992. 16(5): p. 0784-0789.

24.   Davis, F.M., D.L. Rateri, and A. Daugherty, Mechanisms of aortic aneurysm formation: translating preclinical studies into clinical therapies. Heart, 2014. 100(19): p. 1498-505.

25.   Szekanecz, Z., et al., Human atherosclerotic abdominal aortic aneurysms produce interleukin (IL)-6 and interferon-gamma but not IL-2 and IL-4: The possible role for IL-6 and interferon-gamma in vascular inflammation. Agents and Actions, 1994. 42(3): p. 159-162.

26.   Johnston, W.F., et al., Genetic and pharmacologic disruption of interleukin-1beta signaling inhibits experimental aortic aneurysm formation. Arterioscler Thromb Vasc Biol, 2013. 33(2): p. 294-304.

27.   Wang, Y., et al., TGF-beta activity protects against inflammatory aortic aneurysm progression and complications in angiotensin II-infused mice. J Clin Invest, 2010. 120(2): p. 422-32.

28.   Davis, F.M., A. Rateri Dl Fau - Daugherty, and A. Daugherty, Abdominal aortic aneurysm: novel mechanisms and therapies. (1531-7080 (Electronic)).

29.   Gargiulo, M., et al., Content and turnover of extracellular matrix protein in human "nonspecific" and inflammatory abdominal aortic aneurysms. (0950-821X (Print)).

30.   Longo, G.M., et al., Matrix metalloproteinases 2 and 9 work in concert to produce aortic aneurysms. Journal of Clinical Investigation, 2002. 110(5): p. 625-632.

31.   McMillan, W.D. and W.H. Pearce, Increased plasma levels of metalloproteinase-9 are associated with abdominal aortic aneurysms. Journal of Vascular Surgery, 1999. 29(1): p. 122-129.

32. Goodall, S., et al., Ubiquitous elevation of matrix metalloproteinase-2 expression in the vasculature of patients with abdominal aneurysms. (1524-4539 (Electronic)).

33. Ailawadi, G., J.L. Eliason, and G.R. Upchurch, Current concepts in the pathogenesis of abdominal aortic aneurysm. Journal of Vascular Surgery, 2003. 38(3): p. 584-588.

34. Thompson, R.W., et al., Pathophysiology of abdominal aortic aneurysms: insights from the elastase-induced model in mice with different genetic backgrounds. Ann N Y Acad Sci, 2006. 1085: p. 59-73.

35. Thompson, R.W., et al., Production and localization of 92-kilodalton gelatinase in abdominal aortic aneurysms. An elastolytic metalloproteinase expressed by aneurysm-infiltrating macrophages. (0021-9738 (Print)).

36. Pyo, R., et al., Targeted gene disruption of matrix metalloproteinase-9 (gelatinase B) suppresses development of experimental abdominal aortic aneurysms. (0021-9738 (Print)).

37. Manning, M.W., L.A. Cassis, and A. Daugherty, Differential effects of doxycycline, a broad-spectrum matrix metalloproteinase inhibitor, on angiotensin II-induced atherosclerosis and abdominal aortic aneurysms. Arterioscler Thromb Vasc Biol, 2003. 23(3): p. 483-8.

38. Ramadan, A., et al., Loss of vascular smooth muscle cell autophagy exacerbates angiotensin II-associated aortic remodeling. J Vasc Surg, 2018. 68(3): p. 859-871.

39. López-Candales, A., et al., Decreased vascular smooth muscle cell density in medial degeneration of human abdominal aortic aneurysms. (0002-9440 (Print)).

40. Rombouts, K.B., et al., The role of vascular smooth muscle cells in the development of aortic aneurysms and dissections. Eur J Clin Invest, 2022. 52(4): p. e13697.

41. Holmes, D.R., et al., Smooth muscle cell apoptosis and p53 expression in human abdominal aortic aneurysms. Ann N Y Acad Sci, 1996. 800: p. 286-7.

42. Liao, S., et al., Accelerated replicative senescence of medial smooth muscle cells derived from abdominal aortic aneurysms compared to the adjacent inferior mesenteric artery. J Surg Res, 2000. 92(1): p. 85-95.

43. Chi, C., et al., Vascular smooth muscle cell senescence and age-related diseases: State of the art. Biochim Biophys Acta Mol Basis Dis, 2019. 1865(7): p. 1810-1821.

44. Chen, H.-Z., et al., Age-Associated Sirtuin 1 Reduction in Vascular Smooth Muscle Links Vascular Senescence and Inflammation to Abdominal Aortic Aneurysm. Circulation Research, 2016. 119(10): p. 1076-1088.

45. Liao, S., et al., Accelerated replicative senescence of medial smooth muscle cells derived from abdominal aortic aneurysms compared to the adjacent inferior mesenteric artery. (0022-4804 (Print)).

46. Ailawadi, G., et al., Smooth muscle phenotypic modulation is an early event in aortic aneurysms. J Thorac Cardiovasc Surg, 2009. 138(6): p. 1392-9.

47.	Mao, N., et al., Phenotypic switching of vascular smooth muscle cells in animal model of rat thoracic aortic aneurysm. (1569-9285 (Electronic)).

48.	Alexander, M.R. and G.K. Owens, Epigenetic control of smooth muscle cell differentiation and phenotypic switching in vascular development and disease. Annu Rev Physiol, 2012. 74: p. 13-40.

49.	Mao, N., et al., Phenotypic switching of vascular smooth muscle cells in animal model of rat thoracic aortic aneurysm. Interact Cardiovasc Thorac Surg, 2015. 21(1): p. 62-70.

50.	De Meyer, G.R., et al., Autophagy in vascular disease. Circ Res, 2015. 116(3): p. 468-79.

51.	Gatica, D., et al., The role of autophagy in cardiovascular pathology. Cardiovasc Res, 2022. 118(4): p. 934-950.

52.	Jia, G., et al., Insulin-like growth factor-1 and TNF-alpha regulate autophagy through c-jun N-terminal kinase and Akt pathways in human atherosclerotic vascular smooth cells. Immunol Cell Biol, 2006. 84(5): p. 448-54.

53.	Zhang, Y.Y., et al., Autophagy: a killer or guardian of vascular smooth muscle cells. J Drug Target, 2020. 28(5): p. 449-455.

54.	Miller, F.J., Jr., et al., Oxidative stress in human abdominal aortic aneurysms: a potential mediator of aneurysmal remodeling. Arterioscler Thromb Vasc Biol, 2002. 22(4): p. 560-5.

55.	McCormick, M.L., D. Gavrila, and N.L. Weintraub, Role of oxidative stress in the pathogenesis of abdominal aortic aneurysms. Arterioscler Thromb Vasc Biol, 2007. 27(3): p. 461-9.

56.	Guzik, B., et al., Mechanisms of oxidative stress in human aortic aneurysms--association with clinical risk factors for atherosclerosis and disease severity. International journal of cardiology, 2013. 168(3): p. 2389-2396.

57.	Li, Y. and P.J. Pagano, Microvascular NADPH oxidase in health and disease. (1873-4596 (Electronic)).

58.	Daugherty, A. and L.A. Cassis, Mouse models of abdominal aortic aneurysms. Arterioscler Thromb Vasc Biol, 2004. 24(3): p. 429-34.

59.	Golledge, J., Abdominal aortic aneurysm: update on pathogenesis and medical treatments. Nat Rev Cardiol, 2019. 16(4): p. 225-242.

60.	Liu, S., et al., Mineralocorticoid receptor agonists induce mouse aortic aneurysm formation and rupture in the presence of high salt. Arterioscler Thromb Vasc Biol, 2013. 33(7): p. 1568-79.

61.	Cassis, L.A., et al., ANG II infusion promotes abdominal aortic aneurysms independent of increased blood pressure in hypercholesterolemic mice. Am J Physiol Heart Circ Physiol, 2009. 296(5): p. H1660-5.

62.	Daugherty, A., L.A. Manning Mw Fau - Cassis, and L.A. Cassis, Angiotensin II promotes atherosclerotic lesions and aneurysms in apolipoprotein E-deficient mice. (0021-9738 (Print)).

63.	Daugherty, A., L.A. Cassis, and H. Lu, Complex pathologies of angiotensin II-induced abdominal aortic aneurysms. J Zhejiang Univ Sci B, 2011. 12(8): p. 624-8.

64. Eagleton, M.J., et al., Early increased MT1-MMP expression and late MMP-2 and MMP-9 activity during Angiotensin II induced aneurysm formation. J Surg Res, 2006. 135(2): p. 345-51.

65. Lu, H., et al., The role of the renin-angiotensin system in aortic aneurysmal diseases. (1534-3111 (Electronic)).

66. Barisione, C., et al., Rapid dilation of the abdominal aorta during infusion of angiotensin II detected by noninvasive high-frequency ultrasonography. J Vasc Surg, 2006. 44(2): p. 372-6.

67. Daugherty, A. and L. Cassis, Chronic Angiotensin II Infusion Promotes Atherogenesis in Low Density Lipoprotein Receptor −/− Mice. Annals of the New York Academy of Sciences, 1999. 892(1): p. 108-118.

68. Alsiraj, Y., et al., Female Mice With an XY Sex Chromosome Complement Develop Severe Angiotensin II-Induced Abdominal Aortic Aneurysms. Circulation, 2017. 135(4): p. 379-391.

69. Rowinska, Z., et al., Establishment of a new murine elastase-induced aneurysm model combined with transplantation. PLoS One, 2014. 9(7): p. e102648.

70. Wang, Y., S. Krishna, and J. Golledge, The calcium chloride-induced rodent model of abdominal aortic aneurysm. Atherosclerosis, 2013. 226(1): p. 29-39.

71. Karatas, A., et al., Deoxycorticosterone Acetate-Salt Mice Exhibit Blood Pressure–Independent Sexual Dimorphism. Hypertension, 2008. 51(4): p. 1177-1183.

72. Weiss, D. and W.R. Taylor, Deoxycorticosterone Acetate Salt Hypertension in Apolipoprotein E−/− Mice Results in Accelerated Atherosclerosis. Hypertension, 2008. 51(2): p. 218-224.

73. Liu, S., M.C. Gong, and Z. Guo, A New Mouse Model for Introduction of Aortic Aneurysm by Implantation of Deoxycorticosterone Acetate Pellets or Aldosterone Infusion in the Presence of High Salt. (1940-6029 (Electronic)).

74. Lederle, F.A., et al., Open versus Endovascular Repair of Abdominal Aortic Aneurysm. N Engl J Med, 2019. 380(22): p. 2126-2135.

75. Shen, Y.H. and S.A. LeMaire, Molecular pathogenesis of genetic and sporadic aortic aneurysms and dissections. Curr Probl Surg, 2017. 54(3): p. 95-155.

76. Isselbacher, E.M., Thoracic and abdominal aortic aneurysms. Circulation, 2005. 111(6): p. 816-28.

77. Lu, H. and A. Daugherty, Aortic Aneurysms. Arterioscler Thromb Vasc Biol, 2017. 37(6): p. e59-e65.

78. Koenig, S.N., et al., Notch1 haploinsufficiency causes ascending aortic aneurysms in mice. JCI Insight, 2017. 2(21).

79. El-Hamamsy, I. and M.H. Yacoub, Cellular and molecular mechanisms of thoracic aortic aneurysms. Nat Rev Cardiol, 2009. 6(12): p. 771-86.

80. Rateri, D.L., et al., Angiotensin II induces region-specific medial disruption during evolution of ascending aortic aneurysms. Am J Pathol, 2014. 184(9): p. 2586-95.

81. Loeys, B.L., et al., A syndrome of altered cardiovascular, craniofacial, neurocognitive and skeletal development caused by mutations in TGFBR1 or TGFBR2. Nat Genet, 2005. 37(3): p. 275-81.

82. Feng, Y., et al., The machinery of macroautophagy. Cell Res, 2014. 24(1): p. 24-41.

83. Mizushima, N. and M. Komatsu, Autophagy: renovation of cells and tissues. Cell, 2011. 147(4): p. 728-41.

84. Ravikumar, B., et al., Regulation of mammalian autophagy in physiology and pathophysiology. Physiol Rev, 2010. 90(4): p. 1383-435.

85. Kuma, A., M. Komatsu, and N. Mizushima, Autophagy-monitoring and autophagy-deficient mice. Autophagy, 2017. 13(10): p. 1619-1628.

86. Stead, E.R., et al., Agephagy - Adapting Autophagy for Health During Aging. Front Cell Dev Biol, 2019. 7: p. 308.

87. Zheng, Y.H., et al., Osteopontin stimulates autophagy via integrin/CD44 and p38 MAPK signaling pathways in vascular smooth muscle cells. J Cell Physiol, 2012. 227(1): p. 127-35.

88. Giusti, B., et al., Gene expression profiling of peripheral blood in patients with abdominal aortic aneurysm. Eur J Vasc Endovasc Surg, 2009. 38(1): p. 104-12.

89. Ramadan, A., M. Al-Omran, and S. Verma, The putative role of autophagy in the pathogenesis of abdominal aortic aneurysms. Atherosclerosis, 2017. 257: p. 288-296.

90. Clement, M., et al., Vascular Smooth Muscle Cell Plasticity and Autophagy in Dissecting Aortic Aneurysms. Arterioscler Thromb Vasc Biol, 2019. 39(6): p. 1149-1159.

91. Oyabu, J., et al., Autophagy-mediated degradation is necessary for regression of cardiac hypertrophy during ventricular unloading. Biochem Biophys Res Commun, 2013. 441(4): p. 787-92.

92. Masuyama, A., et al., Defective autophagy in vascular smooth muscle cells enhances atherosclerotic plaque instability. (1090-2104 (Electronic)).

93. Muniappan, L., et al., Inducible Depletion of Calpain-2 Mitigates Abdominal Aortic Aneurysm in Mice. Arterioscler Thromb Vasc Biol, 2021. 41(5): p. 1694-1709.

94. Subramanian, V., et al., Pioglitazone-induced reductions in atherosclerosis occur via smooth muscle cell-specific interaction with PPAR{gamma}. Circ Res, 2010. 107: p. 953-958.

95. Porrello, E.R., et al., Angiotensin II type 2 receptor antagonizes angiotensin II type 1 receptor-mediated cardiomyocyte autophagy. Hypertension, 2009. 53(6): p. 1032-40.

96. Steckelings, U.M. and T. Unger, Angiotensin receptors and autophagy: live and let die. Hypertension, 2009. 53(6): p. 898-9.

97. Mondaca-Ruff, D., et al., Angiotensin II-Regulated Autophagy Is Required for Vascular Smooth Muscle Cell Hypertrophy. Front Pharmacol, 2018. 9: p. 1553.

98. Daugherty, A., M.W. Manning, and L.A. Cassis, Angiotensin II promotes atherosclerotic lesions and aneurysms in apolipoprotein E-deficient mice. J Clin Invest, 2000. 105(11): p. 1605-12.

99. Dai, S., et al., Systemic application of 3-methyladenine markedly inhibited atherosclerotic lesion in ApoE(-/-) mice by modulating autophagy, foam cell formation and immune-negative molecules. Cell Death Dis, 2016. 7(12): p. e2498.

100. Seglen Po Fau - Gordon, P.B. and P.B. Gordon, 3-Methyladenine: specific inhibitor of autophagic/lysosomal protein degradation in isolated rat hepatocytes. (0027-8424 (Print)).

101. Wu, Y.T., et al., Dual role of 3-methyladenine in modulation of autophagy via different temporal patterns of inhibition on class I and III phosphoinositide 3-kinase. J Biol Chem, 2010. 285(14): p. 10850-61.

102. Morita, T., Celastrol: a new therapeutic potential of traditional Chinese medicine. Am J Hypertens, 2010. 23(8): p. 821.

103. Xu, S., et al., Celastrol in metabolic diseases: Progress and application prospects. Pharmacol Res, 2021. 167: p. 105572.

104. Li, H.Y., et al., Celastrol induces apoptosis and autophagy via the ROS/JNK signaling pathway in human osteosarcoma cells: an in vitro and in vivo study. Cell Death Dis, 2015. 6: p. e1604.

105. Divya, T., A. Sureshkumar, and G. Sudhandiran, Autophagy induction by celastrol augments protection against bleomycin-induced experimental pulmonary fibrosis in rats: Role of adaptor protein p62/ SQSTM1. Pulm Pharmacol Ther, 2017. 45: p. 47-61.

106. Daugherty, A. and L. Cassis, Angiotensin II-mediated development of vascular diseases. Trends Cardiovasc Med, 2004. 14(3): p. 117-20.

107. Yue, Z., et al., Beclin 1, an autophagy gene essential for early embryonic development, is a haploinsufficient tumor suppressor. (0027-8424 (Print)).

108. Wendling, O., et al., Efficient temporally-controlled targeted mutagenesis in smooth muscle cells of the adult mouse. (1526-968X (Electronic)).

109. Gawriluk, T.R., et al., Beclin-1 deficiency in the murine ovary results in the reduction of progesterone production to promote preterm labor. Proceedings of the National Academy of Sciences, 2014. 111(40): p. E4194-E4203.

110. Angelov, S.N., et al., TGF-β (Transforming Growth Factor-β) Signaling Protects the Thoracic and Abdominal Aorta From Angiotensin II-Induced Pathology by Distinct Mechanisms. (1524-4636 (Electronic)).

111. Doerflinger, N.H., B. Macklin Wb Fau - Popko, and B. Popko, Inducible site-specific recombination in myelinating cells. (1526-954X (Print)).

112. Daugherty, A., et al., Angiotensin II infusion promotes ascending aortic aneurysms: attenuation by CCR2 deficiency in apoE−/− mice. Clinical Science, 2010. 118(11): p. 681-689.

113. Kwon, Y., et al., Effects of 3-methyladenine, an autophagy inhibitor, on the elevated blood pressure and arterial dysfunction of angiotensin II-induced hypertensive mice. Biomed Pharmacother, 2022. 154: p. 113588.

114. Wang, C., et al., Celastrol suppresses obesity process via increasing antioxidant capacity and improving lipid metabolism. Eur J Pharmacol, 2014. 744: p. 52-8.
115. Fashandi, A.Z., et al., Female Mice Exhibit Abdominal Aortic Aneurysm Protection in an Established Rupture Model. J Surg Res, 2020. 247: p. 387-396.
116. Feng, X., et al., IL1R1 is required for celastrol's leptin-sensitization and antiobesity effects. (1546-170X (Electronic)).
117. Wang, B., et al., Celastrol prevents high-fat diet-induced obesity by promoting white adipose tissue browning. (2001-1326 (Electronic)).
118. Liu, Y., et al., Calorie restriction protects against experimental abdominal aortic aneurysms in mice. (1540-9538 (Electronic)).
119. Maguire, E.M., et al., Matrix Metalloproteinase in Abdominal Aortic Aneurysm and Aortic Dissection. Pharmaceuticals (Basel), 2019. 12(3).
120. Guo, J., et al., Celastrol Attenuates Intrahepatic Cholestasis of Pregnancy by Inhibiting Matrix Metalloproteinases-2 and 9. (1665-2681 (Print)).
121. Kim, Y., et al., Celastrol inhibits breast cancer cell invasion via suppression of NF-κB-mediated matrix metalloproteinase-9 expression. (1421-9778 (Electronic)).
122. Mi, C., et al., Celastrol induces the apoptosis of breast cancer cells and inhibits their invasion via downregulation of MMP-9. (1791-2431 (Electronic)).
123. Sanders, K.M., et al., Regulation of gastrointestinal motility--insights from smooth muscle biology. (1759-5053 (Electronic)).
124. Owens, A.P., 3rd, et al., Angiotensin II induces a region-specific hyperplasia of the ascending aorta through regulation of inhibitor of differentiation 3. (1524-4571 (Electronic)).
125. Poduri, A., et al., Fibroblast Angiotensin II Type 1a Receptors Contribute to Angiotensin II-Induced Medial Hyperplasia in the Ascending Aorta. (1524-4636 (Electronic)).
126. Mondaca-Ruff, D., et al., Angiotensin II-Regulated Autophagy Is Required for Vascular Smooth Muscle Cell Hypertrophy. (1663-9812 (Print)).

VITA

Education

University of Kentucky-Saha Cardiovascular Research Center
Lexington, Kentucky
PhD Candidate, Nutritional Sciences

2018 –2022
Emphasis: Biochemical and Molecular Nutrition

University of Kentucky- Dept. of Pharmacology and Nutritional Sciences
 Lexington, Kentucky
Master of Science, Nutritional Sciences
2014 – 2016
Emphasis: Biochemical and Molecular Nutrition

Science and Research Branch, IAU
Tehran, Iran
Bachelor of Science, Nutritional Sciences
2008-2012
Emphasis: Human Nutrition

Professional Positions

University of Kentucky-Saha Cardiovascular Research Center

Lexington, Kentucky
Part Time Lab Technician
2015-2016
Full Time Lab Technician

2016-2018

Honors and Awards

Honorable Mention-Research Presentation
Fall 2020

Physiology Research Retreat
Lexington, KY

Outstanding Research Presentation
Spring 2019

Barnstable Brown Obesity and Diabetes Research Day
Lexington, KY

Research Blitz
Spring 2018

Barnstable Brown Obesity and Diabetes Research Day
Lexington, KY

ATVB Travel Awards for Young Investigators
Spring 2018

Vascular Discovery
San Francisco, CA

International Student Tuition Scholarship

Fall 2015

University of Kentucky
Lexington, KY

Publications

1. Latha Muniappan, PhD, * ^ Michihiro Okuyama, MD, PhD, * Aida Javidan, MS,* Devi Thiagarajan, PhD, * Weihua Jiang, BS, Jessica J. Moorleghen, BS, Lihua Yang, BS, Anju Balakrishnan, MS, Deborah A. Howatt, BS, a Haruhito A. Uchida MD, PhD, c Takaomi C. Saido, MD, PhD, Venkateswaran Subramanian, PhD. Inducible Depletion of Calpain-2 Mitigates Abdominal Aortic Aneurysm in Mice. ATVB 2021, 120.315546

2. Michihiro Okuyama, Weihua Jiang, Aida Javidan, Jeff Zheying Chen, Deborah A Howatt, Lihua Yang, Mika Hamaguchi, Takumi Yasugi, Jun Aono, Roberto Irenardo Vazquez-Padron, Venkateswaran Subramanian. Lysyl Oxidase Inhibition Ablates Sexual Dimorphism of Abdominal Aortic Aneurysm Formation in Mice. Circulation 2020, 119.044986

3. Aida Javidan, Weihua Jiang, Michihiro Okuyama, Devi Thiagarajan, Lihua Yang, Jessica J. Moorleghen, Latha Muniappan & Venkateswaran Subramanian. miR-146a Deficiency Accelerates Hepatic Inflammation Without Influencing Diet-induced Obesity in Mice. Scientific Reports 2019, 10.1038/s41598-019-49090-4

4. Muniappan L, Javidan A, Jiang W, Mohammadmoradi S, Moorleghen JJ, Howatt DA, Balakrishnan A, Baud L, Subramanian V[*]. Calpain Inhibition Attenuates Adipose Tissue Inflammation and Fibrosis in Diet-induced Obese Mice, Scientific Reports 2017, 10.1038/s41598-017-14719-9

Manuscript under revesion

Aida Javidan, Weihua Jiang, Lihua Yang, Venkateswaran Subramanian. Celastrol Supplementation Ablates Sexual Dimorphism of Abdominal Aortic Aneurysm Formation in Mice. (ATVB-Brief Report)

Abstracts

1. Javidan A, Jiang W, Lihua L, Subramanian V Celastrol Supplementation Profoundly Activates Aortic MMP-9 and Abolishes Sexual Dimorphism of Abdominal Aortic Aneurysm in Mice. Saha Cardiovascular Research Day, July 2021, Lexington, USA
2. Javidan A, Jiang W, Lihua L, Subramanian V Celastrol Supplementation Profoundly Activates Aortic MMP-9 and Abolishes Sexual Dimorphism of Abdominal Aortic Aneurysm in Mice. , Vascular Discovery June 2021 (Virtual Meeting)
3. Depletion of Calpain-2 Attenuates Obesity-accelerated Abdominal Aortic Aneurysms in mice. AHA ,November 2017, Anaheim, California

4. Javidan A, Jiang W, Moorleghen JJ, Balakrishnan A, Howatt DA, Subramanian V[*]. Role of Calpain- 2 in obesity associated accelerated abdominal aortic aneurysms in mice. Department of Physiology Research Retreat 2016, Lexington, Kentucky, USA
5. Muniappan L, Javidan A, Jiang W, Moorleghen J.J, Balakrishnan A, Howatt D.A, Subramanian V[*].
   Inducible Depletion of Calpain-2 Attenuates Angiotensin II-induced Cytoskeletal Structural Protein Destruction During Abdominal Aortic Aneurysm Development in Mice. ATVB 2016, Nashville, TN, USA

Organizations

American Heart Association

2016-2022

Aida Javidan